268 301

THE
ANTENNA
LABORATORY

RESEARCH ACTIVITIES in ---

Automatic Controls   Antennas   Echo Area Studies
Microwave Circuits   Astronautics   E M Field Theory
Terrain Investigations   Radomes   Systems Analysis
Wave Propagation   Submillimeter Applications

An Airport Glide-Path System Using
Flush-Mounted, Traveling-Wave
Runway Antennas, Vol. II

by

Richard H. McFarland
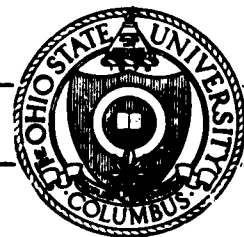
Contract FAA/BRD-116

891-2   31 March 1961

Department of ELECTRICAL ENGINEERING

**THE OHIO STATE UNIVERSITY
RESEARCH FOUNDATION**
Columbus , Ohio

An Airport Glide-Path System Using
Flush-Mounted, Traveling-Wave
Runway Antennas, Vol. II

by

Richard H. McFarland

Contract FAA/BRD-116

891-2   31 March 1961

REPORT

by

THE OHIO STATE UNIVERSITY RESEARCH FOUNDATION
COLUMBUS 12, OHIO

Cooperator

Federal Aviation Agency
Bureau of Research and Development
Washington 25, D.C.

Contract

FAA/BRD-116

Investigation of

Engineering Services for Glide Path
Antenna System Research

Subject of Report

An Airport Glide-Path System Using
Flush-Mounted, Traveling-Wave
Runway Antennas, Vol. II

Submitted by

Richard H. McFarland
Antenna Laboratory
Department of Electrical Engineering

Date

31 March 1961

ABSTRACT

A discussion of a new glide-path system is presented which utilizes conventional airborne receiving equipment to provide a pilot with veritical guidance to touchdown on an airport runway. This system uses five flush-mounted runway antennas to radiate the UHF glide-path signal from the precise destination of the aircraft. Inasmuch as the antennas are in the ground (runway) no image antennas are present; thus the path becomes virtually independent of the terrain. Also,no component of the system except possible monitor antennas need extend above ground, thereby eliminating obstruction hazards.

The basic theory for this endfire, transverse-electric, traveling wave, dielectric-filled antenna is given, together with results of scale-model measurements made at X-band frequencies. Several full-scale models designed to operate near 332 mc were built, in which steatite, asphalt, salt, and polystyrene were used as dielectric fillers, and the findings from the use of these are presented and compared with theoretical values. Results show excellent correlation.

Five array antennas containing polystyrene were built, and impedance and phase velocity tests show them to perform within 2 per cent of predicted values. Gain of the runway antenna in the glide-path region is 0 db compared to a one-half wavelength dipole located one wavelength above ground.

iv

The glide path is obtained with receiving equipment that detects and compares the quantities of 90 and 150-cycle audio present on the received signal. A predominance of 90-cycle modulation will be presented to the pilot as a fly-down command. Predominance of 150-cycle audio indicates to the pilot that he is below path and should fly up.

Two of the runway antennas are used to radiate the basic path, while the other three are used to broaden the path in azimuth. By using the conventional glide-path transmitter, at least a 15-mile coverage is obtained at one degree elevation and full fly-up signal is available at treetop level out to 7 miles.

An automatic servo phase controller is incorporated in the system to provide maximum path-angle stability. This type of monitor not only has the capability of detecting deviations in the path but also can make adjustments to maintain the desired path angle.

The glide path system was established at the Ohio State University Airport and over 90 hours of flight data were obtained . Results show an excellent path which can be flown to the touchdown region of the runway. Because of array near-field effects, the path limits no longer converge when within 600 feet of the array; instead, they remain essentially parallel. This feature has allowed the path to be repeatedly flown in to the touchdown region, thus giving evidence that this flush-mounted glide-path system radiating a signal from the aircraft's destination is an important step toward obtaining a zero-zero landing system.

v

ACKNOWLEDGMENTS

CONTENTS

LIST OF TABLES

LIST OF ILLUSTRATIONS

CHAPTER I

HISTORY OF INSTRUMENT LANDING SYSTEM GLIDE PATHS

1.1 Introduction

Since the beginning of aviation, the success and safety of air travel has been necessarily dependent on in-flight and terminal weather conditions. The Wright brothers in 1903 moved their aircraft, which was to make the first man-carrying powered flight in history, more than 500 miles to Kitty Hawk, North Carolina, to obtain optimum winds for the flight. Even today with modern airplanes it is occasionally necessary to land at airports other than those of the planned destination in order to obtain better weather conditions for a safe landing. These undesirable excursions certainly reduce the advantages and effectiveness of air travel.

The strides made in the safety and dependability of travel during these past 57 years have been tremendous. One of the most formidable problems of aviation that have been ever present is the possibility of below-minimum-operating terminal weather conditions. The minimum values defining operational weather have changed during the years and fortunately have changed to permit aircraft operations during a greater percentage of time.

During the late 1920's pilots began practicing a type of flying known as instrument or blind flying, during which time all reference was made to instruments or equipment that was carried aboard the

1

aircraft. This is in contrast to the type known as contact flying during which the pilot refers to the natural horizon for attitude of the plane, and to roads, terrain features, etc., for his position. The presence of clouds or precipitation can prevent this visual method from being used. When instrument flying is required, navigation is done solely through the use of radio aids. When flying from one city to another, tolerances required on position are moderate and easily held by the average pilot. However, when the aircraft must be oriented, then placed on a portion of the earth's surface 150 feet wide and 2000 feet long, a significant increase in accuracy of position is required. Present operational systems permit a pilot to descend no lower than 200 feet above the airport surface unless he has the runway in sight. The criterion quoted is based on legal standards which in turn are based on such factors as system accuracy, airport size, and sur-rounding terrain, aircraft type and characteristics, and pilot ability. Should the pilot not see the airport runway at 200 feet, he must begin a climb to a designated safe altitude and proceed to another airport.

1.2 Definition and Purpose of Instrument-Landing Systems

The present instrument-landing system is a collection of four radio aids which provide the pilot with navigational information during his approach to an airport.

The localizer is a 108 to 112 mc radio signal modulated with 90- and 150-cycle audio which is received aboard the aircraft to

effectively provide an extended runway centerline and thus give lateral guidance to the pilot.

The glide path is a 329 to 335-mc signal modulated with 90 and 150-cycle audio which provides the pilot with vertical guidance during an approach.

The outer marker is a 75-mc signal modulated with a periodic 400-cycle audio signal that is beamed vertically to provide a known reference approximately 5 miles from the airport. It is at this fix the pilot begins his descent on the glide path from an interception altitude of nearly 1500 feet above the surface.

The middle marker is a 75-mc signal of the same type as the outer marker but modulated with a periodic 1300-cycle audio that provides a fix to indicate that the aircraft is less than a mile from the airport and that visual contact with the runway should be established by this time.

Several additional aids are usually added to the system to provide increased safety:

Compass locator at the outer marker is a non-directional radio beacon operating in the 200 to 400-kc range providing a signal on which an automatic direction finder (ADF) aboard the aircraft is used to home to this point of interception with the glide path.

Compass locator at the middle marker is another non-directional

radio beacon in the same 200 to 400-kc band which provides an
additional reference for an ADF during an approach.

Approach lights are high intensity incandescent or flashing
strobe lights provided from the middle marker to the runway edge to
aid in establishing visual contact, especially at night, as a supplement
to the runway lighting itself. Figure 1   shows a typical arrangement
of instrument landing system radio aids.

By use of the glide path the pilot is able to establish the proper
angle and rate of descent of his aircraft and thereby to ensure adequate
clearance of hazards in the approach region. The glide path can be
thought of ideally as an inclined plane surface on which an aircraft is
flown to the touchdown on the runway. In practice the surface may not
be planar and may not extend to the runway. In many respects, produc-
ing this vertical reference for the pilot has been the most difficult
problem technically, especially when irregular terrain surrounds
many of the nation's airports.

1.3 Goals of Present Work

Although completely blind landings were accomplished as long
ago as 1929 , they were of an experimental nature and did not have the
qualities of safety and reliability that are associated with the aviation
industry as it is known today. Complicating the problem through the
past two decades has been the steady increase in the operating and
landing speeds of aircraft. The early landings were made with aircraft

5
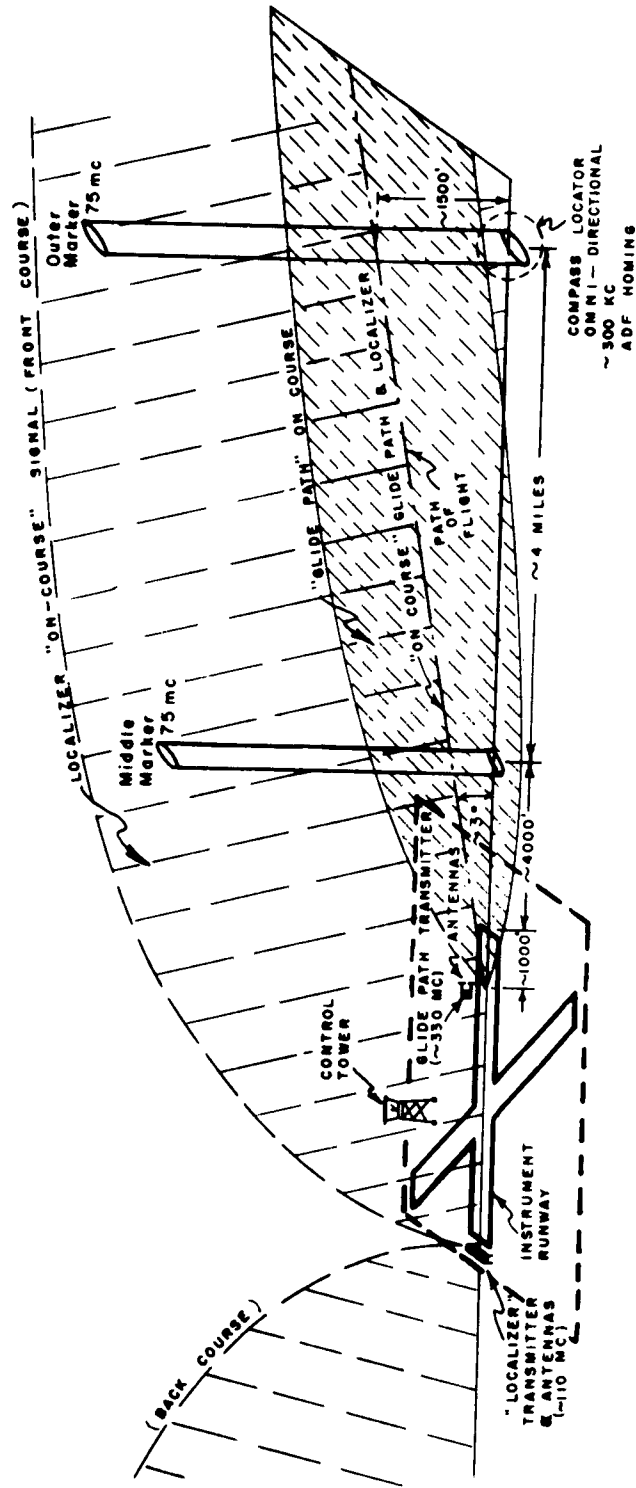
Fig. 1. Typical arrangement of instrument landing system components with course indications.

approaching at speeds of 50 to 60 miles per hour, whereas present
aircraft may approach at 150 mph with accompanying greater rates
of descent and decreased maneuverability. In other words, speed of
aircraft increased at a greater rate than did the improvements on
landing systems.

As instrument landing systems have become more accurate and
reliable, the term "minimum weather" has come to mean conditions
of lower and lower vertical and horizontal visibility. Two goals have
been established towards which the work herein described has been
directed. The first goal is to provide increased air safety. The second
goal is to provide the capability for safe aircraft landings during
conditions when the pilot cannot see the ground until he has flown
the glide path and other aids to touchdown. Landing under these
conditions is known as a zero-zero landing (zero ceiling and zero
visibility).

1.4 Early Glide Path Development

As early as 1919, the National Bureau of Standards began
experimenting with a radio-spark, 300-kc, landing-field localizer
system. However, progress was slow and it was September 1929
when Lt. James Doolittle made the first completely blind landing.
In 1933 James L. Kinney went into the clouds one mile from the air-
port at College Park, Maryland, and flew on instruments until emerg-
ing from the overcast when passing over the boundary of the Newark,

N. J., airport. With him on the flight was Harry Diamond, who since 1929 had been working at the National Bureau of Standards on a localizer and glide-path system which could be presented to the pilot in visual form[1].

By 1933 the demands of air mail flights and of increasing passenger traffic were being heard, with the result that the U.S. Army, U.S. Bureau of Air Commerce, United Air Lines, and Bendix Corp. began actively participating in the development of an improved instrument landing system. Aviators were harassed by radio noise, since low frequency signals were easily disturbed by atmospheric electricity which provided unreliable indications. The glide paths then in use were of the constant-intensity type on which the aircraft was maneuvered to maintain a constant signal strength as they approached and descended to the landing area. The resulting flight path would describe a curve in the shape of the antenna radiation pattern, becoming tangent to the earth at the touchdown region (Figure 2). Although the path had a desirable flare at the earth's surface, the path was generally unsatisfactory in that it was difficult to fly with a high initial rate of descent followed by almost level flight near the airport at such altitude that it would not always allow

---

[1] H. Diamond and F.W. Dunmore, "A Radio Beacon and Receiving System for Blind Landing of Aircraft," Bureau of Standards Journal of Research, Vol. 5, paper 238, October, 1930, also Proc. I.R.E., Vol. 19, pp 585-626, April 1959.

8
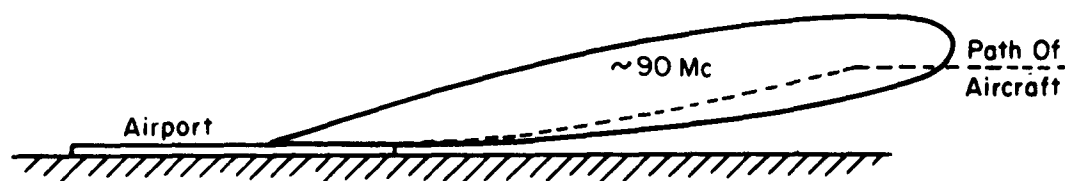
Fig. 2. A constant intensity glide path with pilot's indicator
and early flight test airplane of National Bureau of Standards.

clearance of obstacles. Two requirements came into focus that are

applicable today :

1. A straight-line glide path is to be preferred.

2. Frequencies should be in the Very High Frequency band to

provide freedom from static.

In 1935 at Indianapolis, Indiana, the Bureau of Air Commerce

began testing a 90-mc constant intensity glide path that had been the

result of work done by United Air Lines and Bendix at Oakland , California.

From 1935 to 1940 several glide-path systems were tested by the Bureau of Air Commerce, which in 1939 became the Civil Aeronautics Administration (CAA). Among these was the Lorentz (German) system which used a constant intensity contour of the localizer antenna pattern. Several of these were in operation in Europe.

1.5 The Equi-Signal Glide Path

The first step in eliminating the requirement for a constantly changing attitude of the aircraft came in 1940 when the CAA let a contract with International Telephone and Telegraph Company to develop a 330-mc straight-line glide path. The path information would be provided by comparing the quantities of 90 and 150-cycle modulation present during the approach. Proportional to the deviation above or below path would be the quantity of 90 and 150-cycle modulations, respectively, and when on path equal quantities would be received. The name "equi-signal" was therefore applied to this type of system. Note that airborne equipment designed to operate on this type of system can be used on present glide-path systems and on the system discussed in this paper. A discussion of the receiving equipment is presented on page 85 .

In the equi-signal system approximately one-half of the generated

rf energy was amplitude-modulated at 90 cps while the remainder was

modulated at 150 cps. As shown in Figure 3, the 90-cycle modulated
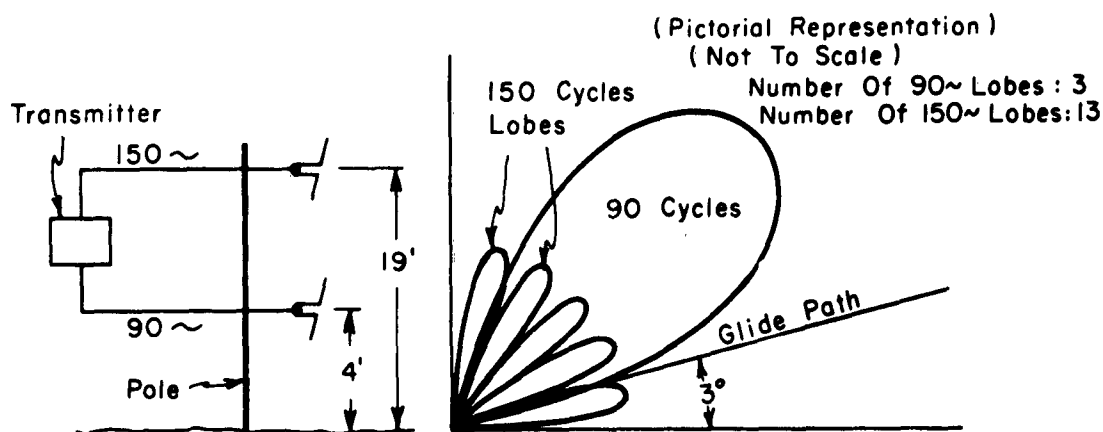
Fig. 3. Formation of the equi-signal glide path.

signal was fed to a dipole located 4 feet above a point, 500 feet to the

side, and 1000 feet from the approach end of the airport runway. (With

the relatively new capability to generate powerful UHF signals, antenna

heights were quite realistic to produce 3° glide paths). This produced

a large lobe of radiation in the approach region to the airport. The

150-cycle modulated signal went to an antenna located 15 to 20 feet above

the other, thus producing a radiation pattern with several lobes. The

superposition of these two radiation patterns produces a relatively

flat surface near 3° elevation where equal 90 and 150-cycle tones would

be received. The line of flight is formed by the intersection of the glide-path surface with that of the localizer.

Unfortunately the effective height of the antennas will change by a relatively large percentage with snow cover. The result of the ground plane being raised is to increase significantly the glide-path angle. Because of this instability, this type of glide path was unacceptable for airports in northern areas.

1.6 The Null-Reference Glide Path, the Present Operational System

One approach to a solution of the aforementioned problem was to design a system that would use higher antenna positions. During the late 1940's a system known as the Null-Reference System evolved, which allowed antennas to be placed on the order of 15 and 30 feet above the ground. Considerable modification had to be made in the transmission line networks in the transmitter, but no changes were necessary in airborne equipment[2].

Through bridge circuitry the carrier frequency may be eliminated from a portion of the signals resulting from the modulation. This energy consisting of 4 frequencies (upper and lower 90 and 150-cycle sidebands)

---

[2] This fact is more important than one would perhaps think at first. If a user has expensive equipment obsoleted, he is less likely to procure new equipment immediately but would probably wait to be sure that the new equipment is not outdated. With the rapid advances that are sometimes noted this might mean that more conservative users might never purchase the equipment, thus defeating the purpose of its existence.

is fed to the higher antenna. The remaining part of the energy which has not had the carrier frequency canceled is fed to the lower antenna. The height of the lower antenna, called the carrier antenna, is adjusted so that the maximum of the radiated beam occurs at the glide path angle, which is usually set between 2.5 and 3.0 degrees, depending on the obstacles in the approach region.

The height of the upper antenna, known as the sideband antenna, is set so that the first null occurs at the path angle, thus giving rise to the name of the system. Figure 4 shows that on path only the energy from the lower antenna which contains equal quantities of 90- and 150-cycle information is received. Phasing is so adjusted in the feeds that the 90-cycle sidebands are partially canceled below path and the 150-sidebands are partially canceled above path. It should be emphasized that the patterns shown in Figure 4 are of magnitude only and that the second lobe above ground has a 180-degree phase reversal. This is necessary to produce the desired cancellation.

When inspecting the geometry closely, it becomes apparent that there may be more than one straight line path produced, each with a progressively higher angle. With the equi-signal system the first false path was above 15 degrees. In practice these false paths cause no difficulty. In flying the glide path the pilot intercepts the path at a given altitude at a given reference, namely, the outer marker. The first false path, some 1700 feet higher, occurs with reverse sensing, and

Modulated R.F. Source

C $\angle 0$
C $\pm 90 \angle 0$

180°

$T_c \left\{ \begin{array}{l} C = \text{Carrier Frequencies} \\ C \pm 90 = \text{90 Cycle Side Band Frequencies} \\ C \pm 150 = \text{150 Cycle Side Band Frequencies} \end{array} \right\} T_s$

C $\angle 0$
C $\pm 150 \angle 0$

Carrier Antenna

Sideband Antenna

C $\angle 0$
C $\pm 90 \angle 0$
C $\pm 150 \angle 0$

C $\pm 150 \angle 0$
C $\pm 90 \angle -180$

Sideband Horizontal Dipole Antenna $\left. \right\} T_s$

Carrier Horizontal Dipole Antenna $\left. \right\} T_c$

26'

12'
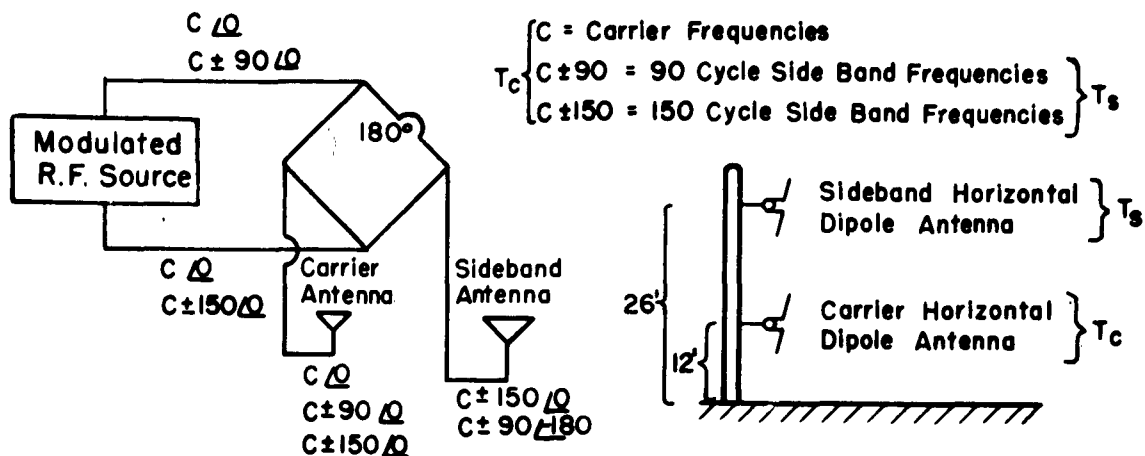
From Lobe 1 (From Sideband Antenna) $\left\{ \begin{array}{l} C \pm 90 \ \underline{\angle -180} \\ C \pm 150 \ \underline{\angle 0} \end{array} \right.$

Lobe 2 (From Sideband Antenna) $\left\{ \begin{array}{l} C \pm 90 \ \underline{\angle 0} \\ C \pm 150 \ \underline{\angle -180} \end{array} \right.$

Lobe 3 (From Carrier Antenna) $\left\{ \begin{array}{l} C \ \underline{\angle 0} \\ C \pm 90 \ \underline{\angle 0} \\ C \pm 150 \ \underline{\angle 0} \end{array} \right.$

Region: Below Glide Path Gives
Lobe 1 + Lobe 3 = $\left\{ \begin{array}{l} C \ \underline{\angle 0} \\ C \pm 150 \ \underline{\angle 0} \end{array} \right.$

Above Glide Path Gives
Lobe 2 + Lobe 3 = $\left\{ \begin{array}{l} C \ \underline{\angle 0} \\ C \pm 90 \ \underline{\angle 0} \end{array} \right.$

Sideband

Carrier

Additional Lobes

Glide Path

$\sim 3°$
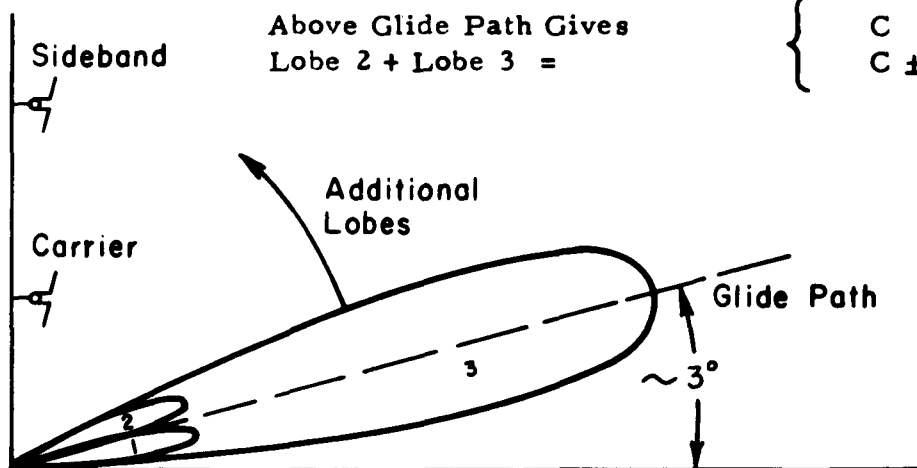
Fig. 4. Radiating system for the null-reference glide path.

should the pilot by some error intercept this path, any correction he would make to hold the path would further displace him from the on-course. The path is inverted in this region with 150 cycles above path and 90 cycles below.

Above the inverted path, 2 degrees or more, is the first false up-right path. To follow this the pilot would have to maintain an abnormally high rate of descent, essentially a dive, which would quickly alert him to the fact that he was not flying the proper path.

The null-reference system alleviated the snow problem inasmuch as it is the higher antenna which now controls the path, and a few inches change in 30 feet makes little change in the path angle. (Tolerances in the path angle are usually held to within .20 degrees.) The path is symmetrical vertically, with indication below path almost linear with displacement.

Two penalties are incurred, however, by this change. First, the higher antenna tower near the runway increases the collision hazard; and, second, and much more significant, with the higher antenna the regions of the earth that act as reflecting surfaces are moved farther from the antenna location. Since part of the signal that is used to form the path comes from a reflection (image antenna), relatively smooth areas for long distances ahead of the antenna are necessary in order to produce a straight path. Occasionally an airport is so located that the land is found to rise or fall abruptly in the approach region.

Examples of such airfields are Charleston, West Virginia; Lexington, Kentucky; Knoxville, Tennessee; and Huntington, West Virginia. At such airports it has been difficult or impossible to obtain an acceptably straight glide path.

1.7 Directional Glide Path

Intuitively the solution to the null-reference problem would be to replace the image antenna with a real antenna and form a path which is produced from direct radiation.

The plan of arraying glide-path antennas horizontally rather than vertically was conceived by A. G. Kandoian[3] in 1942. Little was done with this idea until L. N. Spinner[4] of the CAA established a path at Charleston, West Virginia, in 1956, using eight-element Yagi antennas located one wavelength above the ground. This type is called a directional glide path.

The horizontal array employed to establish a glide path must be used as an end-fire system, i.e., one that radiates predominantly along its longitudinal axis. This is in contrast to the equi-signal and null-reference system radiators that operate in the broadside sense. The associated geometries of on-course indications of the two systems

---

[3] A. G. Kandoian, "Glide Path Beacon", U.S. Patent 2,367,680 U.S. Patent Office; 1942.

4. T. H. Bottoms, H. C. Hurley, L. N. Spinner, and J. W. Watt, "A Directional Glide Path", Technical Development Report No. 336, Civil Aeronautics Administration; February 1956.

are illustrated in Figure 1-5. The broadside radiator produces a broad

conical surface whose vertex angle is near 174 degrees, while the end-

fire semi-cone has a vertex angle of 3 degrees. The result is that the

end-fire path is very narrow in azimuth coverage and must be broad-

ened.

1.8 Other Systems

For completeness, mention should be made here of a side band

reference system, modified side band reference system, and the "B"

and "M" arrays of the International Radio and Telegraph Laboratories[5].

These consist generally of vertical arrays similar to the null-reference

system but with emphasis on the reduction of terrain illumination.

These have all been designed to improve glide-pa'ʰ flyability, which

has been achieved in some instances.

Ground Controlled Approach, GCA, is a radar system, used

primarily by the military and involving a ground-based operator, who

observes the aircraft on the radar screen and then communicates its

position to the pilot by radio. This system has not found widespread

use with civil aviation except for monitor purposes. Perhaps the

greatest drawback in its present form is that its operation is dependent

on a human operator on the ground. It is the feeling of pilots that

---

[5] F. W. Iden, "Glide-Slope Antenna Arrays for Use Under Adverse Siting Conditions", I. R. E. Transactions on Aeronautical and Navigational Electronics, Vol. ANE-6, pp. 100-111 ; June 1959.
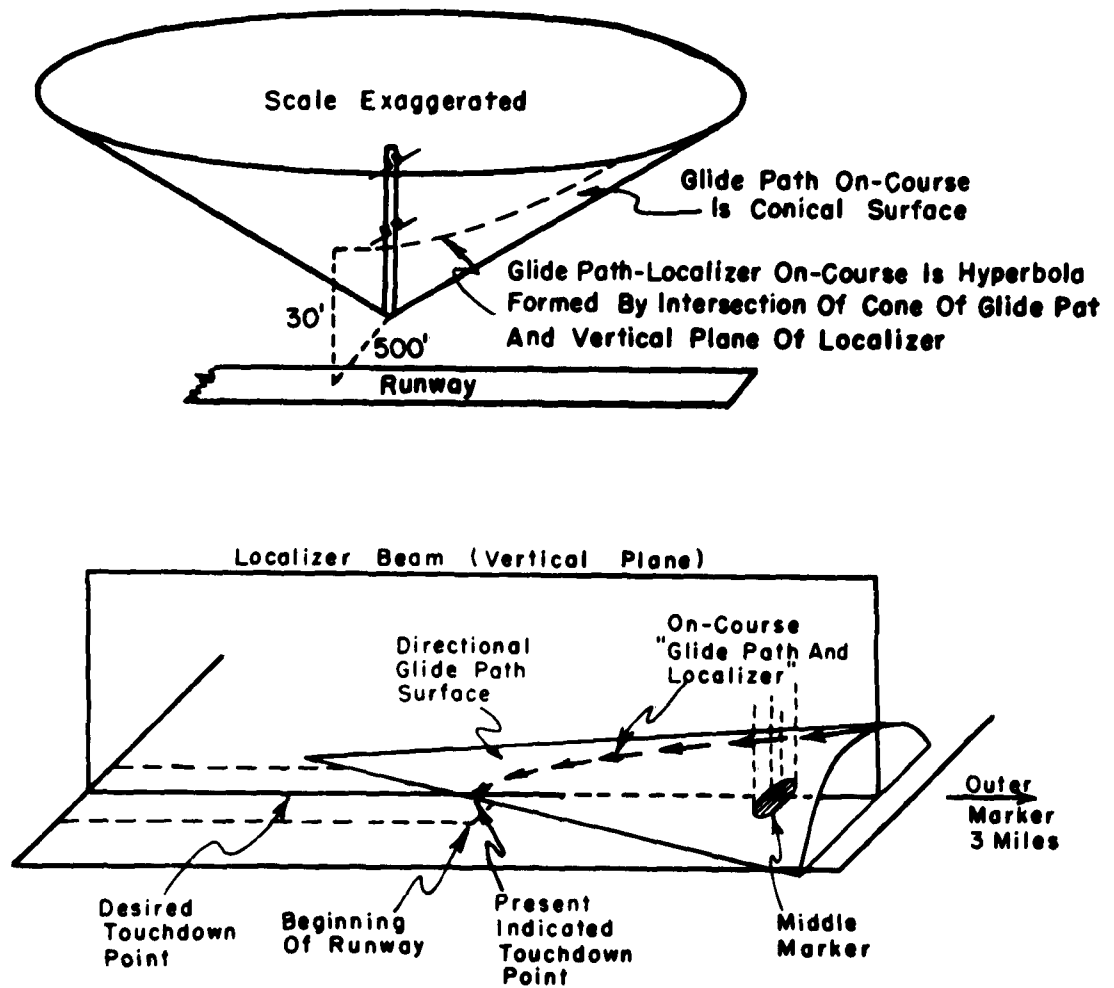
Fig. 5. Geometries of null reference and directional
glide-path surfaces using off-runway antennas.

command of the airplane should be from the air, since motivation for maintaining the safety of the flight cannot be higher than when one's own life depends on it. Work is being done at present on a radar system which involves no human in the relay of information to the pilot.

Table 1 is offered as a summary of the merits and problems of the glide-path systems prior to 1958.

1.9 On-Course Geometries

Because of the heretofore requirement of placing the source of radiation alongside the active runway or landing area, it is important to look at the indicated flight paths of various systems. The localizer providing lateral guidance can be thought of as a vertical plane intersecting the centerline of the runway and perpendicular to its surface. The curve formed by the intersection of this plane with the null-reference glide-path surface is an hyperbolic section opened upward with its apparent vertex some 30 feet above the runway. This thirty-foot minimum height on the glide path is a direct result, of course, of the necessity of having the antenna tower (axis) located 500 feet from the runway for purposes of safety. Because of this minimum height which the path reaches, it is not feasible for this system to provide sufficient information for completely blind landings. Although attempts have been made to modify

TABLE I

COMPARISON OF GLIDE-PATH SYSTEMS

GLIDE-PATH SYSTEM	MERITS	DEFICIENCIES
Constant intensity	Simplicity	Path shape difficult to fly. Close-in path too low to clear obstacles.
Equi-signal	Straight line path	Path angle seriously affected by ground cover.
Null Reference	Stable straight-line path	Irregular terrain in approach region produces path irregularities. Path does not extend to touchdown. Obstacle near runway.
Sideband Reference	Less affected by terrain in approach region because of lower antennas.	Stability poor in presence of ground changes.
Directional glide path with off-runway antennas	Straight-line path with no dependence on ground reflections to form path.	Convex curvature on localizer path. Horizontal path width must be increased by using more antennas in the array.

the path in the touchdown region, no completely acceptable method
has been forthcoming.

Figure 5 also shows that an end-fire array located to the side
of the runway produces a convex curvature in the on-course just
before touchdown. These undesirable geometries resulting from the
location of the antennas adjacent to the runway suggest that the
glide path should be radiated directly from the runway.

This discussion of glide-path systems and their deficiencies
has not been given here for the purpose of degrading these systems,
but rather to show the evolution and to provide motivation for ad-
vancement of the glide-path concept. Never has a navigational aid
been commissioned for public use in the United States if there was
serious question of its capability to provide adequate safety for its
users. Utilization rather than safety is the factor that is always
compromised when operating such navigational systems as the glide
path.

References are given in the bibliography to detailed discussions
of the glide path systems herein mentioned.

CHAPTER II

THE TRAVELING-WAVE, FLUSH-MOUNTED,

RUNWAY ANTENNA ELEMENT

2.1 Introduction

Figure 5 shows that the cause for the downward curvature of the

flight path with the directional glide path is the non-coincidence of the

axis of the cone and the centerline of the runway. Should they be

coincident, the glide path would be a straight line to touchdown,

provided the aircraft remained exactly on the localizer course.

To make the path practical and allow for deviation along the localizer

course, the path must be broadened.

The necessary coincidence of the two geometries can be ob-

tained by radiating the glide path directly from the touchdown region

of the runway. Intuitively, this is the correct place for radiation to

take place, since this is the desired destination of the aircraft. It is

well known that "homing" or tracking to a source provides information

that allows progressively more accurate position fixing. Homing

also produces continuing increase in signal strength, resulting in

more reliable receiver response.

2.2 Requirements

To allow radiation from a region that must accept the wheel

traffic of landing aircraft, a special antenna has been designed to meet

the electrical requirements of a glide-path system and the mechanical requirements for runway installation.

Specifically, these are the electrical requirements:

a. Gain should be such as to provide a three to five microvolt signal 15 miles from the airport, 1000 feet above the airport level, with 1 watt fed to the two antennas forming the path. This gain is 0 db compared to a wavelength dipole, one-wavelength above ground.

b. The antenna should be sufficiently broadbanded to operate satisfactorily in the glide-path band of 329.0 to 335.0 mcs.

c. The input impedance to the antenna should be 50 ohms to be compatible with transmitting equipment.

d. The antenna should radiate horizontally polarized energy in the approach region.

e. The radiation pattern should be of an end-fire type in order to reduce radiation in undesirable directions and to improve the gain at 3 degrees elevation for the flight path.

Horizontally polarized energy is required for compatibility with present aircraft antennas. Because no tangential electric field can exist at the boundary of a perfect conductor, there will be, inherent in the radiation field of the glide-path antenna, lower signal at low elevation angles. In spite of this, sufficient signal must be present from

1 to 5 degrees elevation to provide the necessary information during an approach to the airport. As will be shown later in this chapter, sufficient signal is available from the flush-mounted antenna to provide a safe coverage over all the required region.

2.3 Theory of the Traveling-Wave Runway Antenna

It will be useful in the understanding of the operation of the traveling-wave, flush-mounted, glide-path antenna to derive

a. an expression for the electric field intensity in the far field;

b. an expression for determining the critical dimensions of the antenna.

2.31 Derivation of an Expression for the Far Electric Field

Consider a waveguide in which a TE_{10} mode is propagating. If one-half of the guide were removed, as is shown in Figure 6 , the aperture would contain an electric field

$$\bar{E} = \hat{y}\, E_y \qquad (2\text{-}1)$$

as indicated.

While there are other types of traveling-wave slot antennas that might be considered, it will be shown that this simple type gives a strong signal of the proper polarization in the glide-path region.

To facilitate the analysis of this traveling-wave source, the equivalence principle will be used. Bronwell and Beam[1] discuss this

[1]. A.B. Bronwell and R.E. Beam, Theory and Application of Microwaves, McGraw-Hill Book Co.,Inc.,New York, N.Y., pp. 451-453 ; 1947.
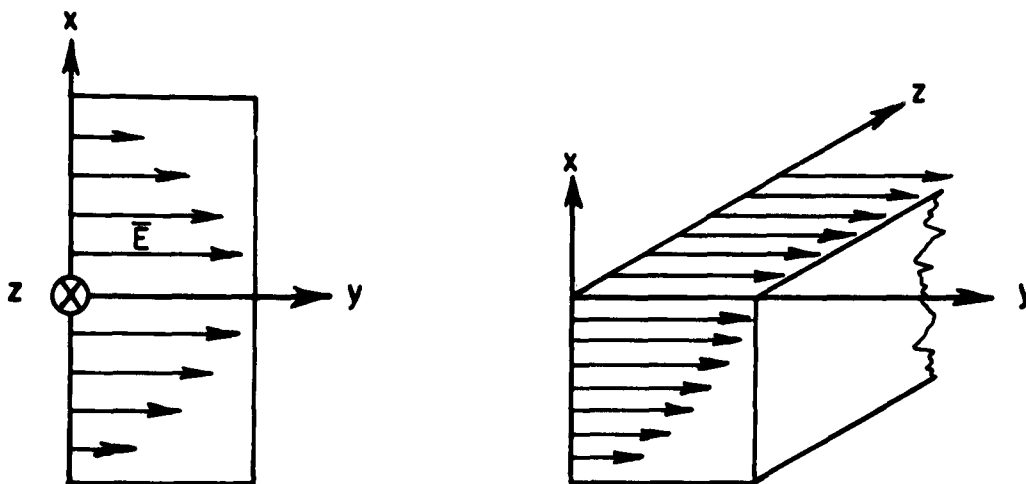
Fig. 6. TE_{10} mode (rms values) with one-half of the
guide removed.

principle, which will here be applied to the plane aperture of the run-

way antenna shown in Figure 7. In this application the surface enclosing
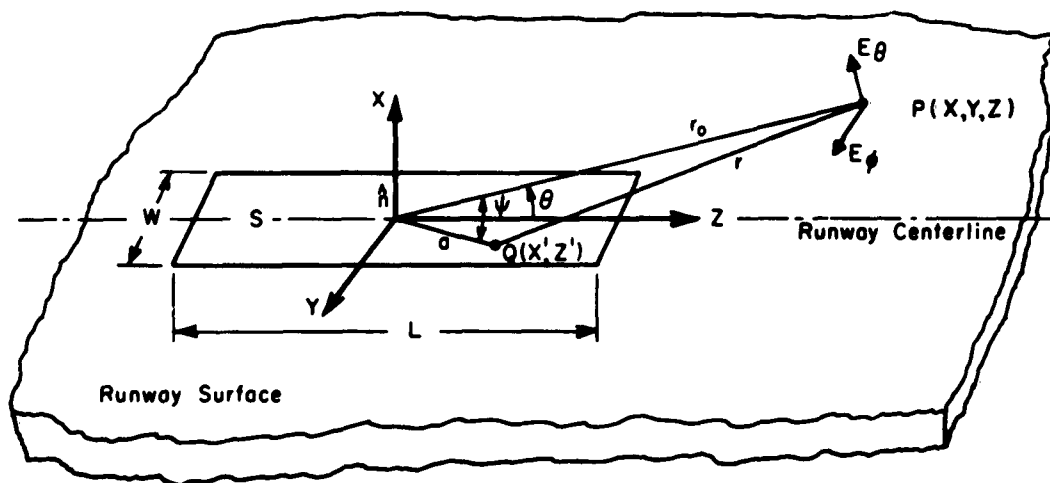
Fig. 7. Coordinate system used in analysis.

the source of electromagnetic energy is the surface of the earth, including the aperture of the antenna; i.e., all sources of energy are below ground level insofar as radiation is concerned. To a good approximation, the surface of the earth may be treated as a plane surface of infinite extent. The earth is assumed to be a perfect conductor; therefore, the component of the $\bar{E}$ tangential to the surface S must be zero everywhere except in the aperture of the antenna.

In general, fictitious electric and magnetic currents are consid-eredto flow on the surface S in accordance with the relations

$$J_{es} = \hat{n} \times \bar{H} = \hat{x} \times \bar{H}, \qquad (2\text{-}2)$$

$$J_{ms} = \bar{E} \times \hat{n} = \bar{E} \times \hat{x}. \qquad (2\text{-}3)$$

These currents, distributed over the entire earth plane S, are equivalent to the original radiating source in the sense that the fields produced by these currents are the same everywhere above the earth as those produced by the actual sources.

By the principle of superposition, the field at any point in space may be calculated by adding (integrating) the contributions from currents flowing at each point on S. Bronwell and Beam give the resulting electric field as

$$\bar{E} = \frac{j \omega \mu}{4 \pi} \int_{s} \frac{(\dot{n} \times \bar{H})}{r} \, e^{-j\beta r} \, dS$$

$$- \frac{j}{4 \pi \omega \epsilon} \nabla \left[\nabla \cdot \int_{s} \frac{(\acute{n} \times \bar{H})}{r} \, e^{-j\beta r} \, dS \right]$$

$$+ \nabla \times \left[\frac{1}{4 \pi} \int_{s} \frac{(\hat{n} \times \bar{E})}{r} \, e^{-j\beta r} \, dS \right] \qquad (2\text{-}4)$$

where

β = phase constant, 2π/ wavelength,

r = distance to point of observation (see Figure 7),

S = surface of the source .

Harmonic variation with respect to time has been assumed and is suppressed.

However, the calculations may be greatly simplified by noting that boundary conditions require that the discontinuity in the tangential field components be equal to the corresponding surface current density on S. The fields immediately above S are equal to the actual fields, and the fields immediately below S are zero. That is, the fictitious surface current density provides exactly the proper magnitude to require a discontinuity in the field, changing from its actual value above to zero below S.

Since the fields due to the equivalent currents are zero everywhere below S, a body or surface of arbitrary shape and electromagnetic properties may be introduced below S without disturbing the fields above S. Since tangential $\bar{E}$ is zero everywhere on the infinite plane except in the antenna aperture, it is desirable, if possible, to eliminate the integrals involving $n \times \bar{H}$. This may be done by placing a fictitious plane sheet, which is a perfect conductor of electricity, an infinitesimal distance below S. The contributions from

$$\bar{J}_{es} = \hat{n} \times \bar{H} \qquad (2-5)$$

are canceled by corresponding image currents, and the contributions from

$$\bar{J}_{ms} = \bar{E} \times \hat{n} \qquad (2-6)$$

are doubled by contributions from the image currents. Therefore, the expression may be simplified to

$$\bar{E} = 2 \nabla \times \left[\frac{1}{4\pi} \int_s \frac{\hat{n} \times \bar{E}}{r} e^{-j\beta r} dS \right] . \qquad (2-7)$$

Details of this operation are given in the Appendix. Instead of facing the problem of evaluating three integrals over an infinite surface, the problem has been reduced to evaluation of a single integral over the antenna aperture alone.

Furthermore, the remaining expression may be interpreted simply as the fields produced by an array of longitudinal magnetic dipoles along the aperture of the antenna. Since the fields of a magnetic dipole are the same as those of an electric current loop[2], the problem is reduced to that of calculating the fields from an array of loop antennas whose axes are longitudinal and are distributed continuously along the antenna aperture.

In the application at hand, interest is restricted to the horizontally polarized signal on the localizer path, i.e., $\phi = 0°$. As discussed in the Appendix, these restrictions allow the integrand to be simplified. Thus the following expression is obtained:

$$E_{\phi}(r_o\ ,\ 0\ ,\ \theta) = \frac{-j\beta e^{-j\beta r_o}}{2\pi r_o}\ \sin\theta\ \int_{s} E_y(y',\ z')e^{j\beta a\cos\psi}\ dS \qquad (2\text{-}8)$$

Assuming $\qquad E_y = E_o\ e^{-jK z'} \qquad\qquad (2\text{-}9)$

as in a traveling wave where

$$K = \alpha_g + j\beta_g\ ,$$

α_g = losses due to radiation, the dielectric and the conductors with finite conductivity, and

$\beta_g = \dfrac{\omega}{v}$ = phase constant of cavity.

---

2. J. D. Kraus, <u>Antennas</u> , McGraw-Hill Book Co., Inc., New York, N. Y. , p. 157 ; 1950 .

Integrating over the aperture with area A = LW gives

$$E_\phi(r_o, \, 0, \, \theta) = \frac{-j\beta e^{-j\beta r_o}}{2\pi r_o} \, A \, E_o \, \sin\theta \, \frac{\sin X_o}{X_o} \qquad (2\text{-}10)$$

where

$$X_o = (\, K - \beta \cos\theta \,)\frac{L}{2} \qquad (2\text{-}11)$$

Several important observations can be made at this point. The field strength is proportional to the area of the aperture. Increasing the length, or within limits the width, will increase the signal strength in the region of interest. Also, the sin θ factor tends to reduce low elevation angle radiation. Although there was an early concern about whether sufficient signal would be available for operation of glide-path receivers, the signal has been found to be adequate and the sin θ factor becomes a benefit, inasmuch as it reduces the illumination on reflecting objects, such as knolls and buildings in the approach region.

2.32 Determining the Cavity Phase Velocity

The direction of maximum radiation is a function of the phase velocity of the cavity. Considering discrete sources, end-fire radiation takes place when the phase delay between elements is equal to the element spacing in free-space wavelengths[3]. This applied to a

---

3 Ibid; p. 80.

continuous source requires that the cavity phase velocity equals that of the speed of light, i.e.,

$$\frac{c}{v} = 1 \ . \tag{2-12}$$

Some lowering of the beam maximum will take place because of the currents in the ground plane near the aperture, but the effect will be small. Equation (2-10) effectively gives the upper bound, since no ground plane effects have been taken into account. In Figure 8 is shown the plot of

$$(\sin \theta) \left\{ \frac{\sin (K - \beta \cos \theta) \frac{L}{2}}{(K - \beta \cos \theta) \frac{L}{2}} \right\} \ . \tag{2-13}$$

L is 20 feet, $K = \beta = \beta_o = \frac{2\pi}{\lambda_o}$.

As was seen, the desired aperture fields can be obtained by using a horizontal electric probe to excite a pseudo-waveguide structure with one wall removed to allow radiation. Since a waveguide is inherently a fast wave structure, while a wave is effectivelly slowed when traveling in a dielectric, it is desirable to combine these two effects properly to obtain a phase velocity of the desired $\frac{c}{v}$ in the antenna. It is necessary then to obtain a relation between the guide dimensions and the dielectric material if optimum properties are to be obtained from the antenna. This relation will be obtained in the next section.
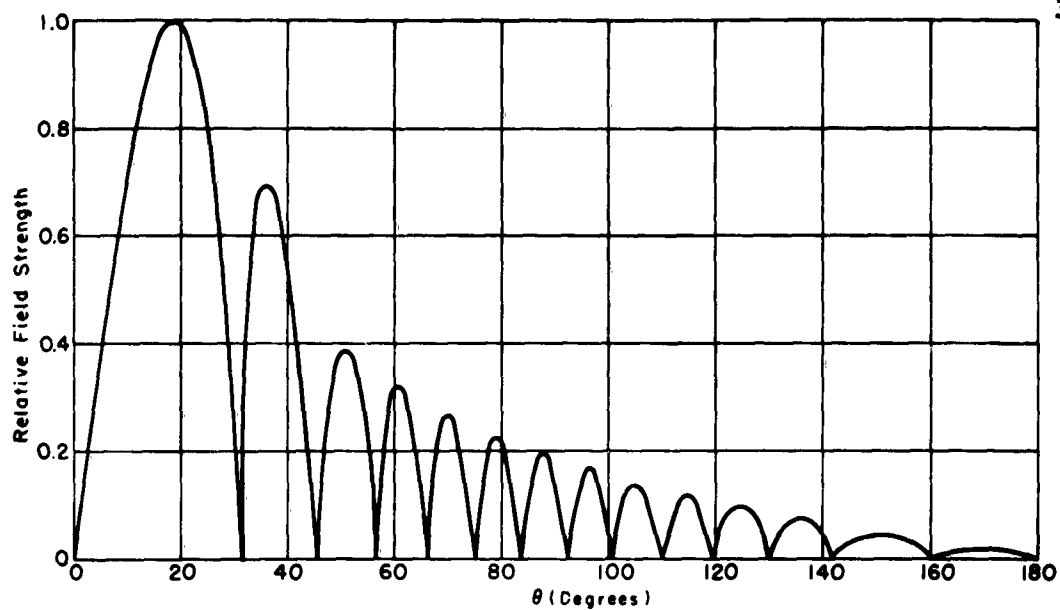
(a) Rectangular
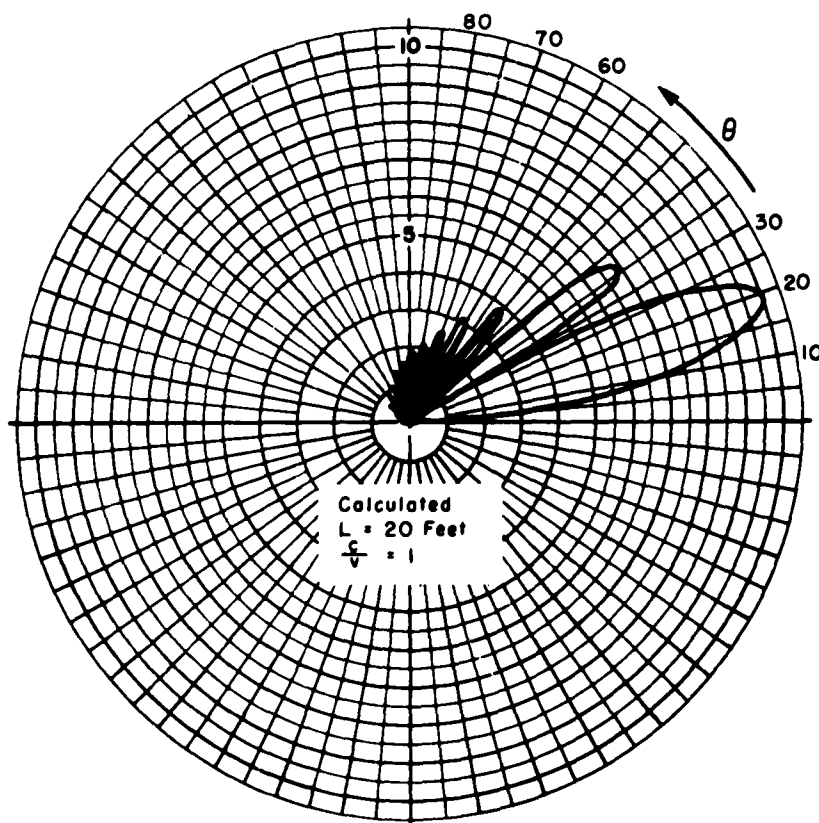
(b) Polar

Fig. 8. Calculated relative radiation patterns for 20-foot traveling-wave antenna.

2.33 Determining the Cavity Dimensions for End-Fire Operation

The model shown in Figure 9 is used to obtain a simple formula which checks with model measurements to within 4 per cent.

Starting with Maxwell's quartet, the following are the expressions for the electric fields in the two regions.[4]

For region II excited with a horizontal probe

$$\bar{E}_2 = \hat{y} \left[E_0 \, e^{j(\omega t - K_{x2}x - K_{z2}z)} + RE_0 \, e^{j(\omega t + K_{x2}x - K_{z2}z)} \right], (2\text{-}14)$$
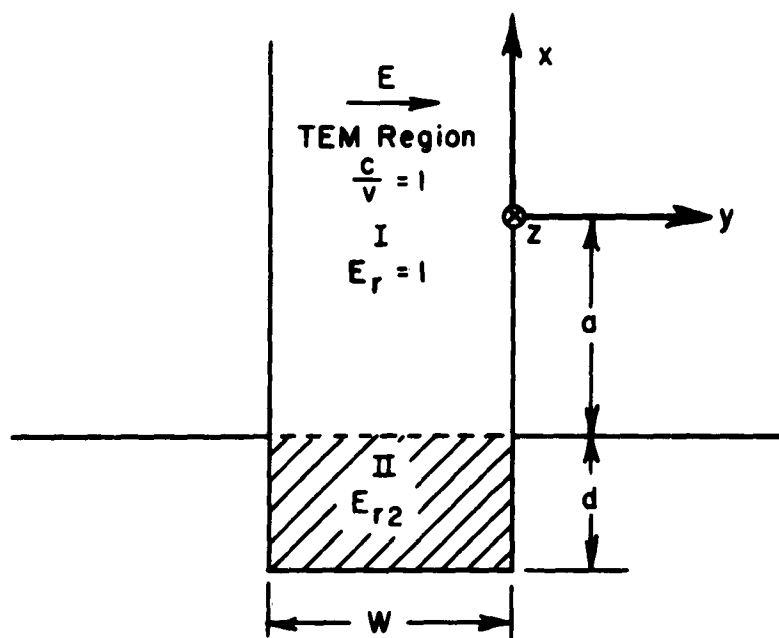
Fig. 9. Model for determining cavity dimensions.

4. Ibid ; pp. 344-348.

and for region I with TEM mode

$$\bar{E}_1 = \hat{y} \left[TE_o \, e^{j(\omega t - K_{z1} z)} \right] \tag{2-15}$$

where T and R are the transmission and reflection coefficients respectively of the interface at $x = -a$, $\omega = 2\pi f$, and k_x and k_z are vector wave numbers.

The magnetic field components are found from

$$-j\omega\mu\bar{H} = \nabla \times \bar{E} = \nabla \times (\hat{y} \, E_y) = -\hat{x} \, \frac{\partial E_y}{\partial z} + \hat{z} \, \frac{\partial E_y}{\partial x} \tag{2-16}$$

to be

$$-j\omega\mu\bar{H}_1 = -\hat{x} \left[\left(-j K_z \right) TE_o \, e^{j(\omega t - K_{z1} z)} \right] + \hat{z} \cdot 0 \tag{2-17}$$

and

$$-j\omega\mu\bar{H}_2 = -\hat{x} \left[(-j K_{z2}) \, E_o \, e^{j(\omega t - K_{x2}x - K_{z2} z)} \right.$$

$$+ (-j K_{z2}) \, RE_o \, e^{j(\omega t + K_{x1}x - K_{z2}z)} \Bigg]$$

$$+ \hat{z} \left[(-j K_{x2}) \, E_o \, e^{j(\omega t - K_{x2}x - K_{z2}z)} \right.$$

$$+ (j K_{x2}) \, RE_o \, e^{j(\omega t + K_{x2}x - K_{z2}z)} \Bigg] \tag{2-18}$$

Because of the TEM wave in the region I, the above statements

verify that

$$H_{z1} \equiv 0 \qquad (2\text{-}19)$$

and because no electric currents are present at the interface $x = -a$,

$$H_{x2} = H_{x1} \qquad (2\text{-}20)$$

$$H_{z2} = H_{z1} = 0 \qquad (2\text{-}21)$$

Then after dividing through by non-zero quantities, equations (2-20)

and (2-21) respectively become, noting that $K_{z2} = K_{z1}$

$$e^{jK_{x2}a} + R\, e^{-jK_{x2}a} = T; \qquad (2\text{-}22)$$

$$-e^{jK_{x2}a} + R\, e^{-jK_{x2}a} = 0. \qquad (2\text{-}23)$$

Further boundary conditions require that at $x = -a$ the

tangential electric fields be equal, thus giving

$$TE_0\, e^{j(\omega t - K_{z1}z)} =$$

$$E_0\, e^{j(\omega t + K_{x2}a - K_{z2}z)} + RE_0\, e^{j(\omega t - K_{x2}a - K_{z2}z)} , \qquad (2\text{-}24)$$

and at $x = -(a+d)$ the tangential electric field vanishes, assuming a

perfectly conducting cavity wall; hence

$$E_0\, e^{j[\omega t + K_{x2}(a+d) - K_{z2}z]} + RE_0\, e^{j[\omega t - K_{x2}(a+d) - K_{z2}z]} = 0. \qquad (2\text{-}25)$$

Simplifying gives

$$T = e^{jK_{x2}a} + R\, e^{-jK_{x2}a} \qquad (2\text{-}26)$$

$$e^{jK_{x2}(a+d)} + R\, e^{-jK_{x2}(a+d)} = 0 . \qquad (2\text{-}27)$$

Solving for R in (2-27) and substituting into (2-23) gives

$$1 + e^{j K_{x2}(2 d)} = 0,$$ (2-28)

or

$$1 + \cos 2 K_{x2}d + j \sin 2 K_{x2}d = 0 .$$ (2-29)

Thus

$$\cos 2 K_{x2} d = -1$$ (2-30)

$$\sin 2 K_{x2} d = 0$$ (2-31)

which requires

$$K_{x2} = \frac{\pi}{2d}$$ (2-32)

for the first mode. Note that this value also satisfies the boundary conditions of (2-22) and (2-26) .

The relation between the vector wave numbers is

$$(K_{x2})^2 + (K_{y2})^2 + (K_{z2})^2 = K_2^2 = \omega^2 \mu \varepsilon .$$ (2-33)

For end-fire radiation it was found that

$$K_{z2} = \frac{2\pi}{\lambda_o} .$$ (2-34)

Also, assuming that $\mu_2 = \mu_0$, and noting that there is no dependence on y allows (2-33) to be rewritten as

$$\left(K_{x2}\right)^2 + \left(\frac{2\pi}{\lambda_o}\right)^2 = \left(\frac{2\pi}{\lambda_o}\right)^2 \epsilon_r. \qquad (2\text{-}35)$$

Now from (2-32)

$$\left(\frac{\pi}{2d}\right)^2 = \left(\frac{2\pi}{\lambda_o}\right)^2 (\epsilon_r - 1) \qquad (2\text{-}36)$$

or

$$d = \frac{\lambda_o}{4\sqrt{\epsilon_r - 1}}. \qquad (2\text{-}37)$$

This is the expression for the depth of the cavity in terms of the relative permittivity of the dielectric filler and the operating wavelength. As can be seen there is no dependence on the width of the cavity, except for the restriction to prevent propagation of higher order modes.

From Equation (2-10) it may be seen that the field strength in the far field is directly proportional to the cavity width; therefore, it is desirable to make W as large as possible without introducing higher order modes in the structure. Making W $\frac{1}{4}$ wavelength is a practical compromise. Numerous measurements verify this expression for d

within 4 per cent and clearly illustrate the independence of W in determining the cavity depth.

Further accuracy could be obtained by considering the fringing effects at the aperture or interface and the finite conductivity of the actual conductors. One advantage of this expression lies in its simplicity, and the 4 per cent deviation can be reduced for design purposes by adding an empirical correction which allows the expressions to be written as

$$d = \frac{.26 \ \lambda_0}{\sqrt{\epsilon_r - 1}}$$ (2-38)

$$W = .25 \ \lambda_o \ .$$ (2-39)

These then provide the cross section dimensions for a TE, dielectric filled, end-fire, traveling wave, slot antenna (Figure 10) .

2.4 Artificially Loaded Antenna Structure

As was pointed out in the preceding discussion, the phase velocity of the energy in the traveling wave antenna must be adjusted to equal the speed of light in order to obtain maximum end-fire radiation. To obtain a slow wave structure a dielectric filler[5] was added. It is clear from equation (2-37) that the higher the dielectric constant of the material used, the smaller will be the physical size of the antennas.

---

[5] The term "dielectric filler" will refer only to solid dielectrics for the case of the runway antenna.
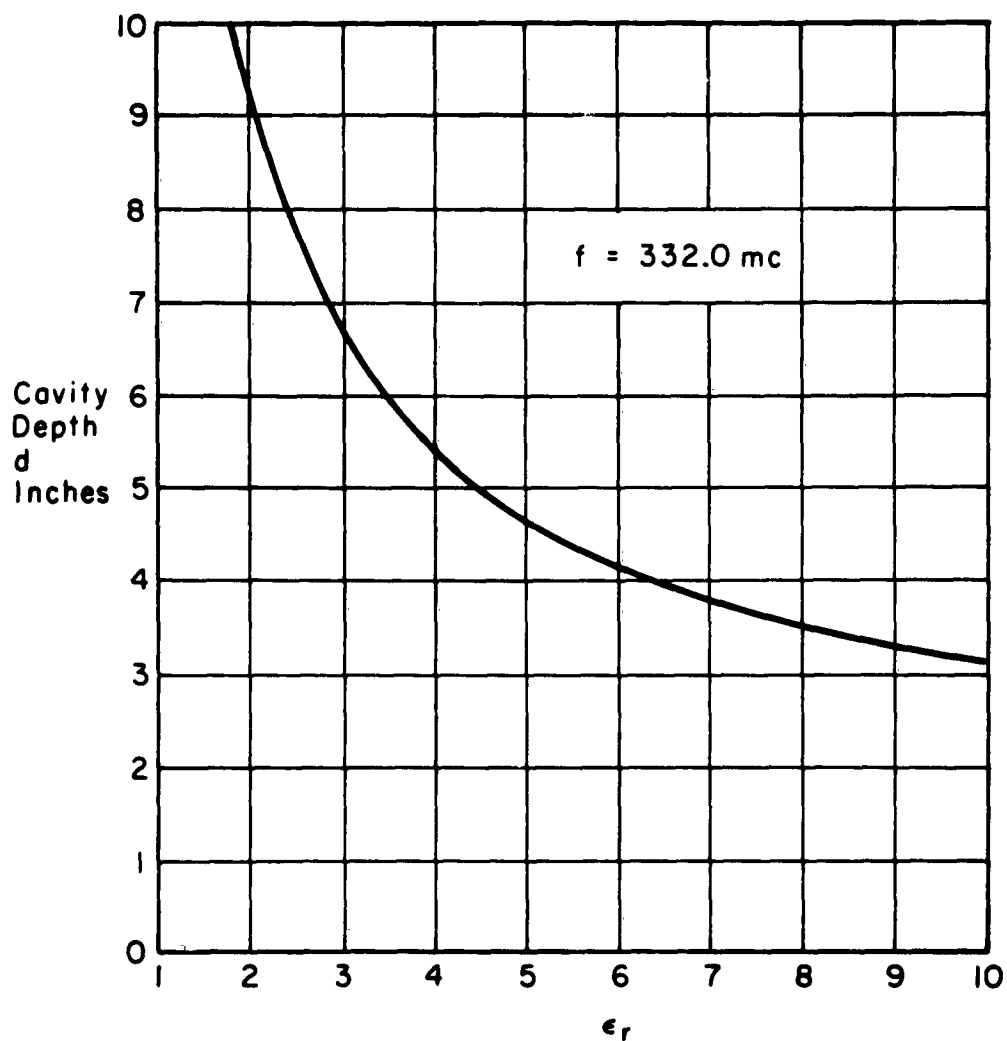
Fig. 10. Cavity depth as a function
of dielectric constant.

This is generally desirable, since these will be placed in an airport

runway, where lower maintenance and construction costs usually

increase with the size of the antennas. Materials such as polystyrene

($\epsilon_r = 2.56$) and steatite ($\epsilon_r \approx 5.7$) have been successfully used in

tests. Should materials with extremely high dielectric constants be used (e.g., barium titanate $\epsilon_r > 1000$), tuning and stability would become more critical.

Fortunately, some of the materials suitable electrically have the strength requirements for runway installation, since the dielectric material will be an integral part of the runway. Under most circumstances it is desirable to add a replaceable radome covering to protect the filler from abrasion.

There may be one disadvantage in having a surface of a solid as the aperture of a radiating structure. Material can collect on this surface, thus causing changes in the phase velocity and changes in the near and far fields. Of particular concern is a layer of water which may collect during rains. A layer of water hosed onto a flat surface can retard the phase of the signal coming from the antenna up to 15 electrical degrees at 330 mc. This has been observed and can be calculated simply using the consideration of oblique transmission through a layer of high permittivity medium. This is illustrated in Figure 11. From this it can be calculated that each 0.001 inch of water will introduce a phase retardation 1.55 electrical degrees. The effects of water layers are eliminated, however, when the antennas radiating the two signals for phase comparison are equally wet. Phase shifts are proportional to the quantity of water on the surface.

Fluids whose dielectric constant are low (ε_r = 2.5 - 4.0) cause no

measurable phase shift.
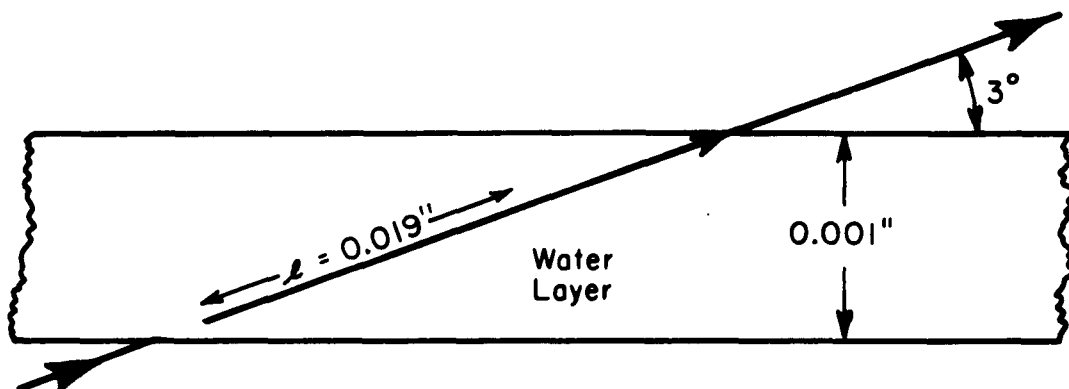
Fig. 11. Transmission through water layer.

To minimize the effect of a layer of water, the shape of the sur-

face was designed so that only a minimum amount could collect on the

antenna. For best drainage a gabled crown was selected, which offers

maximum constant slope for minimum height.

In addition some thought was given to obtaining an antenna that

would be especially insensitive to water at the aperture surface. Since

the absence of water could not be guaranteed, automatic servo phase

control and the removal of the surface were both considered.

Early in 1959 Oliner and Rotman[6,7] published information on

6 A. A. Oliner, and W. Rotman, "Periodic Structures in Trough Waveguide," I.R.E. Transactions on Microwave Theory and Techniques, Vol. MTT-7, pp. 134-142 ; January, 1959 .

7. W. Rotman, and A. A. Oliner, "Asymmetrical Trough Waveguide Antennas", I.R.E. Transactions on Antennas and Propagation, Vol. AP-7, pp. 153-162 ; April, 1959 .

artificially loading a guide or trough with a serrated ridge to control the phase velocity. Such a technique is applicable to controlling the phase velocity in a slotted wave guide which can be used as a radiator.

If a series of longitudinal slots were cut in the guide wall as shown in Figure 12 and these slots were excited with probes extending into the region of strong fields inside the guide, it should be possible to produce horizontally polarized radiation at low elevation angles provided the c/v ratio was maintained at unity. Preliminary studies indicated the importance of taking into account the effects of the probes when determining the type of ridge structure for $c/v = 1$.

The radiating slots could be made narrow enough that aircraft tires would not slip through. Rain water could fall directly into the antenna, which would have a conducting screen base to allow rapid passage to a drain system. In this way no surface of water would be formed, and freedom from undesirable shift could be obtained.

The success of early tests using the full-scale dielectric-filled antenna was the determining factor in the use of this type of antenna to establish the glide path.

2.5 Scale Model Measurements

The use of scale-model measurements in determining the characteristics of the dielectric filler is invaluable. Important in these measurements is the verification of the analytical expression (Equation 2-37) for the cavity depth as a function of the permittivity
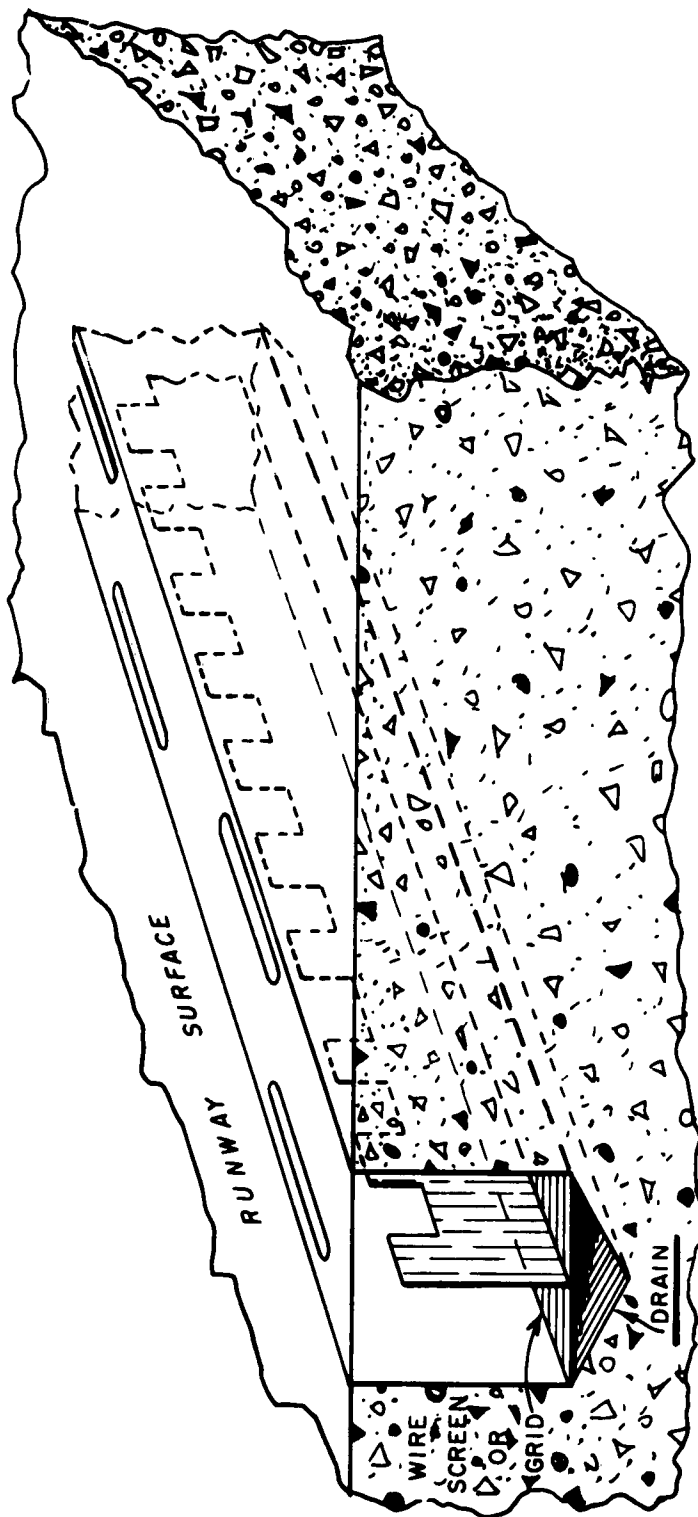
Fig. 12. Antenna with slotted cover.

of the filler material. The use of scale models to obtain basic design data prior to full-scale construction results in great economy of both time and money.

Inasmuch as it is the cavity depth that controls the phase velocity, variations of this dimension (cavity depth referred to wavelength) are easily effected by changing the frequency of the signal used on the scale-model measurements.

Narrower band transmitters at the 330 mc glide path and Federal Communications Comission rules make depth-determining measurements using frequency variation at full scale impractical. Because of the resulting small sizes of models used with frequencies near 10,000 mc, it is possible to use a conventional radiation pattern range and thus determine the lobe structure of the antenna in much more detail.

Fabrication of the scale-model antenna began with a 12-inch bar of brass one inch square in cross section. In this bar was cut a channel 0.400 inch wide, 0.200 inch deep, and 12 inches long. A brass plate was attached at one end of the bar for a termination. At the other end two different attachments were used. For early testing, a taper section going from the 0.200 depth of the channel to the 0.900 inside dimension of X-band was used as a transition from the antenna to the X-band detector mount. Copper foil was bonded to an 18- by 36-inch piece of plywood, forming a conducting ground plane. A

one-inch by 12-inch slot was cut in the ground plane to receive the channel. Figure 13 shows the details of the scale model.

The second attachment that was later used was simply a brass plate , which was attached to the channel when the waveguide and taper section were removed. The detector was then attached to a probe which entered the channel from the side below the ground plane. This was the true scale-model of the actual runway antenna.

It should be mentioned that the principle of reciprocity is used in measuring , since the test antenna is used as a receiving antenna for convenience rather than as a transmitting antenna.

Polystyrene, because of its ease in machining, was first used as a dielectric filler for the brass channel. The length of the radiating aperture was changed by inserting brass slugs in the channel in place of portions of the dielectric. In addition to the polystyrene, asphalt, glass, steatite, and sodium chloride were used in tests as fillers.

A series of tests was made to determine the effect of changing the depth of the channel or cavity of the antenna on the radiation pattern. Figure 14 shows the change of the depth of the antenna from 5.73 in. to 7.55 in. , It is understood that the width and length are also changing here, but from theory and measurements presented later in this chapter, these do not affect the pattern shape - only size or magnitude.

Table 2 presents a comparison between the calculated depth of a

Fig. 13. Scale model of runway antenna used at X-band.
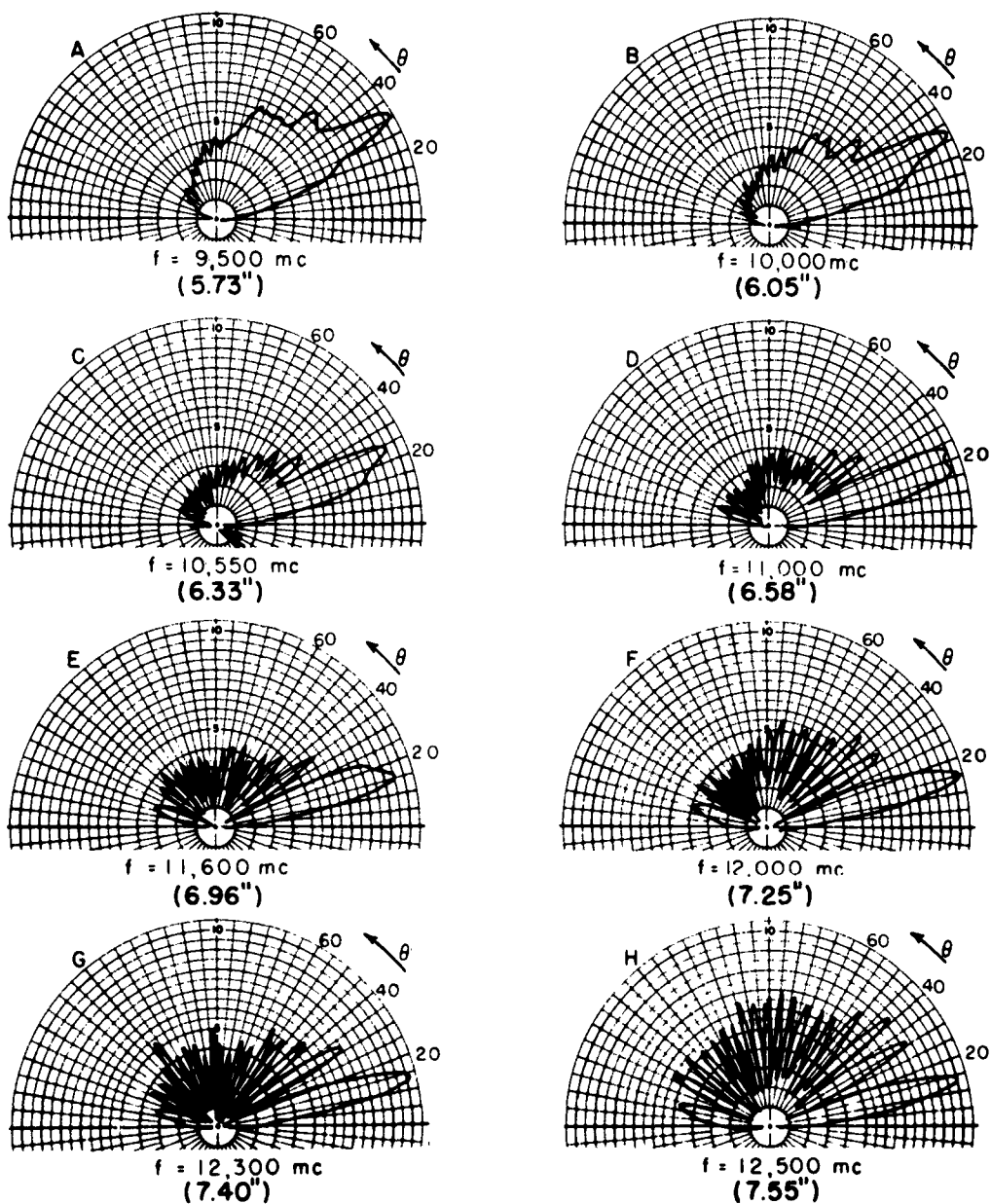
Traveling Wave Slot Antenna
Vertical Plane Radiation Pattern $\phi = 0$ $E_\phi(\theta)$
    Dielectric : Polystyrene
    Aperture : 12 Inch
    Feed   : Probe
    Crown : None
Full Scale Antenna Depth Represented : In Parentheses

Fig. 14. Comparison of radiation pattern shapes
with frequency change.

cavity to produce end-fire radiation and that depth indicated from

measurements where the frequency has been adjusted to produce a

pattern with optimum end-fire pattern.

TABLE 2

Dielectric Filler	Published Relative Dielectric Constant	Frequency for Optimum End-Fire (KMC)	Calculated Depth Eq. (2-38) for 332.0μc (no crown)	Full Scale Depth from Scale Frequency
Polystyrene	2.56	12.3	7.39	7.40
Asphalt	2.56	12.3	7.39	7.40
Salt	5.34	7.4	4.44	4.45
Steatite	5.58	6.6^+ ($^+$with .030" crown)	3.97^+ $^+$Eq. (2-40)	3.94^+ ($^+$with crown)

Ideally, a maximum of radiation from the antenna element

should occur at 3 dgreees elevation. However, because of the sin θ

factor in the expression for the far field radiation pattern (Equation

2-10), the maximum occurs both in the calculated and measured pat-

terns above 13 degrees(Figures 8b and 14g). When operating on the

glide path, the airborne receiver at 3 degrees is working well removed

from the region of maximum radiation. The only absolute criterion for

acceptability is that the signal strength be sufficient to operate

airborne receivers not only at the 3 degree path angle, but at lower angles as well in order to provide the pilot with the information that he is below path. Since the above criterion is satisfied, with no increase in the transmitter power, the radiation pattern shown in Figure 14-G is quite acceptable.

Study of the feed area design was made to minimize the direct radiation from the probe and to effect a better coupling of the energy from the transmission line to the through. Referring to Figure 15, it can be seen that 9db gain is obtained at 15 degrees by using the wave-guide rather than the probe feed. Even so, the waveguide feed was not used in the final design because adequate signal was available from the simpler, less expensive model.

The scale model had 18 inches of ground plane extending in front of the antenna, causing fringing and thus preventing accurate gain measurements from being made at 3 degrees.

Because the brass channel was 12 inches long, (34 feet, full scale) many of the mesurements were made by using the full aperture. Figure 16 indicates a decrease of 2.1 db at 15 degrees when the aperture was reduced to 7 inches (19.4 feet full scale).

The importance of water drainage requires that the maximum practical slope be present at the aperture. To establish data for crown heights, various scale-model crowns were tested, and the results were reduced to graph form and presented in Figure 17.
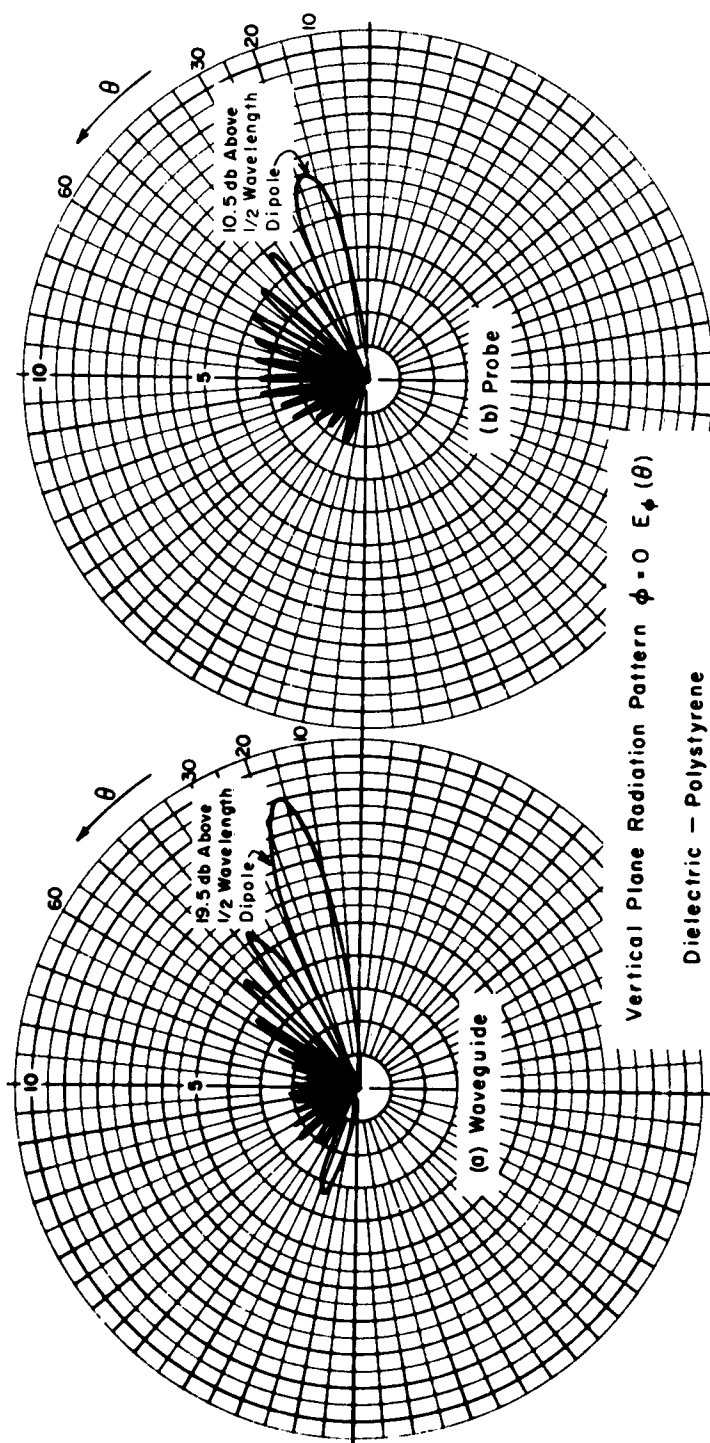
Fig. 15. Comparison of waveguide and probe feeds.

Vertical Plane Radiation Pattern $E_\phi (\theta)$

Dielectric — Polystyrene

Frequency — 11,000 Mc

Crown — 0.0279λ   (1.0 Inch Full Scale)

(a) 12 Inch Aperture

(b) 7 Inch Aperture
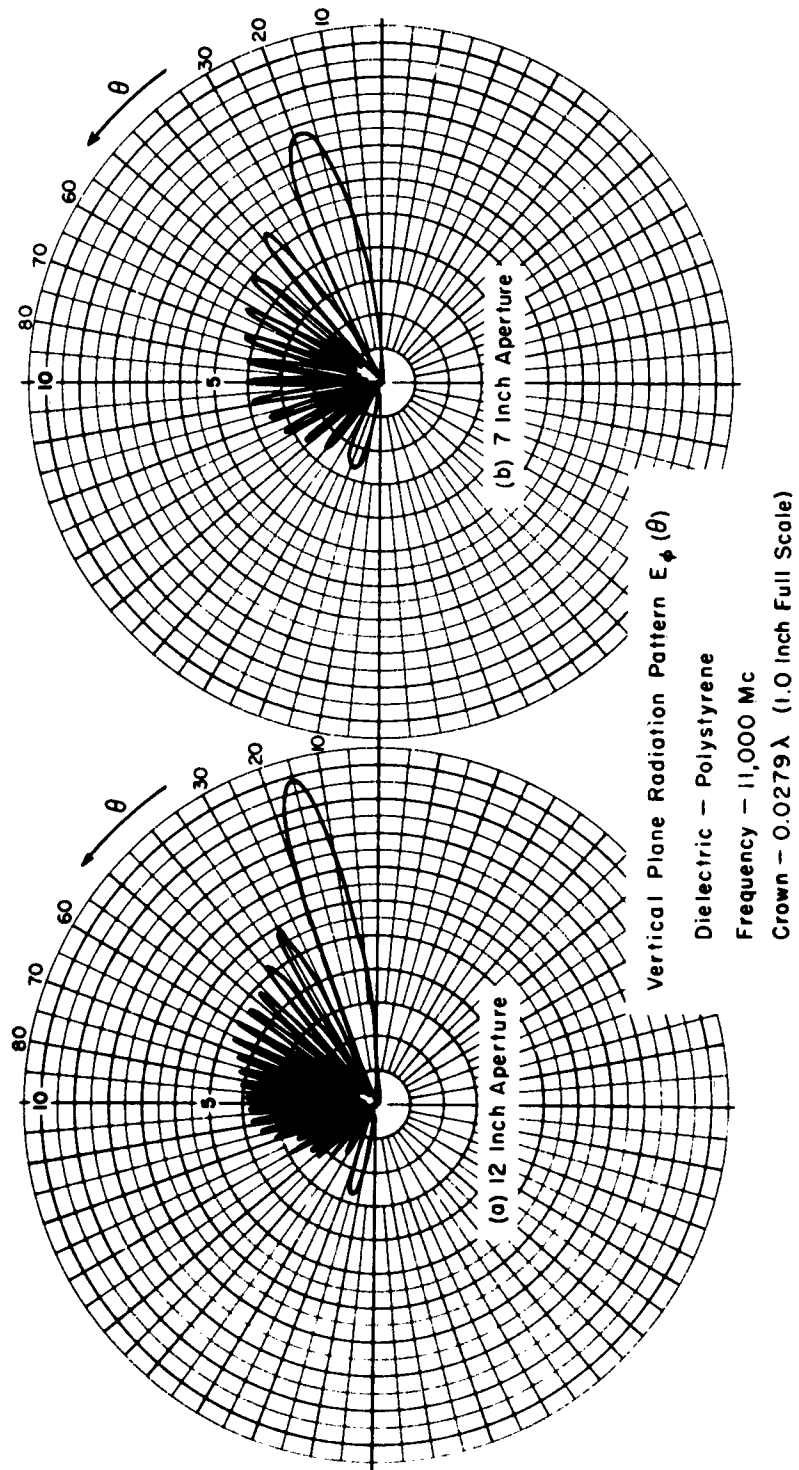
Fig. 16. Effects of a change in aperture length.

For small-crown heights, the depth of the metal cavity may be found

by using the formula

$$d_c = \frac{.26\lambda}{\sqrt{\epsilon_r - 1}} - 0.6 h \qquad (2-40)$$

where d_c is the depth of the metal cavity and h is the crown height.

No deterioration in the radiation pattern is noted between the flat

aperture and one with a simulated 2-inch full-scale crown (Figure 18).
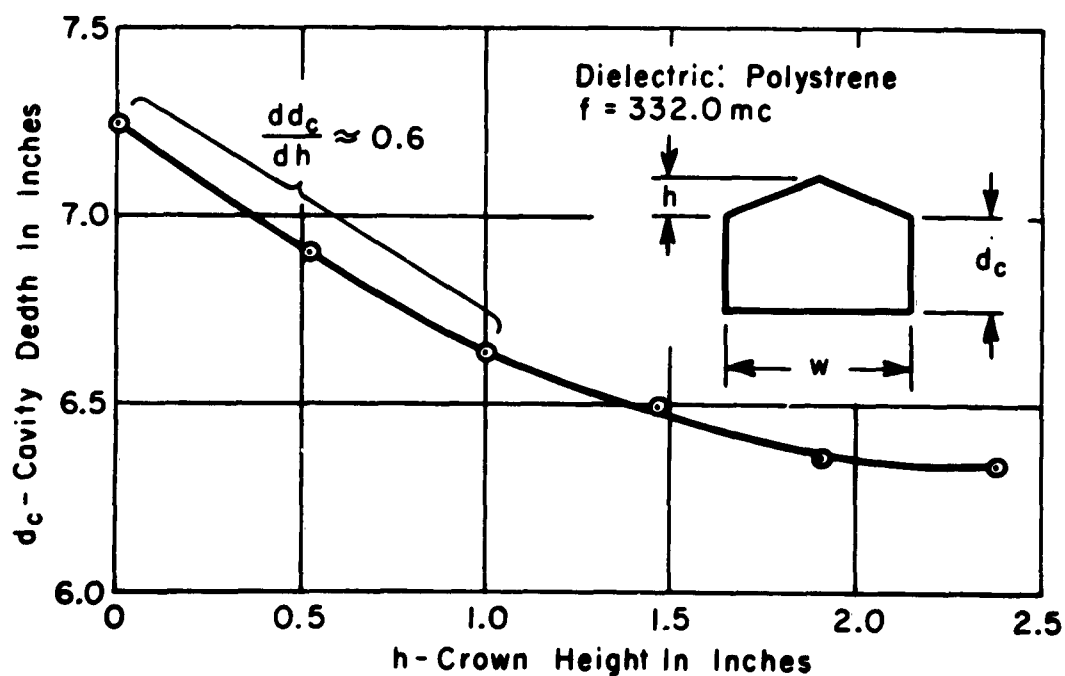
Fig. 17. Required cavity depth for various
crown heights.

The ϕ - component predominates in the far electric field radiated

from a traveling wave structure such as the transverse-electric slot

used as the glide-path antenna. The radiation pattern of a traveling

52

Vertical Plane Radiation Pattern $\phi = 0$ $E_\phi(\theta)$

Dielectric — Polystyrene

Aperture — 12 Inch

Feed — Waveguide

(a) Crown — None
Frequency — 12,300 Mc

(b) Crown — 0.0518 λ
(1.86 Inches Full Scale)

Frequency — 10.2 Mc
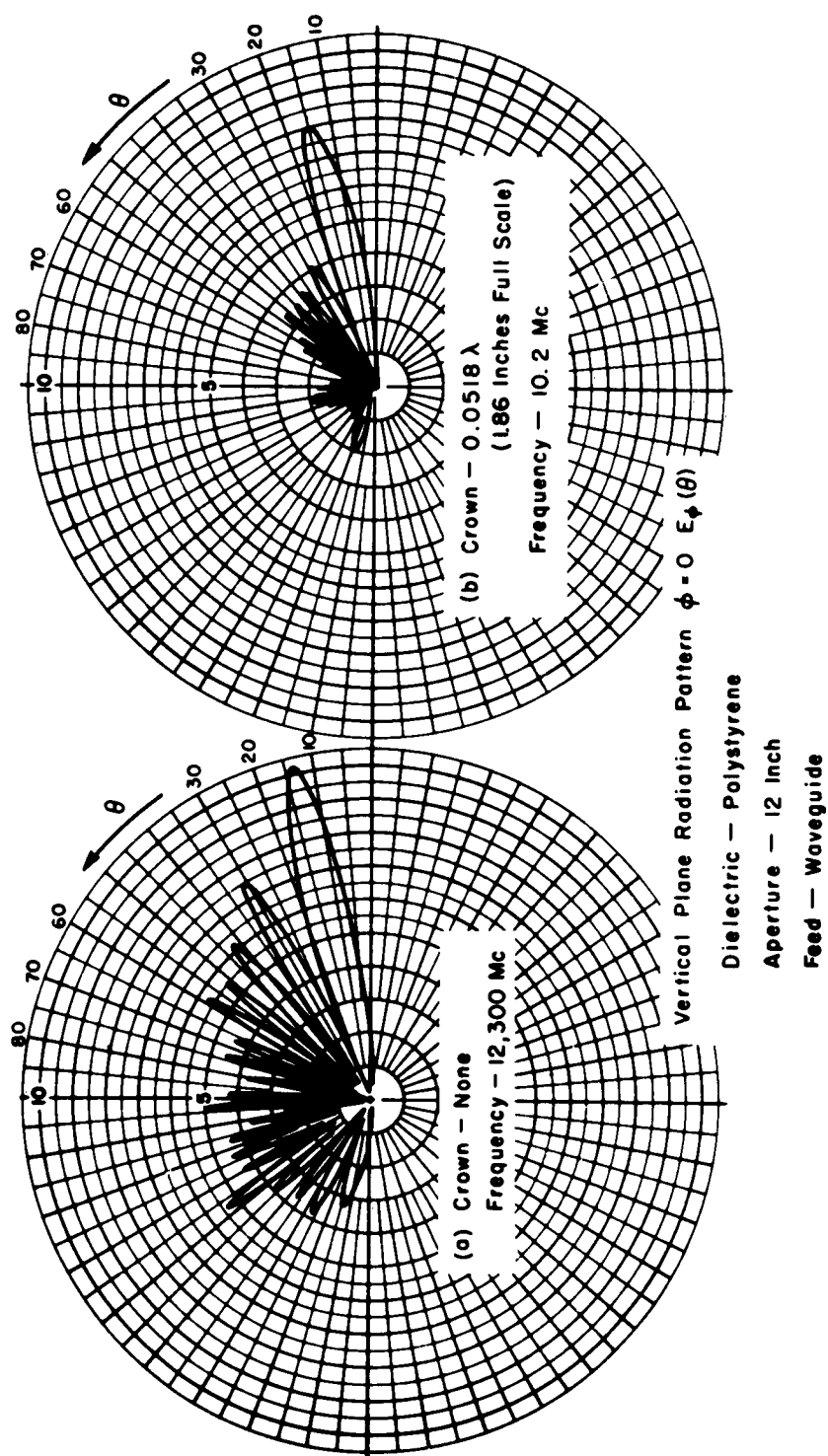
Fig. 18. Comparison of aperture with and without crown.
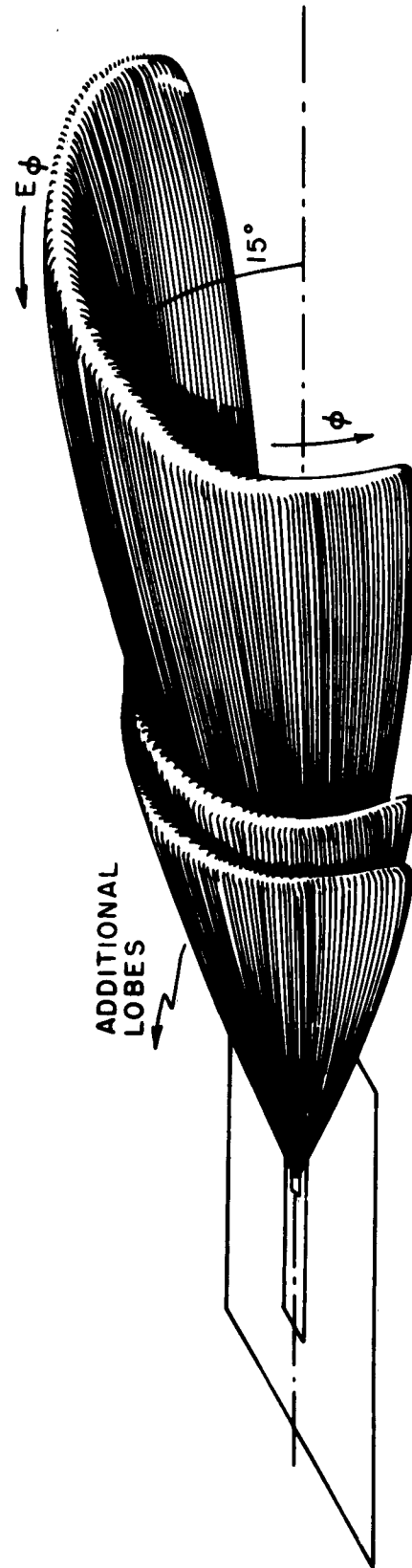
Fig. 19. Three-dimensional view of lobe structure.

wave line source is a figure of revolution about the z-axis when considered in three dimensions. Both model and full-scale antennas tend to be figures of revolution in the upper hemisphere, but depart from this near the horizon because of the presence of the earth or a ground plane (Figure 19).

If the antenna were a pure line source, the lobes would form conical surfaces; however, in practice these surfaces are flattened on top because of the width of the antenna. This flattening desirably increases the region of a horizontally polarized component. From Figure 19 it can be seen that the ϕ - component becomes a vertically polarized component in the yz-plane off the z-axis (runway center line extended). Fortunately this is not a serious disadvantage, since this cone is flattened sufficiently to allow the horizontal component to predominate throughout the region in which the glide path will be used. Figure 20 shows the measured half-power beam width of the horizontally polarized component to be 26 degrees at 3 degrees elevation. No back lobe radiation is observed, since this measurement was taken along a great circle path passing through (r, ϕ, θ) $(r_1, 0, 3^\circ)$, $(r_1, 90, 90)$ and $(r_1, 270, 90)$, and hence was below the ground plane at the $\phi = 180^\circ$ position.

2.6 Full Scale Antenna Measurements

A number of full-scale model antennas designed for 332 mc have been built and tested. Four different dielectric fillers have been used

Great Circle Plane Radiation Pattern $\begin{bmatrix} r,\Phi,\theta \\ r_1,0°,3° \\ r,90°,90° \\ r,270°,90° \end{bmatrix} E_\phi(\phi)$

Dielectric — Polystyrene

Aperture — 12°

Frequency — 12,000 Mc

Crown — None
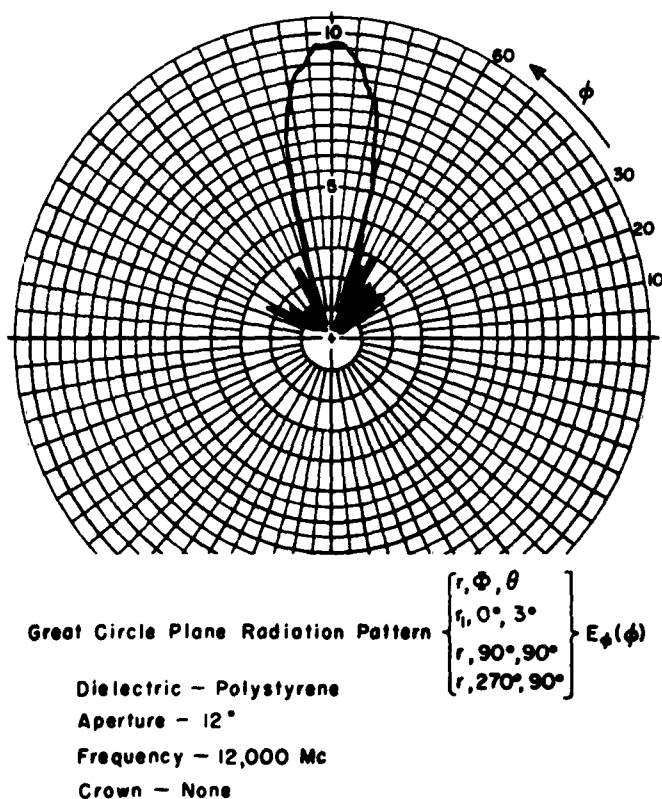
Fig. 20. Pattern indicating quantity of horizontally polarized signal vs ϕ (azimuth).

in various antennas for testing; namely, salt, steatite, asphalt, and polystyrene.

2.61 Dielectric Considerations

The first full-scale model was 20 feet long and used livestock salt blocks for the filler. Salt was used because it was very cheap, research funds were extremely limited, and it made possible worthwhile full-scale tests that could not have been carried out otherwise. A uniform cavity depth of 4.5 inches was calculated from Equation (2-38). The probe entered one-fourth wavelength from one end of

the galvanized-steel trough.   The antenna is shown in Figure 21 .
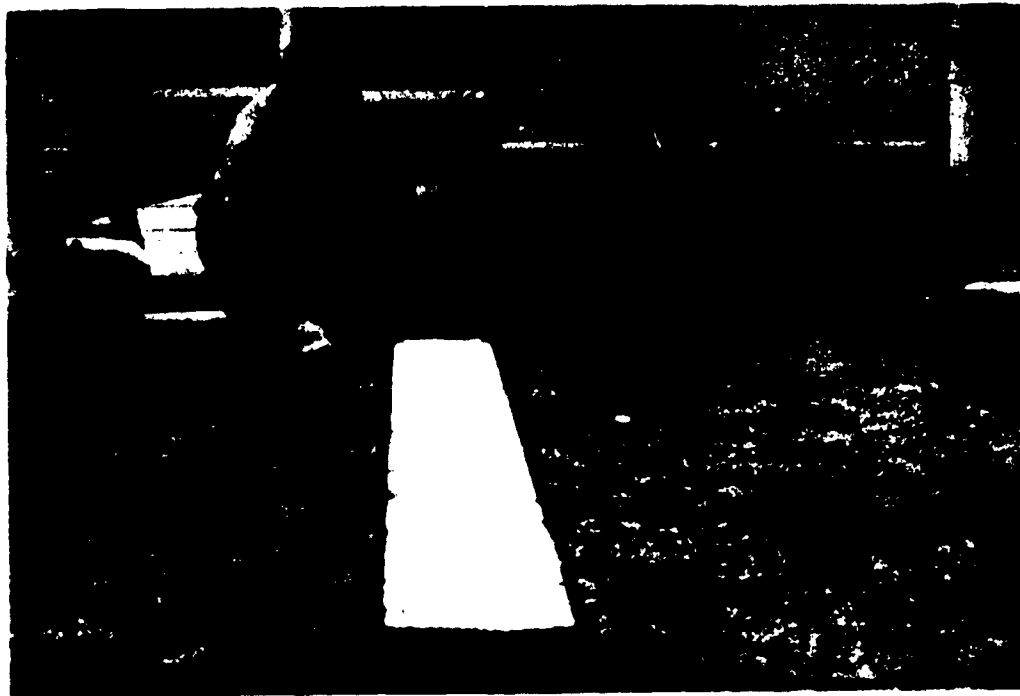
Fig. 21. Photograph of first flush-mounted runway antenna.

Actually dry salt (sodium chloride) is an excellent dielectric from an electrical point of view, but unfortunately it is hygroscopic and soluble in water, so that moisture tends to make the filler a conductor. The initial test results were so good that some effort was devoted to coating and packaging techniques to overcome the moisture problem, but it was felt that the reliability was not adequate.

Next, asphalt was used as a filler for experimental tests because it, too, was cheap and it provided a simple method of studying the effect of adding a crown for water drainage (Figure 22).

Fig. 22. Asphalt filled cavity after crown had fallen due to sun's heating. Dimensions of this cavity were 6.6" x 13.2" x 20'.

Steatite, a ceramic produced by Centralabs, Milwaukee, Wisconsin, was suggested by the Federal Aviation Agency as a material that would not be affected by water and would withstand the tortures of runway operation. This material was obtained in the form of bricks 9" by $4\frac{1}{2}$ "by 1" and placed in a metal trough much as books would be placed on a shelf. In general, this ceramic performed very well even though it was slightly more lossy than salt. However, because it was a fired ceramic, tolerances in production were difficult to hold. It is a most difficult task to cut or change the shape of the blocks after firing. In fact, diamond cutting wheels were the only devices found to be successful in making rough alterations. Because of these limitations, this product was not used for a drainage crown at the aperture. Also, attempts at cementing the bricks together by the FAA brought problems, since suitable cements were lossy and changed the characteristics of the antenna. A close-up view of a block and a filled cavity is shown in Figure 23.

Polystyrene's excellent electrical characteristics were well known through scale-model measurements. Cost of the material in quantity was the chief deterrent to its use in initial tests. Attempts to polymerize the styrene monomer in a mold such as the cavity itself met with little success. Loss of quantities of the material during the polymerization process due to evaporation and the appearance of air bubbles as it was hardening made this method

Fig. 23. FAA steatite #1 stripped of adhesive coating
with a close-up of the steatite blocks.

questionable , especially when quality control was important .

It was learned that one-tenth-inch extruded polystyrene sheets

could be obtained at approximately one-half the price of the styrene

block and these could then be bonded together with a styrene monomer

cement which would introduce no foreign material to the final product.

A sample block was built and found to be good both from electrical

and mechanical considerations (Figure 24). It can be seen that a

crown was machined on the polystyrene block. This was conveniently

done with woodworking equipment. The cross-sectional dimensions

Fig. 24. Sample 5-foot length polystyrene dielectric
filler. The block was sufficiently transparent to
allow the reading of a newspaper through it.

of a block determined from model measurements (Figure 17 or

Equation (2-40)) are 14.6 inches by 7.2 inches, plus a 0.6 inch

crown.

Table 3 is given for comparison of the characteristics of the

various dielectric fillers.

Following in Figure 25 is a view of two cemented steatite

antennas, in shipping crates, a loose steatite-filled cavity with a

radome, and a loose-sheet polystyrene cavity with a radome. The

cross-sectional size increase when polystyrene is used may be

Fig. 25. Antenna test bed at the Ohio State University Airport
(left to right). 1. FAA steatite antenna #1 with epoxy sealer
removed. 2. FAA steatite antenna #2 with epoxy sealer.
(Both #1 and #2 are in uncovered wooden shipping crates.)
3. OSU steatite antenna with loose bricks covered by a 1/16th-
inch thick radome, secured by a rope. 4. Polystyrene prototype
with no crown.

62

TABLE 3

Dielectric	ϵ_r	tan δ	Material cost per antenna. (Dollars)	Effect of moisture	Satisfactory for runway compression?	Actual cavity depth in inches. No crown.
Salt Sodium chloride Morton's Livestock Without Hole	5.34	2×10^{-4}	30	Severe	yes	4.5
Asphalt (Road Quality)	2.56	1.5×10^{-3}	40	None	no	7.3
Steatite Centralabs.	5.5 - 6.5	.001	500	None if cemented	yes	4.5
Polystyrene Kopper's Dylene 8	2.50 - 2.56	2×10^{-4}	550	None	yes	7.3

readily observed. Readings were taken with these antennas above

ground about 10 inches. A 3-db increase in field strength is obtained

because of the elevation.

Of great interest during the first tests was the production of a

50-ohm input impedance and sufficient field strength at low elevation

angles to make this a practical antenna. Because of the finite ground

plane of the scale-model, the gain at 3 degrees elevation was not

accurately known until full-scale tests were conducted.

Impedance tests were made by using the probe as a tuning

device. It was convenient to vary the length of the probe extending

into the cavity and, thereby, obtain a variety of impedances. Figure

26 shows a Smith chart plot of the impedance obtained by using a

Hewlett-Packard 803 R.F. Bridge. It can be seen that one tuning stub

must be added to produce the necessary susceptance for obtaining a

50-ohm input impedance. The desired depth for the probe then to

extend into the cavity is 6.3 inches, giving an impedance of $61/\underline{35}$

ohms with no tuner. A tuner was added to the antennas used in the

glide-path array, and the impedance set at $50/\underline{0}$ ohms. A photograph

of the impedance-measuring equipment is shown in Figure 27.

2.63 Field Strength

Field strength studies and tests were quite important in de-

termining the suitability of the traveling wave runway antenna for

application in a glide path array. Sufficient signal strength must be
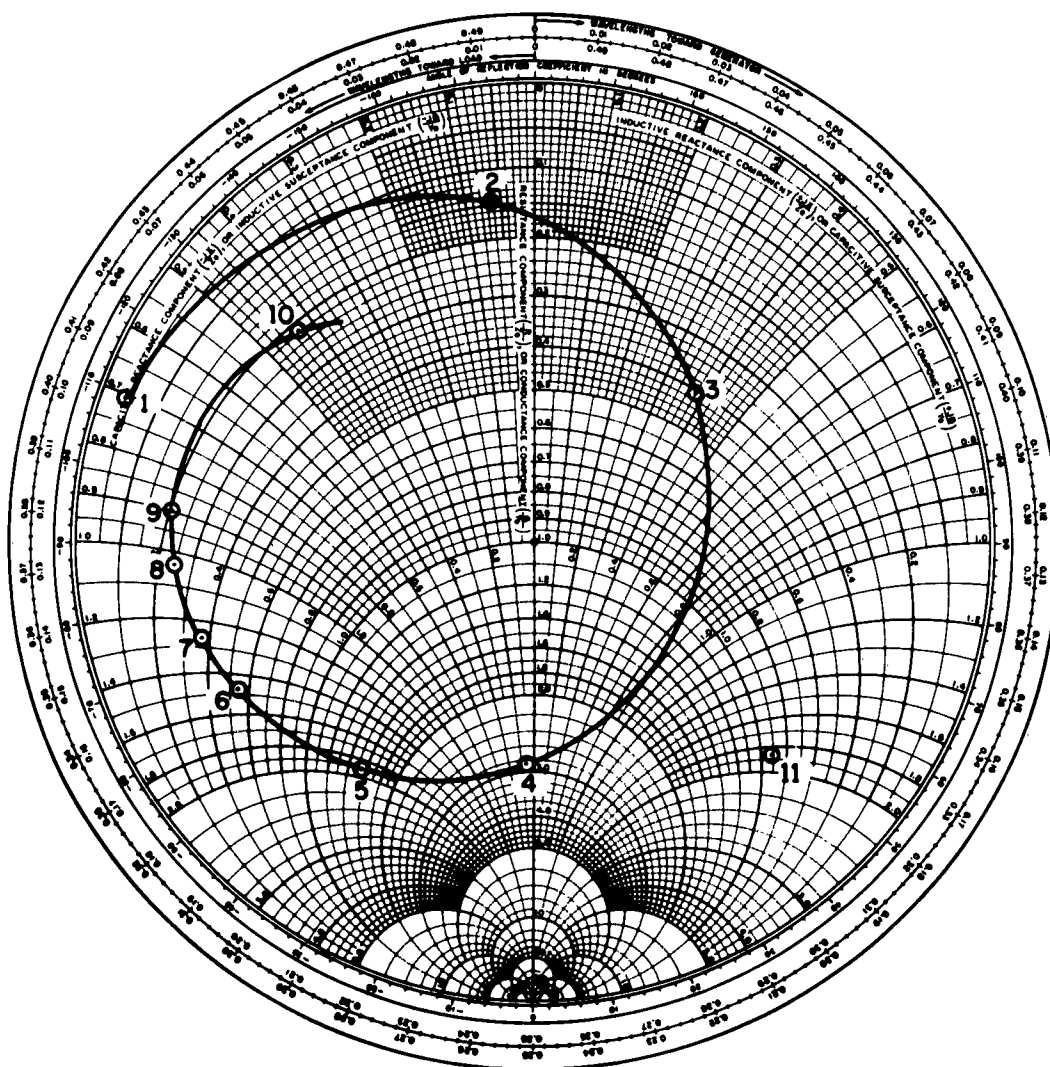
Points		Points	
1	2.00 Inches	6	8.75
2	4.25	7	9.62
3	5.12	8	11.00
4	6.50	9	12.12
5	7.37	10	14.25

Point 11 Admittance Of Point 10
Shorted Tuning Stub Length Calculated 2.80 Inches

Fig. 26. Plot of impedance of runway antenna.

Fig. 27. Measuring the input impedance of a polystyrene array antenna.

present to produce 5 microvolts potential at the airborne receiver terminals when the aircraft is flying 1500 feet above the airport surface and 15 miles from the field. Many factors, of course, enter here, such as the power to the glide path array, gain of the array, gain of the airborne antenna, and loss in the transmission line to the receiver.

For reference purposes we will consider that power of the order of $\frac{1}{2}$ watt will be delivered to each of the two antennas forming the path; the airborne or probe antenna will have a gain of 0 compared to a half wave dipole; and the transmission line is lossless going to the mobile receiver. With these established, all field strength values will be given in microvolts of receiver terminal voltage. Cathode current in the last IF stage of a Collins Radio Co. 51-V glide-path receiver may be used as a convenient measure of receiver input voltage. Absolute calibration is obtained by switching the receiver input to a calibrated signal generator with known output and by adjusting the signal generator to give the same receiver cathode current. In this case a Hewlett-Packard 608-C generator is used. Photographs are shown in Figure 28 .

Field strength readings were taken by ground-based and airborne techniques. With 0.5 watt fed into the polystyrene filled cavity, 8 microvolts were read at 10 miles. Compatibility between ground-based measurements and those made in the airplane was good, as can be seen from Figure 29, and the 1/r relation can be seen to hold
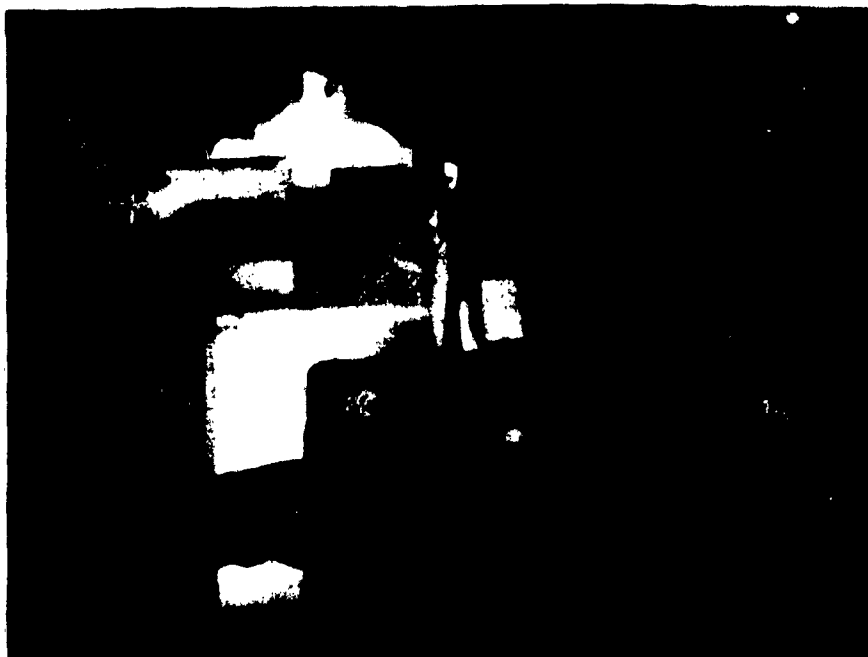
Fig. 28. Mobile probe unit showing the telescoping tower, power unit, and receiving equipment inside. A signal generator with a calibrated output is being used to determine the received signal strength.
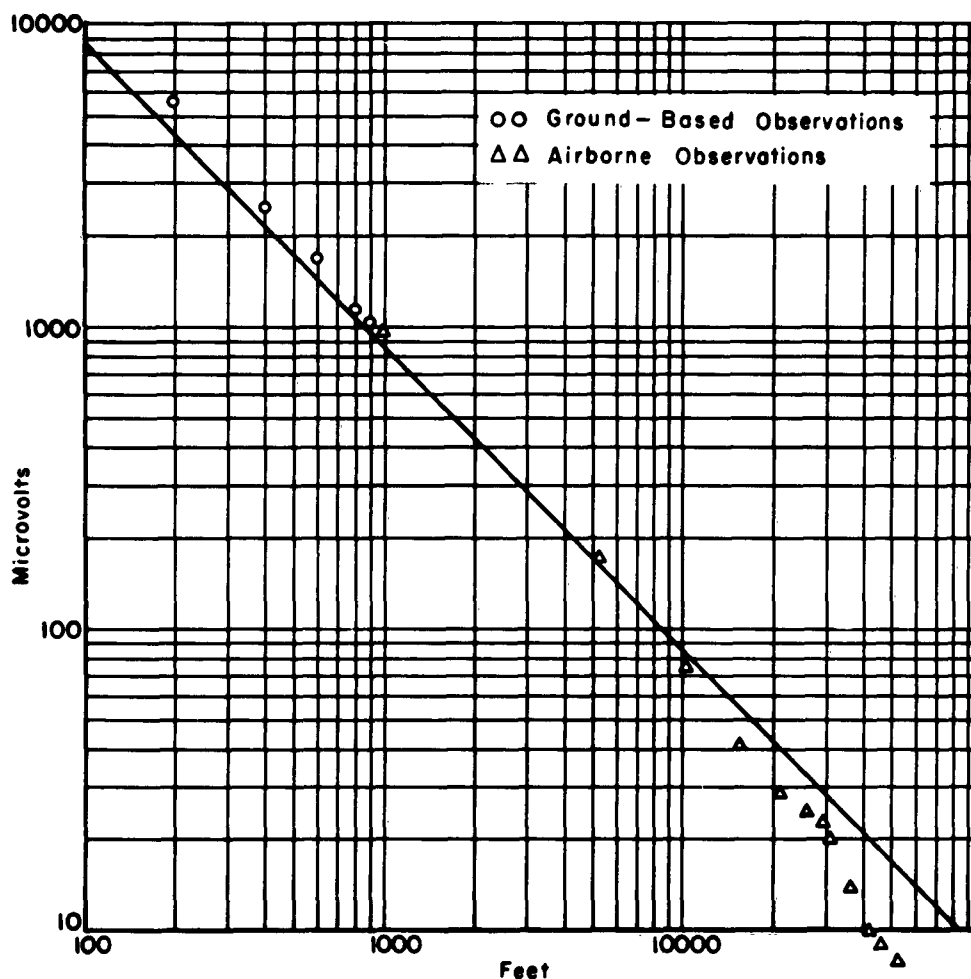
Fig. 29. Field strength at 3° elevation versus distance
(r) for a single runway antenna with reference line 1/r.

rather closely. Readings with the accuracy implied by the graph were

difficult beyond 5 miles and hence may account for the deviation from

the expected straight line.

Readings taken on the back side of the antenna at 3 degrees

showed the back lobe radiation to be down 15.2 db from the front. This

back radiation could be further reduced or virtually eliminated by

putting an absorbing load at the end of the trough opposite the probe,

for it is the reflected energy from the conducting end plate that causes the reverse traveling wave and hence the back radiation. In the frontal region near 3 degrees elevation, the signal from the poly-styrene-filled cavity was 0.5 db below that from a one-half wavelength dipole located one wavelength above ground.[8]

In probing the fields on either side of the antenna axis, the results confirmed that of theory and model measurement as shown in Figures 30 and 31. The conical lobe structure is verified by the comparison of the vertical and horizontal component patterns. Oscillations in the records are interference effects due to direct radiation from the transmitter.

Because the E_ϕ component is of most interest when forming the glide path, measurements of the relative amplitude of this component were made versus elevation, and were plotted in Figure 32. These can be compared directly to calculated values (Figure 8) or scale model values (Figure 15b). The data for Figure 32 were obtained from horizontal probe positions located on a line perpendicular to the ground plane and not on the arc of a circle centered at the antenna. The amplitude error introduced by this procedure when measuring at positions less than 20 degrees elevation is less than 8 per cent and is insignificant when comparing the relative patterns.

[8]A $\frac{1}{2}$-wavelength dipole, with a transformer to produce an impedance of $50\underline{/0^\circ}$ ohms and located 1-wavelength above screened ground, was used as a standard for all gain measurements.
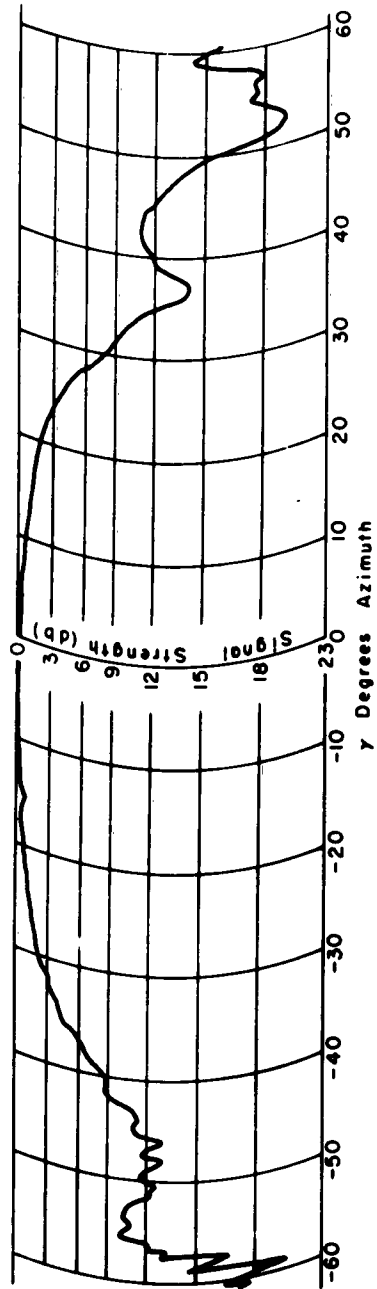
Fig. 30. Horizontally polarized radiation (relative) vs. azimuth
#1 array antenna. Distance: 280 feet. Angle: 3° earth's surface.
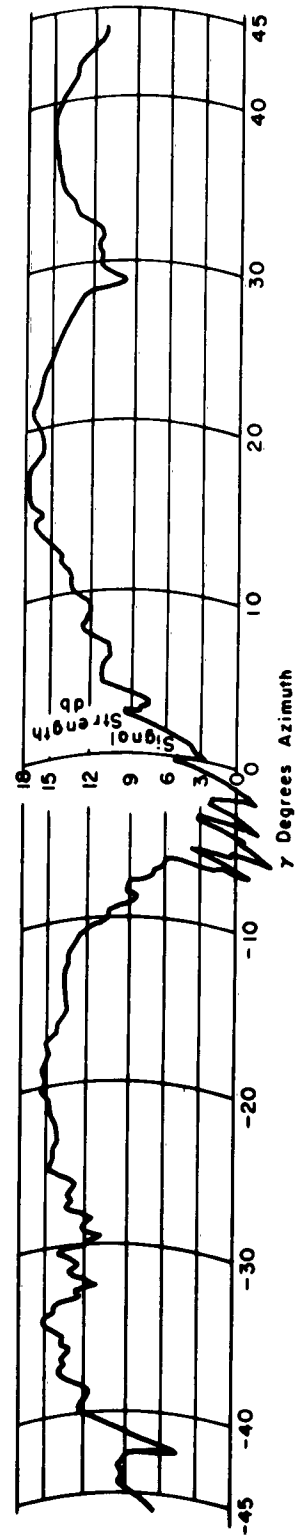
Fig. 31. Vertically polarized radiation (relative) vs azimuth
#1 array antenna. Distance: 280 feet. Angle: 3° earth's surface.

71
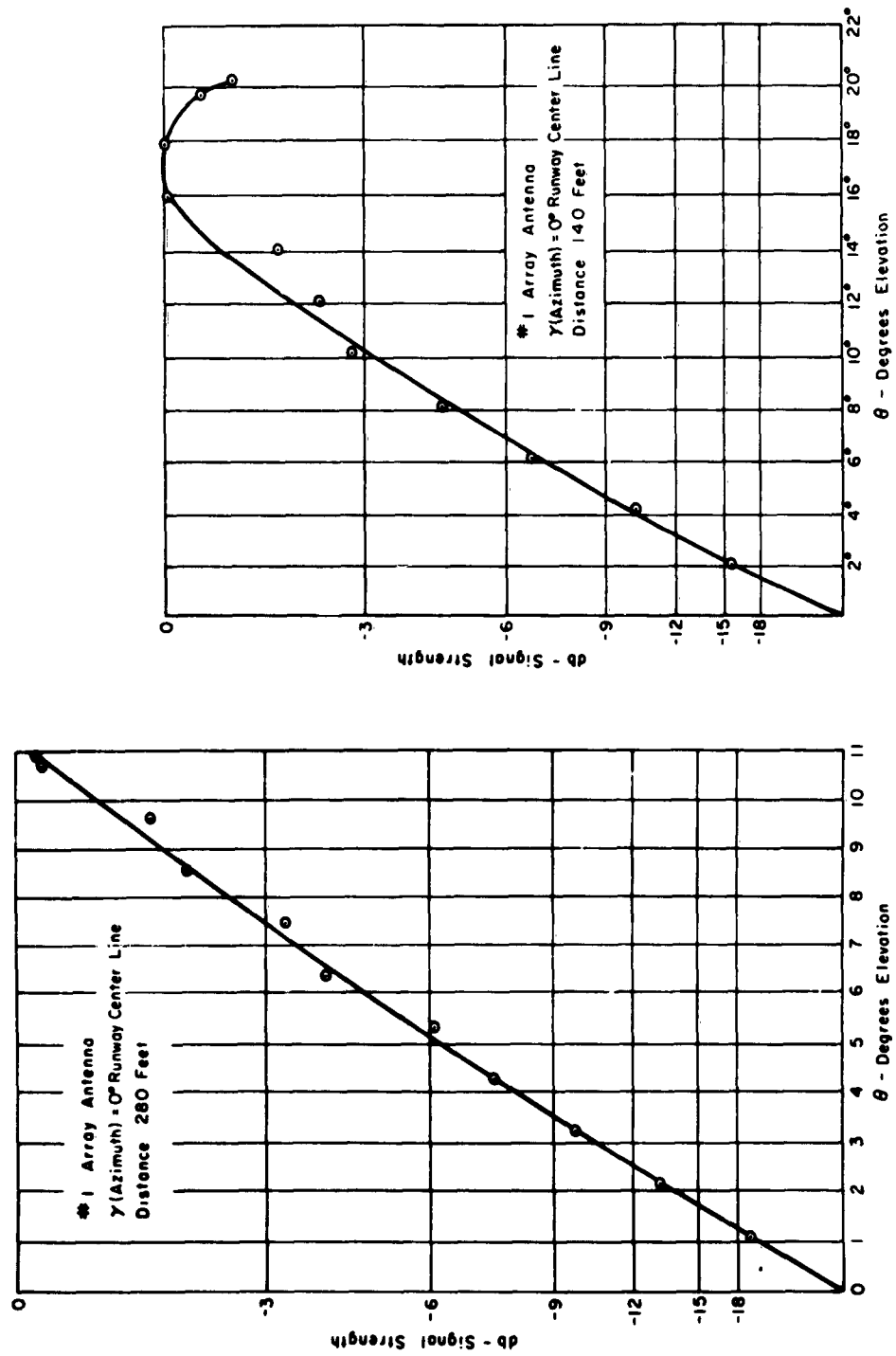
Fig. 32. Signal strength versus elevation.

With the available 50-foot tower to support the probe antenna, it was possible to get above the first beam maximum by taking the measurements 140 feet from the antenna. This position is less than the value prescribed by the usual textbook criterion of

$$R = \frac{2 L^2}{\lambda}$$

where

R is the distance from the source to point of observation,

λ is the wavelength,

L is the length of the source (here 20 feet).

This criterion is established on the basis of a maximum allow-able deviation of 1/16 wavelength in phase across a broadside aperture when an incident spherical wave front originating at a distance R is compared to a plane wave (point source at infinity).

Since the angle of elevation was restricted to 20 degrees or less, the equivalent broadside aperture can conservatively be considered as its projection, 6.9 feet at 20 degrees, with

$$R = 31.5 \text{ feet} .$$

This value was greatly exceeded in all measurements.

In an attempt to exploit fully the possibility of using steatite, two antennas were built by the Federal Aviation Agency for which nominally 1-inch by $4\frac{1}{2}$ - inch by 9   - inch bricks in a $4\frac{1}{2}$ - inch by 9-inch by 20-foot cavity were used. These were shipped to the Ohio

State University test site for evaluation. Both of these cavities had the bricks bonded with an epoxy resin adhesive. In the 20-foot cavity there was a total effective length of resin equaling 7 inches.

Available also was the cavity used previously at the Ohio State University with the salt filler. This was filled with unbonded steatite bricks.

The epoxy adhesive used to bond the steatite degraded the performance of the two antennas by introducing loss. Also, the metal cavity depth originally designed for salt was too deep for the steatite with its higher dielectric constant. This condition caused $\frac{c}{v} > 1$, which reduced the main beam and increased the side lobe level. The low phase velocity was clearly indicated by the low values of guide wavelength (note Table 5). Interestingly enough the third cavity in which there were loose bricks had sufficient air entrapped to effectively lower the average dielectric constant and compensate for its cavity being too deep.

Both FAA antennas had been coated with approximately 1/16 inch of the adhesive for sealing purposes. When this was removed, the signal strength was increased by 4.2 db. Since these cavities were already too deep, the additional dielectric coating effectly made them still deeper and further reduced the field strength in the glide path region. A comparison of these antennas is given in Table 4, with tuning accomplished by varying the probe depth.

TABLE 4

GAIN COMPARISON OF TRAVELING WAVE ANTENNAS

ANTENNA	GAIN IN DB
1/2 Wavelength Dipole 1 Wavelength above ground	Reference 0
OSU Steatite (unbonded)	0
FAA #1 Steatite	- 15.1
FAA #2 Steatite	- 11.8
FAA #1 Adhesive Removed from top	- 10.9

2.64 Determining Phase Velocity

Within limits the direction of maximum radiation from the

traveling-wave antenna is a direct function of phase velocity. Notwith-

standing the fact that a sine θ element factor is present, maximum

radiation near three degrees elevation is obtained by adjusting for the

endfire condition, i.e., $\frac{c}{v} = 1$. It is therefore desirable for optimizing

purposes to have a means of measuring v. In the antennas built for

testing, the termination of the guide was a metal plate which reflected

the energy that had not radiated. Standing waves were formed in the

traveling-wave structure which could be measured easily. This is

analogous to investigation of a standing wave on a lossy transmission

line, the primary loss here due to radiation. Figure 33 shows a graph

of measured values (relative) of voltage along the antenna aperture,

indicating a radiation attenuation of 7.8 db per antenna length and an

average guide wavelength $\lambda g = 35.3$. For endfire operation $\frac{c}{v} = 1$,

and the λg can be seen to be

$$\lambda g = \frac{c}{v} \lambda = \lambda \qquad\qquad (2.41)$$
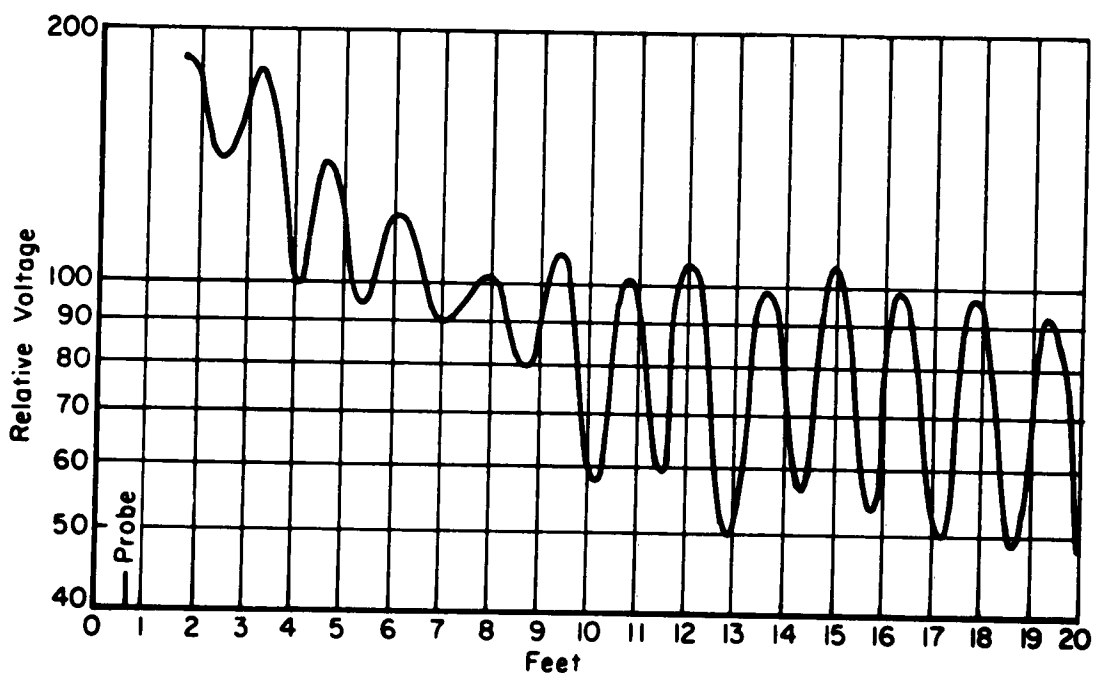
Fig. 33. Relative voltage along antenna aperture.

By measuring the guide wavelength, a value for the relative phase velocity in the cavity can be determined, and thus the angle of maximum radiation can be calculated. Table 5 shows the guide wavelength for a number of antennas that were available for this measurement.

Guide wavelength measurements can be used to determine the effective dielectric constant of the filler material. To obtain such an expression use is made of equation (2-33).

$$(K_{x2})^2 = \omega^2 \mu \epsilon - (K_{z2})^2 \tag{2-42}$$

or

$$\left(\frac{\pi}{2d} \right)^2 = \left(\frac{2 \pi c}{\lambda_o} \right)^2 \frac{1}{c^2} \cdot \epsilon_r - \left(\frac{2 \pi c}{\lambda_o} \right)^2 \frac{1}{v^2} \tag{2-43}$$

then

$$\frac{v}{c} = \frac{1}{\sqrt{\epsilon_r - \left(\frac{\lambda_o}{4d} \right)^2}} \quad . \tag{2-44}$$

This relative phase velocity when adjusted with the same empirical factor of Equation (2-36) becomes

$$\frac{v}{c} = \frac{1}{\sqrt{\epsilon_r - \left(\frac{\lambda_o}{3.83\, d} \right)^2}} \quad . \tag{2-45}$$

The expression for the effective dielectric constant then is

$$\epsilon_r = \left(\frac{c}{v} \right)^2 + \left(\frac{\lambda_o}{3.83\, d} \right)^2 \tag{2-46}$$

TABLE 5

ANTENNA GUIDE WAVELENGTH AND RELATIVE
PHASE VELOCITY

ANTENNA		λ_g at 329.6mc	Relative Phase Velocity
OSU Salt Filled		35.0" (at 331.4mc)	.98
OSU Steatite Filled	Without Radome	34.4"	.96
	With 1/16" Radome	33.7"	.94
FAA #1 Steatite Filled		32.0"	.89
FAA #2 Steatite Filled		32.4"	.90
FAA #1 Adhesive Cover Removed		32.4"	.90
OSU Polystyrene, no crown		35.5"	.99
Glide Path Antenna #1	6.9" Poly with aircrown and radome	36.0"	1.01
	Loose sheet stock with poly crown cap	35.8"	1.00
Glide Path Antenna #2	6.9" Poly with aircrown and radome	35.8"	1.00
	Loose sheet stock with poly crown cap	35.7"	.99
Glide Path Antenna #3	6.9" Poly with aircrown and radome	35.6"	.99
	Loose sheet stock with poly crown cap	35.8"	1.00
Glide Path Antenna #4	6.9" Poly with aircrown and radome	35.8"	1.00
	Solid poly block	35.3"	.98
Glide Path Antenna #5	6.9" Poly with aircrown and radome	35.9"	1.00
	Loose sheet stock with poly crown cap	35.6"	.99

The effects of air in the cavities can clearly be seen for the polystyrene glide-path antennas. In all cases the phase velocity was higher with the air present.

The contract for the manufacture of the five glide-path array antennas was made with the knowledge that there would be air entrapped between the 77 sheets of laminated polystyrene. A polystyrene specimen with air bubbles between sheets was furnished by the contractor and the effective dielectric constant was measured as 2.45 . Unfortunately, the manufacturer was unable to bond the plastic by the technique he used, and consequently the air entrapment pattern was not as planned. One 20-foot block of polystyrene was laid up nearly air-free by the personnel in the machine shop of the Department of Electrical Engineering. By using a squeegee method, the sheets would adhere to the block being built, forming an almost instant bond which required no curing. Table 5 shows #4 antenna which was designed to accommodate the entrapped air to have a slightly lower phase velocity than the other antennas when it is filled with a solid block. This did not prevent the antenna from performing satisfactorily in the array and would indicate that manufacturing tolerances can be reasonable.

A simple experiment was conducted to determine the effects of changing the depth of the dielectric in the cavity. One by one loose polystyrene sheets in the cavity were removed, and the resulting

field strength variations were recorded and are shown in Figure 34 .

The change produced by the removal of one sheet was within the range

of observational error - hence the non-uniform distribution of data

points. Some of the change in field strength must be attributed to the

impedance change and the resulting mismatch, since the cavities

were not retuned after the initial adjustment.
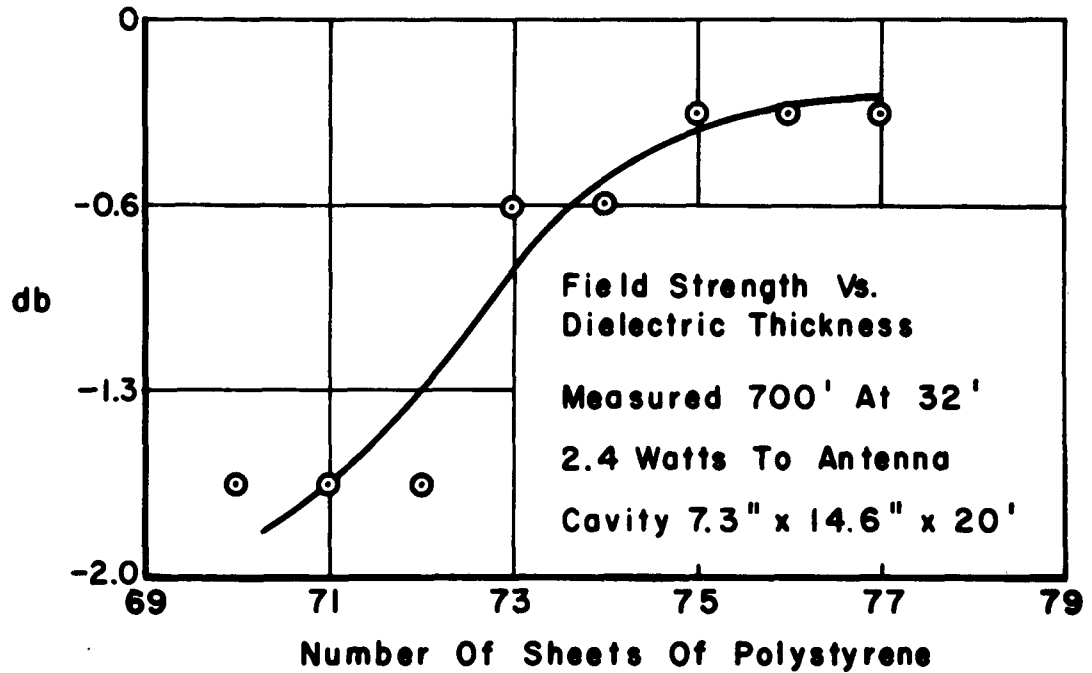
Fig. 34. Measured field strength change with variation
in the thickness of dielectric filler.

The foregoing observations make it apparent that a conservative

manufacturing tolerance could be given as $\pm$ 0.05 inch , but if neces-

sary $\pm$ 0.10 inch would be acceptable.

Table 6 shows calculated values of antenna depths required by

air entrapment or different operating frequencies. The second decimal

place is shown only to illustrate the effects of the numerical change in the dielectric constant, and it is not implied that the accuracy of the required cavity depth is to the nearest one-hundredth of an inch.

The glide-path band is usually considered to be from 329.0 mc to 335.0 mc, with 332.0 mc the mid or design frequency. Operation of the glide-path system at the Ohio State University has been at 329.6 mc by authority of the Federal Communications Commission.

TABLE 6
COMPARISON OF CAVITY DIMENSIONS

Frequency used OSU Test Site	Mid Frequency of Glide Path Band
329.6	332.0
$\lambda = 35.8313$	$\lambda = 35.5729$

$$d_c = d - .6h$$

where

d_c = depth of cavity

$$d = \frac{.26\lambda}{\sqrt{\epsilon_r - 1}} = \text{depth of cavity with no crown}$$

h = height of crown

Values of d in inches are:

	f = 329.6 mc	f = 332.0 mc
No air $\epsilon_r = 2.50$	7.60	7.55
Air bubbles dispersed $\epsilon_r = 2.45$	7.74	7.68

For array cavity f = 332.0

$d_c = 7.22$ h = .6"

$\epsilon_r = 2.5$

THE FLUSH-MOUNTED, FIVE-ELEMENT GLIDE-PATH ARRAY

3.1 Basic Concepts and Requirements

The basic purpose of any instrument landing system glide path is to provide the pilot with vertical guidance during the approach for landing. Essentially, it should provide a planar surface which the airplane may be made to follow. If this path is to be flown all the way to the runway, it is desirable, then, to provide information that will permit the rate of descent of the aircraft to be decreased just above the runway. This is known as "flare out" and is necessary for good landings.

During the early 1930's when completely blind landings were first being tried by pilots, the aircraft was virtually flown into the ground, and the landing gear absorbed the shock. With present high-speed heavy aircraft, the rate of descent is much greater just prior to touchdown, and the gear structures are not designed to take loadings of this kind. For example, a structure was formerly needed that would take 3000 pounds descending at 275 feet per minute, whereas now the requirement may be 200,000 pounds descending at 700 feet per minute.

Intuitively, one would suggest a path with a curve built in approaching the point of touchdown. Technically this could possibly be done by directing a quantity of fly -up signal in the region where the curve is to be present. By carefully adjusting the quantity and shape of the radiation beam, a flare in the path would be produced.

This type of landing path has two significant disadvantages. First, this additional signal would be delicate to maintain and difficult to monitor. Second, aircraft structures are of various sizes and shapes, and the position of the glide-path antenna may vary from 3 to 30 feet above ground when the aircraft would have different points of touchdown and different accompanying rates of descent.

If a straight glide path is present, and if distance measuring is available at the touchdown region, then automatic computations can be made aboard the aircraft so that the height above touchdown is known at every instant. With this information fed to a computer which has a program established for the particular aircraft, pilot, and airport, a custom-built glide path could be indicated to the pilot and autopilot.

Distance measuring equipment is now in operation at many en route navigational facilities throughout the United States. Similar equipment should be suitable for this type of use.

Therefore, the problem at hand is that of producing a straight-line glide path that can be used directly as a reference for either pilot or computer interpretation.

Conventional, above-the-ground dipoles are inappropriate for use in forming a straight-line glide path that must intersect the runway. Any off-the-runway array, as all dipole arrays must be, produces a path curvature near touchdown. This was discussed in Chapter I.

It is proposed here that flush-mounted antennas be used in a horizontal array to provide a straight path directly in to touchdown. Unfortunately, a vertical array is no longer possible, and in using horizontal spacing, a penalty in horizontal path width is incurred if even a two-element array is used. For practical purposes an additional array must be provided for broadening the path in azimuth.

The glide-path antenna array discussed in this paper consists of two flush-mounted antennas which form the basic path, and three additional flush-mounted antennas which form the broadening array. To obtain optimum path width and the vertical thickness required, spacing of the antennas must be as shown in Figure 35. The glide path array axis is coincident with the runway center line. The intersection of this line with the broadening array axis is at a point approximately 1000 feet from the threshold of the runway. Modern airports will have from 4000 to 10,000 feet beyond this point in which the landing roll may be completed.
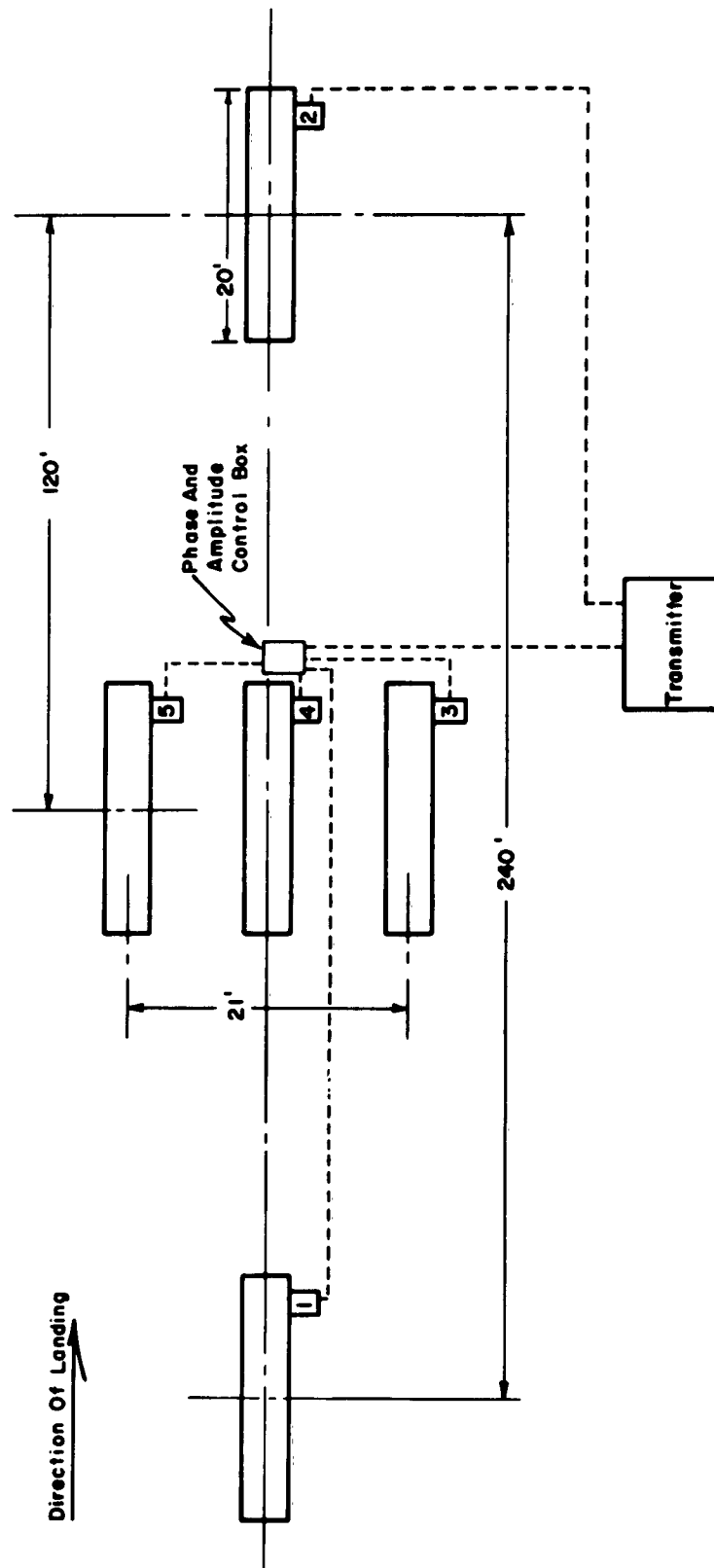
Fig. 35. Plan view of array.

3.2 The Airborne Glide-Path Receiver

To fully appreciate and understand the operation of the glide path it is necessary to be familiar with the airborne presentation and receiving equipment. For flying a glide path to the region of touchdown, special airborne equipment is necessary:

a. Horizontally polarized receiving antenna with transmission line,

b. Sensitive (2μv) ultra-high frequency receiver with associated glide-path detection circuit,

c. Pilot indicator, a $\pm$ 150 microampere meter,

Antennas used for receiving the glide-path signal vary from simple 18-inch dipoles mounted on a supporting shaft to the more elegant flush-mounted cavity found in the nose section of many transport aircraft. These cavities are small broadside radiators manufactured by the Bendix Corporation.

Receivers are of the superheterodyne type, crystal-controlled, and in practice are channelled by tuning the localizer or lateral guidance receiver. The frequencies for the glide path are paired with the VHF channel of the localizer.

Following the second detector of the receiver are two audio pass band filters which are used to separate the 90 and 150 - cycle frequencies present. Following both the 90 and 150-cycle filters, the signal is rectified. The two outputs are fed to a meter which deflects

according to which rectified audio has produced the greater potential.

The glide-path receiver essentially compares the quantities of 90 and 150-cycle modulation and presents a quantitative indication to the pilot. The principle of establishing a glide path, then, is one of establishing a region of rf signal modulated with equal quantities of 90 and 150-cycle audio.

Other methods of forming a glide path are possible, but a system based on a new type of airborne receiver is opposed immediately by the users themselves. Private and corporate-owned equipment, which is valued in the millions of dollars, would be obsolete. Also to be considered would be the time required for such a change-over if it were necessary. Therefore, an important concept in producing a system that will be an advance in the state of the art and can be tried out in flight, is that it be compatible with present airborne glide-path receiving equipment. This compatibility requirement is of great practical significance when a system is proposed for operational use.

Figure 36 shows a block diagram and a photo of an airborne receiver. Given is the relation between the audio voltage ratio and the elevation angle change in degrees. The notation of dots is introduced, since these are the units in which the indicator is calibrated. In Figure 37 is shown a pilot's indicator, which is sometimes called a cross pointed indicator or course deviation indicator
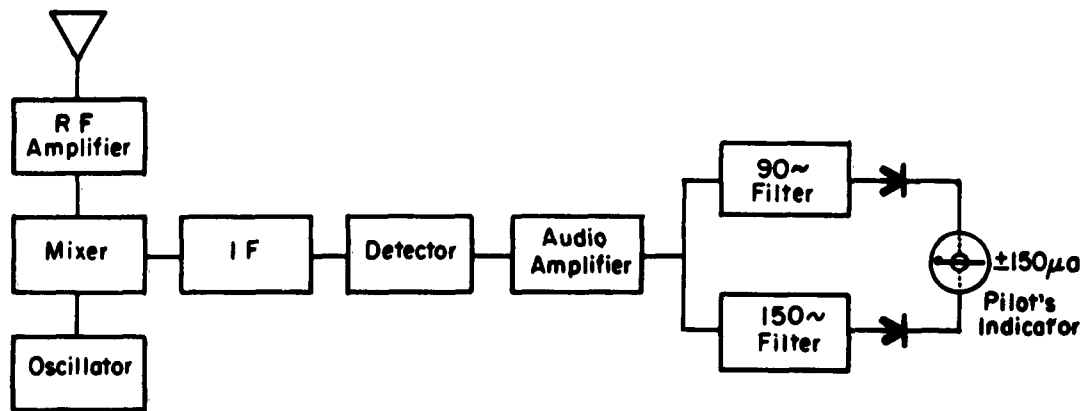
2 db Ratio Of Audio = 77 μa Meter Deflection

150 μa = 5 Dots   (On Indicator)

5 Dots = ~0.7° Change In Elevation Angle = $\frac{1}{2}$ Vertical Paths
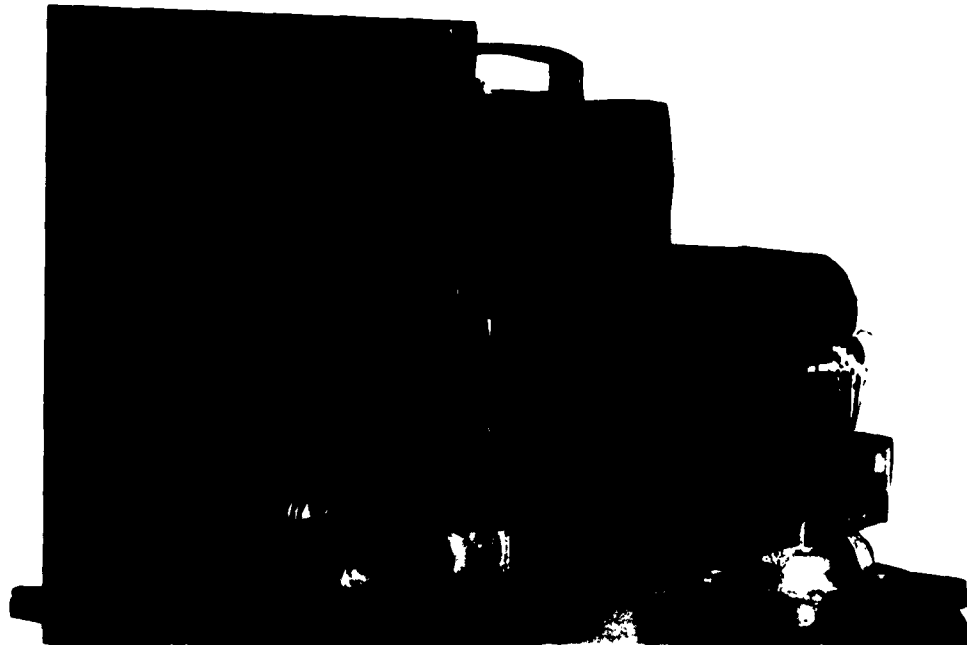
Fig. 36. Block diagram and photograph of an airborne glide-path receiver.
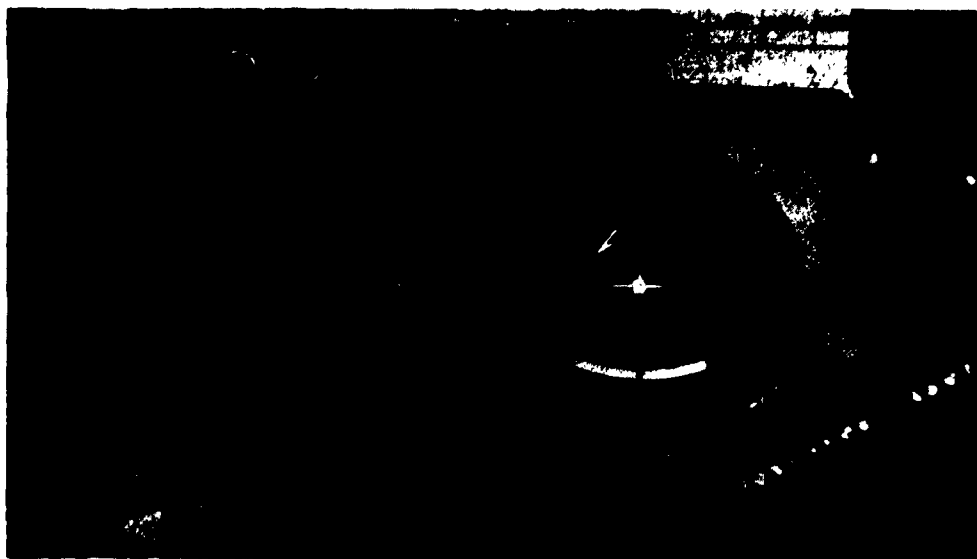
Fig. 37. Illustrated are examples of two types of course deviation indicators. On the left is the ID-387 showing an on-course indication for the glide path (horizontal needle), and a right-of-course indication for the localizer (vertical needle). The ID-48 indicator on the right in this photograph is indicating that the airplane is below the glide path and to the right of the localizer course.

(CDI). Contained in this housing also is another ± 150 micro-ammeter for lateral guidance and two flag meters for both glide path and localizer. These flags fall into view when the carrier signal strength drops below a safe operating level.

3.3 Glide Path Criteria

In considering whether a glide path is satisfactory, a number of points must be assessed. They will be listed here so that the

reader may have in mind, during the following discussion of this flush-mounted five-element glide-path array, the pertinent items relative to the acceptability of this system for actual airport use:

a. Straightness of the glide path,

b. Position and characteristics of false paths,

c. Range and altitude at which sufficient signal is available for full fly-up indication,

d. Adequacy of off-scale indication in the region far below path,

e. Symmetry of path above and below "on-course" as presented to the pilot,

f. Linearity of indication versus elevation angle change,

g. Vertical path width,

h. Horizontal path width,

i. Uniformity of path throughout complete sector,

j. Stability,

k. The system's capability being adequately monitored.

Because the safety of human lives is at stake in the satisfactory operation of aeronautical navigational aids, the maximum in reliability and dependability is demanded. When a question affecting safety is involved, it is resolved conservatively, allowing an ample saftey factor for the unknown or near-impossible cases. A basic premise is that it is better to have no radio aid than to have one which is faulty. This

is the philosophy used in establishing and maintaining radio facilities. To this end is directed the whole monitoring concept, which detects path angle and path width in the case of the glide path. Should these not be as required, an alarm is sounded to radio operators who notify pilots. The equipment is automatically shut down until the fault is corrected.

3.4 Theory of the Flush-Mounted, Glide-Path Array

The theory of the elemental glide path that uses two antennas will first be discussed. This information will then serve as background for a presentation of the theory for the complete 5-element system. The additional three elements, as has been stated, are present solely for the purpose of broadening the path in azimuth.

3.41 The Elemental Array

Consider an rf generator whose output is equally divided into two channels, one of which is amplitude modulated at 90 cps, and the other at 150 cps. In practice the power division is accomplished by using a bridge, and the modulation, by paddle wheels turning within two separate cavities through which the energies must pass on the way to the antennas. Since the paddle-wheel shaft is driven at 1800 rpm by a synchronous motor, the modulating wheels located on opposite ends of this shaft have 3 and 5 paddle elements for the 90 and 150-cycle modulations, respectively. In this way the modulation envelopes maintain a constant phase relation with each other

or, in other words, the side band components produced by the modulation have a fixed angle between their respective resultants. Figure 38 shows the part of the circuit involving the generation of the carrier and side bands.

$$\frac{m}{2}E\sin 2\pi(f_c+90)t \qquad \frac{m}{2}E\sin 2\pi(f_c-90)t$$

$$E\sin 2\pi f_c t$$

$$\frac{m}{2}E\sin 2\pi(f_c+150)t \qquad \frac{m}{2}E\sin 2\pi(f_c-150)t$$

$$E\sin 2\pi f_c t$$

RF Gen — Cross Modulation Bridge — 90~ — Motor — 150~
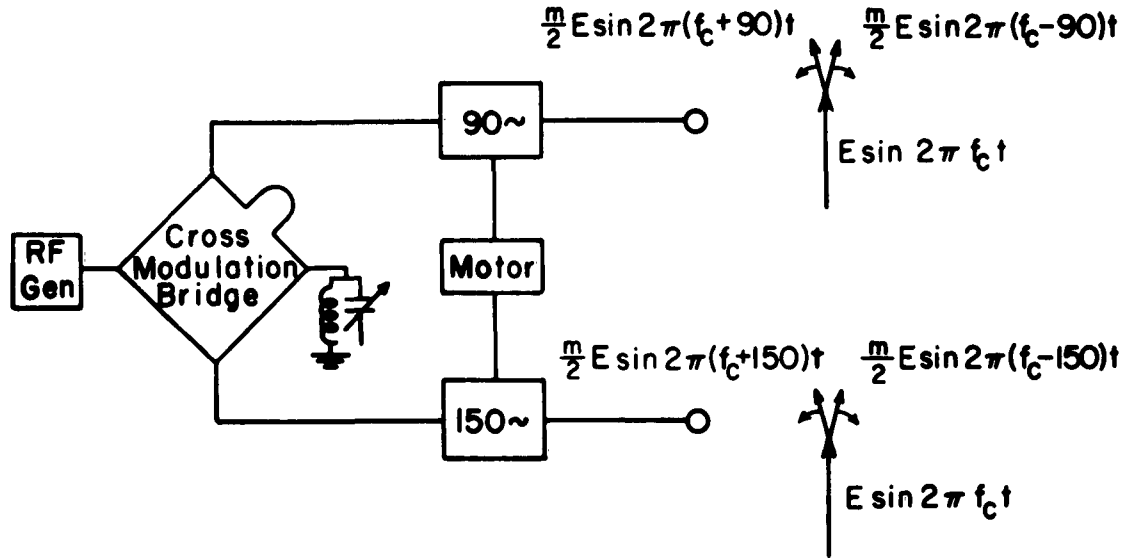
Fig. 38. TUS generator and modulator diagrams.

From the modulator units the 90 and 150-cycle modulated rf is recombined by using a bridge whose arm lengths are so arranged that at one output of the bridge only side band energy is present, while at the other all five frequencies are present.

To these output terminals are normally connected the transmission lines going to the antennas of the null reference system. However, for use with a directional glide path, i.e., one with carrier radiating from all antennas, an additional bridge is used.

Figure 39 indicates how the relative phase of the five frequencies is adjusted to obtain, at the antennas, signals of equal magnitude, but with the 90-cycle sideband phase reference advanced 90 electrical degrees over the 150 cycle for the forward or #1 antenna. The 150 cycle is advanced 90 degrees over the 90 cycle for the rear antenna excitation (see Figure 39). The line stretcher in the line to the rear antenna is adjusted so that the carriers from the two antennas will arrive in phase in space at the path angle, usually 3 degrees.

This bridge arrangement is not unique. However, it is the most satisfactory and convenient because of the availability of the present glide-path transmitter and the problem of maintaining proper impedances in a system that is as critical as one in which the transmitter uses the paddle wheel modulators. An alternate bridge arrangement which is simpler from a circuit standpoint is the one shown in Figure 40.

Consider two point sources spaced 240 feet apart (28,936 electrical degrees at 329.6 mc). Let the phase of the one element be delayed 96 degrees with respect to the other; then the calculated resultant relative radiation pattern for the first 20° elevation is as shown in Figure 41. According to the principle of pattern multiplication, the pattern of the traveling wave antenna element (Figure 8) will be multiplied by the one shown in Figure 41 to produce the glide path pattern with the first maximum corresponding to the glide path.

LEGEND:

CONVENTION: PHASE ADVANCE

$$\text{LET} \begin{cases} \frac{m}{2} E \sin 2\pi(f_c + 90)t \ \text{\&} \ \frac{m}{2} E \sin 2\pi(f_c - 90)t \\ \frac{m}{2} E \sin 2\pi(f_c + 150)t \ \text{\&} \ \frac{m}{2} E \sin 2\pi(f_c - 150)t \\ E \sin 2\pi f_c t \end{cases}$$

BE REPRESENTED BY

C + 90
C + 150

C ± 90
C ± 150

C ± 90
C ± 150

FROM MODULATORS

A

B

0.15 λ

0.65 λ

0.15 λ

0.15 λ

λ/4

λ/2

c ± 150
c + 90

c ± 90

c ± 150
c + 90

c ± 150

c ± 90

C ± 90
C ± 150
C

C + 90
C + 150
C

c ± 90
c ± 150

C + 90
C ± 150 = C + 90
C ± 150

C + 90
C ± 150 = C + 150
C + 90

C ± 150

LINE STRETCHER
TO SET PATH ANGLE

No. 1 ANTENNA AND BROADENING ARRAY

No. 2 ANTENNA

Fig. 39. Method used to obtain proper excitation of directional glide-path antennas.

Maxima at higher angles represent false paths, and the nulls appear

as inverted glide paths with carrier cancellation.
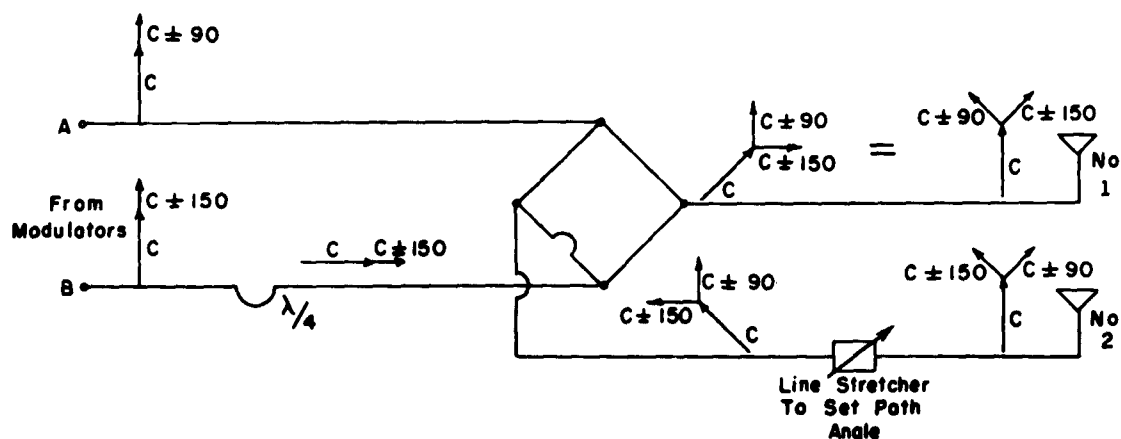
Fig. 40. Alternate bridge arrangement.

By inspecting the phasor representations shown at the antennas

in Figure 39, one can observe that when the two carriers are in

phase, i.e., a maximum in the radiation, there will be equal quanti-

ties of 90 and 150-cycle sidebands present. If the forward antenna is

used as reference and the point of observation is moved above the

angle, where the in-phase condition occurs, the phasors from the

rear antenna will rotate or advance, thus causing some of the 150-

cycle sideband energy to be canceled, and the 90 cycle to be in-

creased. By recalling the operation of the glide path receiver, this

will appear as a predominance of 90-cycle audio after detection, thus
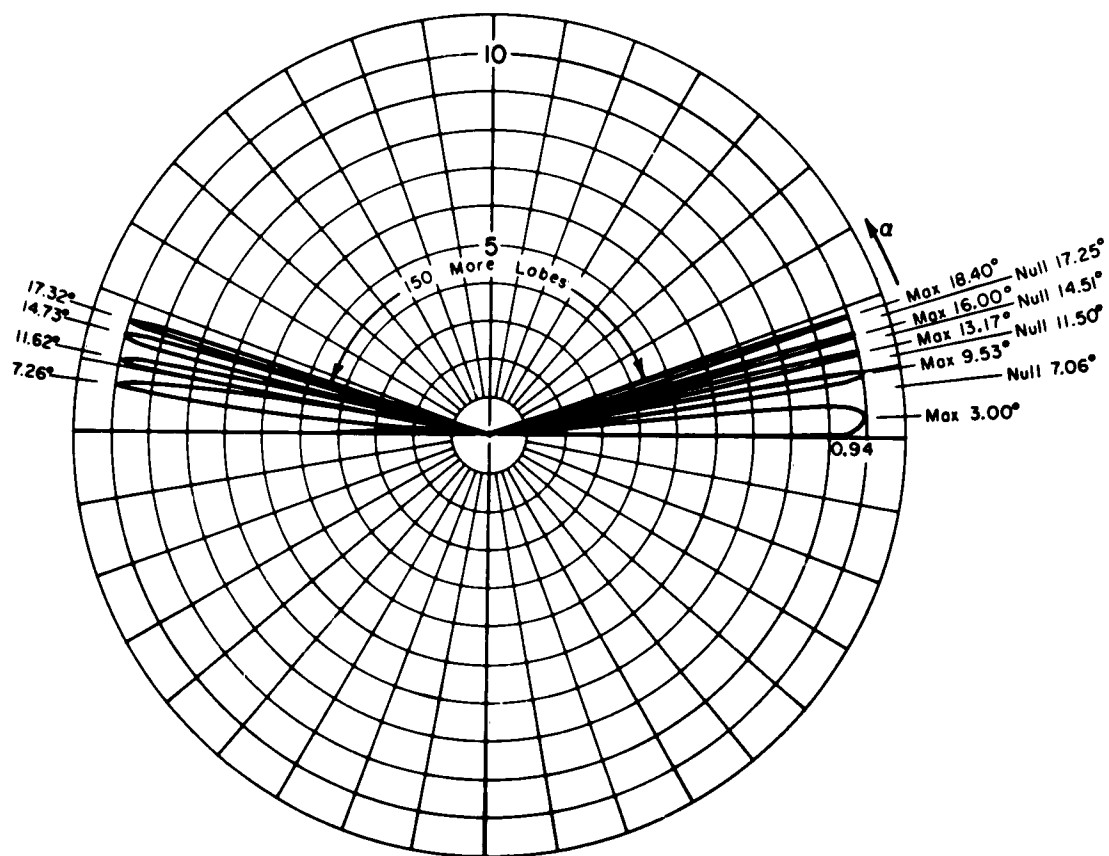
Fig. 41. Array pattern for 240-foot spacing of sources.

causing the pointer to deflect downward. This is the indication for the above path. The pilot's response is then one of flying toward the needle. The opposite indication is observed below the angle of in-phase condition. The 150-cycle sidebands will add; the 90-cycle sidebands will subtract; and the result will be a larger 150-cycle audio voltage in the receiver. This can be seen from Figure 42.
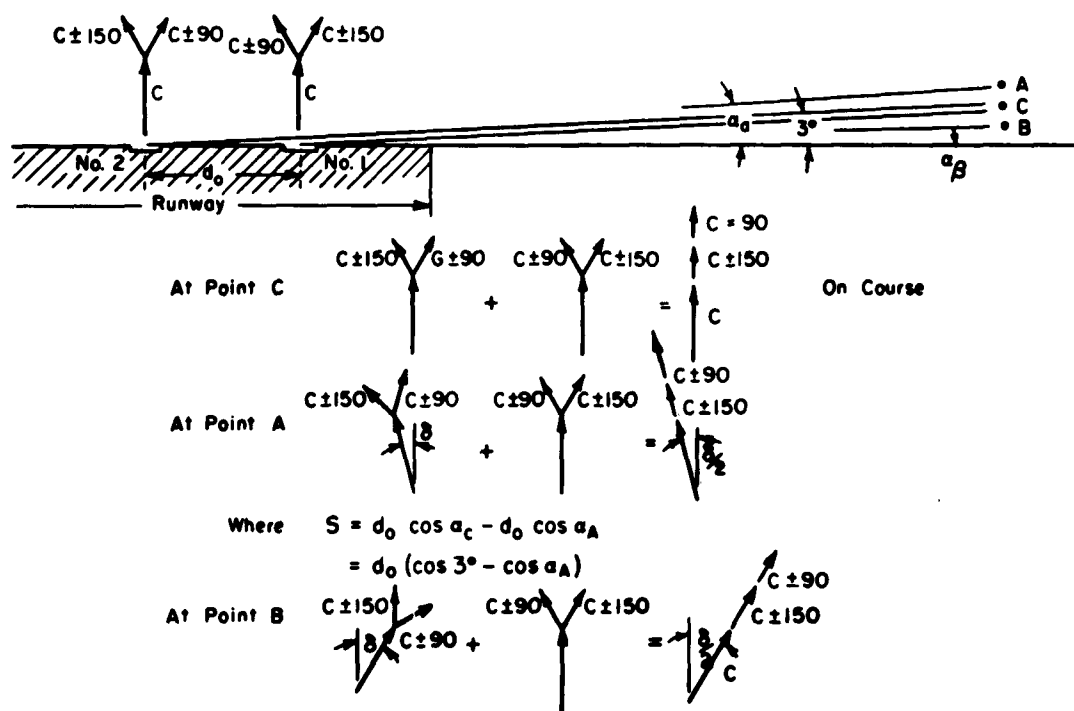
Fig. 42. Phasor addition to produce conditions of above-path, on-course, and below-path.

Experience has shown that a desirable vertical thickness of a glide path is on the order of 1.4 degrees. This is the change in elevation angle required to change the indication from full-scale fly up to full-scale fly down.

The glide path would indeed be hard to fly should the path converge to a point when approaching the antennas. A flight deviation of a few inches near the antenna because of turbulence or pilot ability would be expected to produce off-scale deflection on the course deviation indicator. Two factors tend to minimize this. First, the receiver is designed so that the path is softened through the AVC as the signal strength increases. Second, as the array is approached the distance to the #1 antennas becomes significantly different from the distance to #2. The greater magnitude of the signal from #1 antenna tends to soften the path. Because of these two effects, the path converges to a thickness of approximately 25 feet near the runway threshold. From this region to the array, the thickness remains essentially constant. Figure 43 shows the close-in path structure. It is observed that the on-course signal is omnipresent in the immediate vicinity of the #1 antenna.

When considering flyability it is desirable that the path be symmetrical and linear about the on-course signal. Because trigonometric functions are usually involved, linearity is only approached, but this does not seriously affect the acceptability of this system.
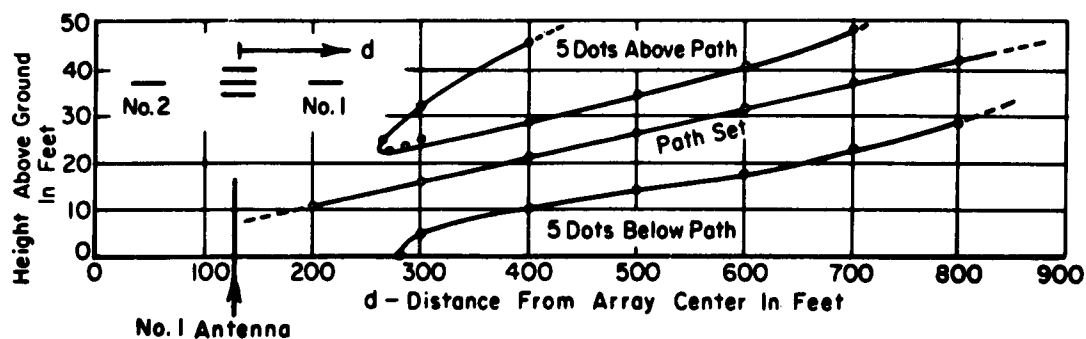
Fig. 43. Close-in glide-path structure.

Although this system does not possess the nearly linear character-
istic of the null reference, no pilot without the recording test equip-
ment would know the difference. For the case of the test system here
discussed, the electrical phase shift δ is given by

$$\delta = d_0 (\cos \alpha_c - \cos \alpha) \qquad (3-1)$$

thus

$$\delta_1 = d_0 (\cos \alpha_c - \cos \alpha_a) \qquad (3-2)$$

$$\delta_2 = d_0 (\cos \alpha_b - \cos \alpha_c) \qquad (3-3)$$

where

δ_1 is phase shift obtained moving 0.7° above path

δ_2 is phase shift obtained moving 0.7° below path

d_0 = spacing between #1 and #2 antennas. Here it is $28,936^\circ$.

α_c = path angle = 3.0° (see Figures 42 and 44)

α_a = above path limit 3.7^O

α_b = below path limit 2.3^O.

Then

$$\delta_1 = 20.55^O \qquad (3\text{-}4)$$

and

$$\delta_2 = 16.22^O. \qquad (3\text{-}5)$$

Fig. 44. Definition of angles used in glide path discussions.

A graph of δ versus α (calculated) is shown in Figure 45.

In Figure 46 is shown the CDI deflection measured with changes in elevation. Following in Figure 47 is a graph of measured Course Deviation Indicator (CDI) deflection versus electrical phase shift here obtained by varying the line length to #2 antenna. Combining these two graphs gives Figure 48, relating the measured

electrical phase shift and elevation angle. This can be compared

directly with the calculated curve in Figure 45. It can be seen that

the glide path in the region of interest is essentially linear and gives

a sensitive indication with correct sensing.

When considering path irregularities, plus or minus one-fifth

full-scale deflection, is generally accepted as the tolerance limit

for an operational glide-path system.
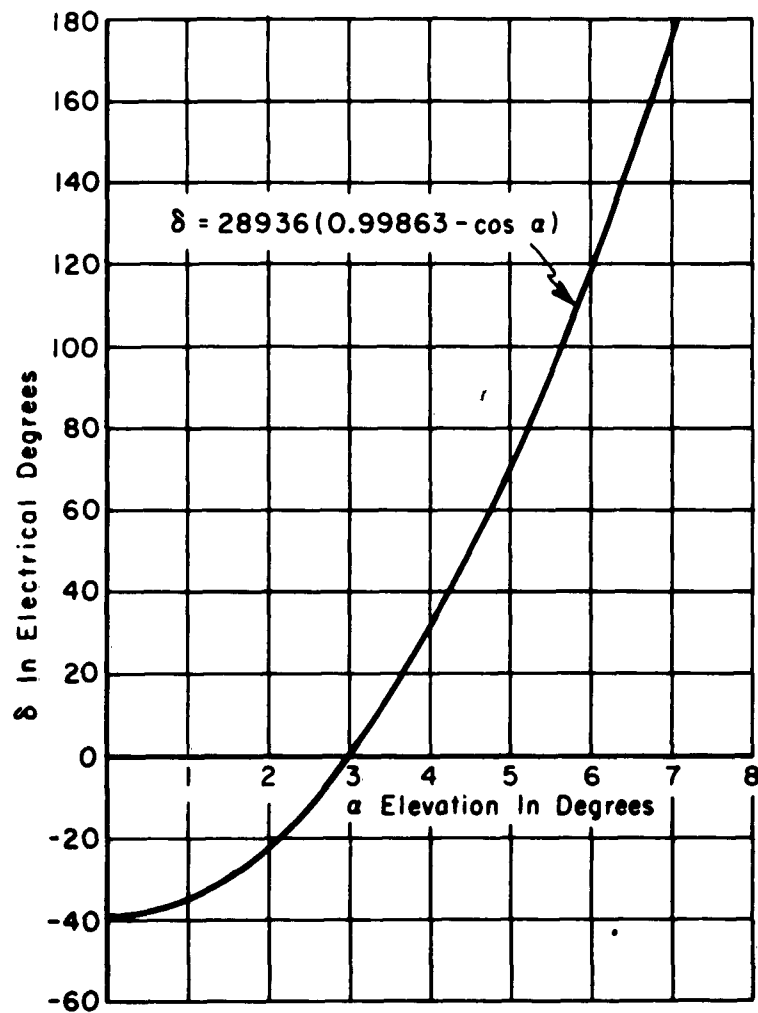
Fig. 45. Calculated electrical phase shift obtained
with change in elevation.
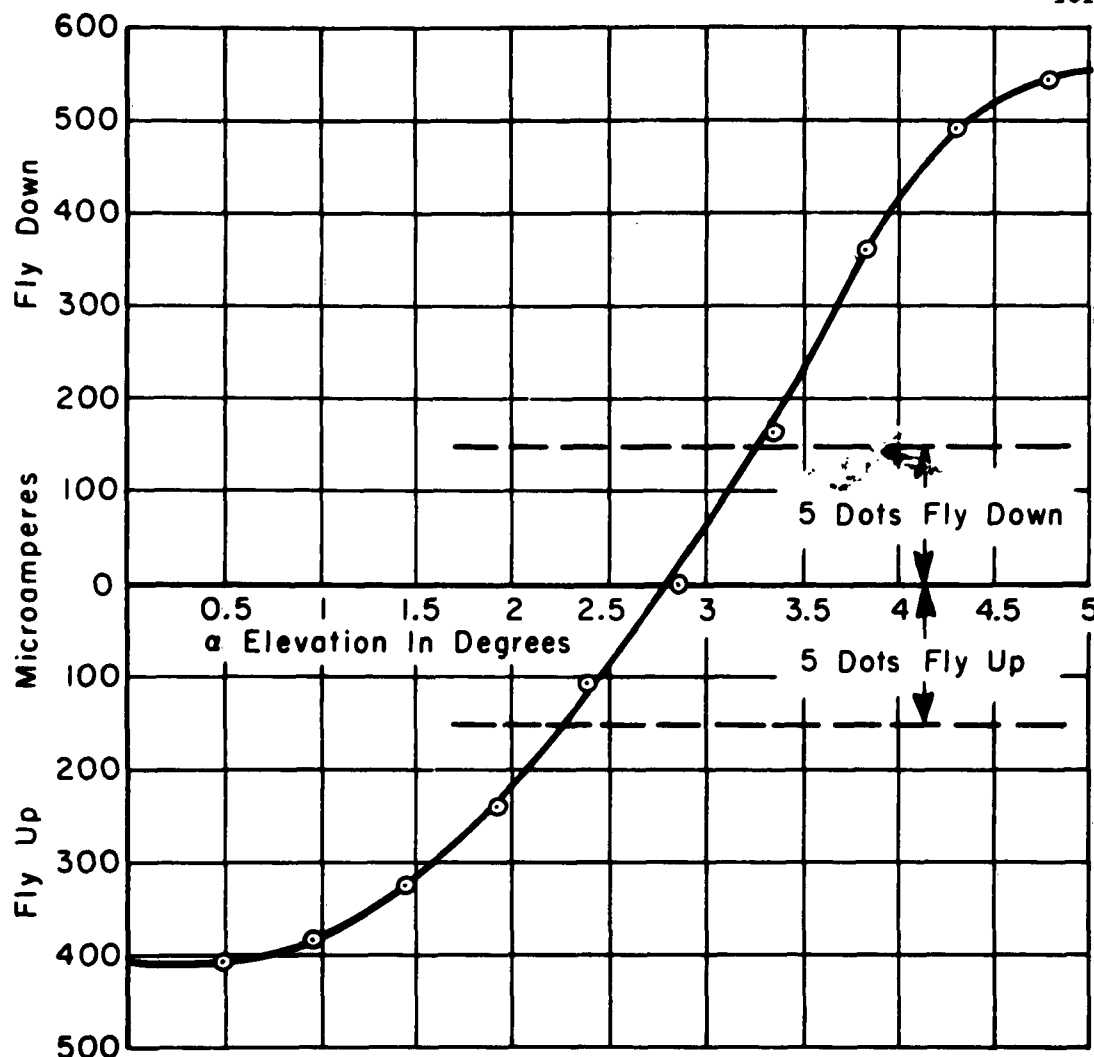
Fig. 46. Indicator deflection versus elevation.

Inasmuch as fewer electrical degrees phase shift was obtained when going below path, a smaller difference in audio voltages will appear when going below path. The angle α represents the desired glide-path elevation angle only on the center line of the runway ($\gamma = 0$). Observation of Figure 44 shows that the locus of constant α describes a conical surface whose vertex angle is 2α .
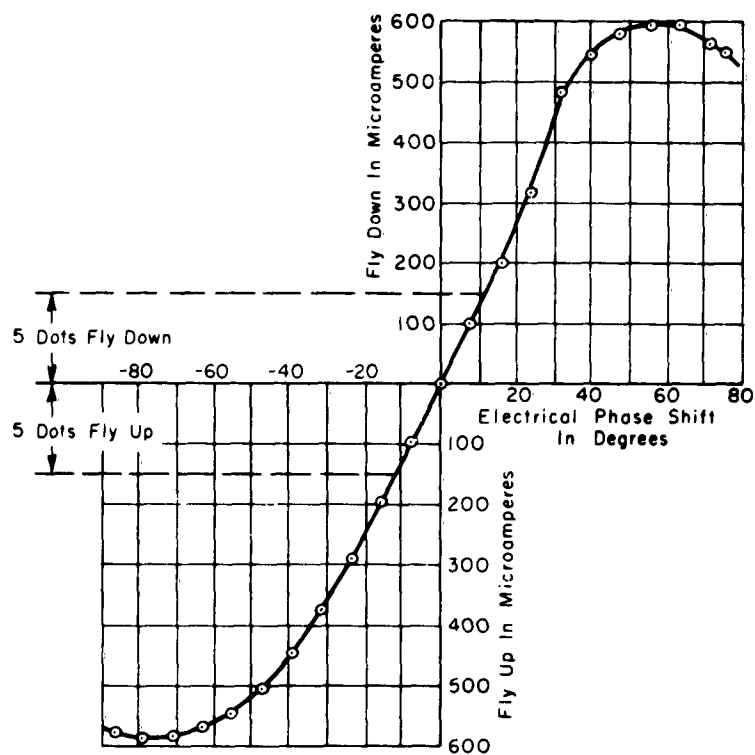
Fig. 47. Indicator deflection versus electrical phase change.
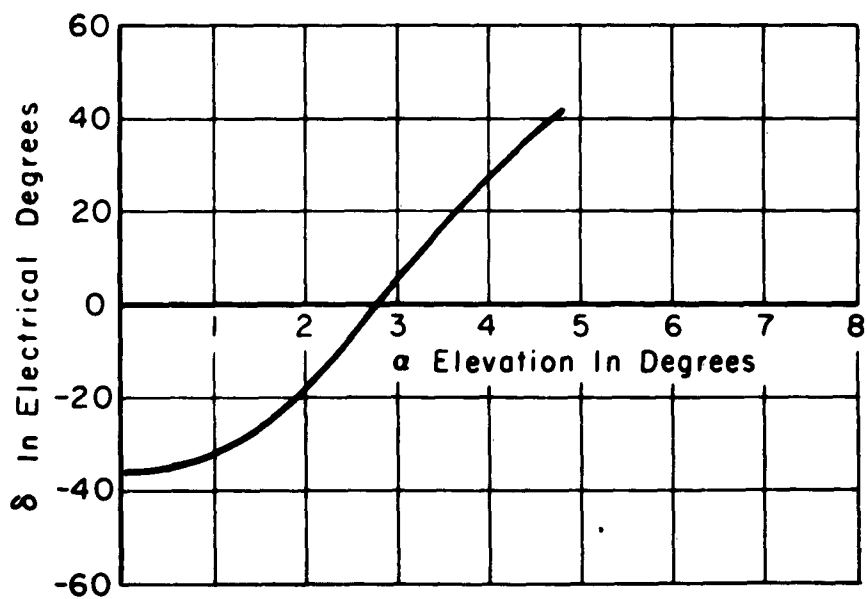
Fig. 48. Measured electrical phase shift versus elevation.

Figure 49 illustrates this conical surface and shows the un-
desirable feature of giving an on-path indication at elevations below
that of the required glide path. It is because of this that the addition-
al elements are added to the array to broaden the path well outside
the limits of the lateral guidance (localizer) path limits.

3.42 Path Broadening

In discussing the path-broadening theory, reference will be
made to the coordinates shown in Figure 44.

The ideal glide-path plane would intersect a plane perpendicular
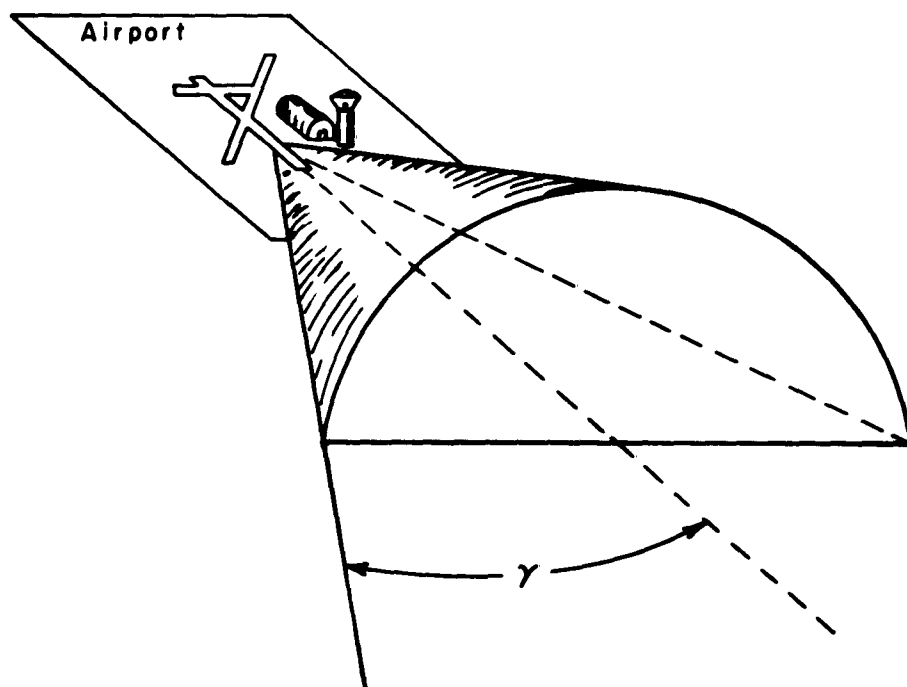
Fig. 49. Illustration of elemental, conical path.

to the runway center line in a line parallel to the tangent plane of the

earth. If a recording is made of the glide-path signals from the

elemental array as a perpendicular run is made on this glide

path, a series of regions with 90 and 150-cycle modulations alternate-

ly predominating is encountered. Figure 50 shows that in traveling

from A to B, various path indications are obtained. When starting

above the runway centerline, an on-course is observed which rapidly

changes to a fly down (90-cycle modulation). This is in agreement

with the theory that says the path is a semi-cone with the perpendicular
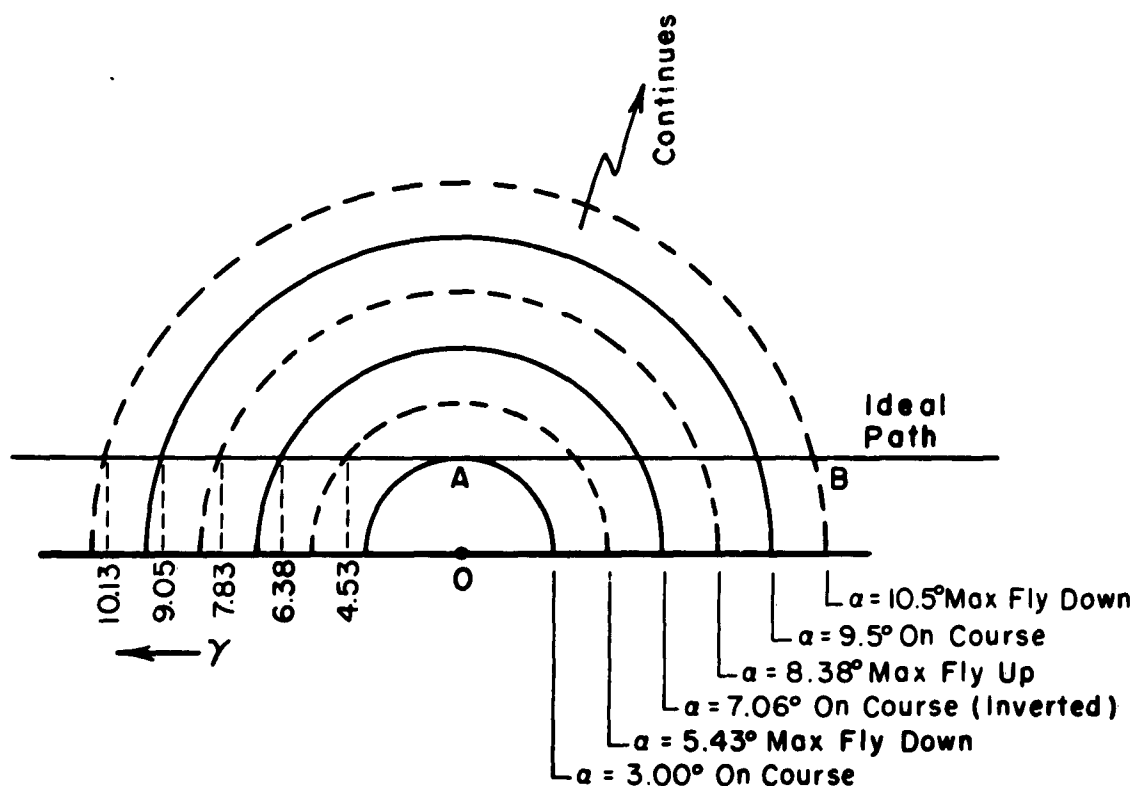
Fig. 50. Intersections of various paths with a plane
perpendicular to the runway centerline.

cross sections evident as arcs of circles. An actual flight pattern is shown in Figure 51.

The numerous path crossovers found when moving away from the runway centerline plane point to the increasing complexity that would be present in a modifying system as the requirement for a flat path in azimuth is increased. An important question then becomes : What is the azimuth angle to which this path must be essentially straight ? To answer this in a realistic manner reference must be made to the lateral guidance system. The localizer gives full-scale deflection on the pilot's indicator at $2\frac{1}{2}$ degrees either side of the centerline. This means that once the aircraft exceeds $2\frac{1}{2}$ degrees, there is no further information provided, i.e., the indication is the same at 3 degrees as at, say, 30 degrees. Therefore, no reference should be made to the glide path outside the $\pm 2\frac{1}{2}$ degree limits of the localizer unless the glide path is a constant elevation angle at all azimuth angles. It is generally accepted as proper piloting technique to refer to the glide path only when on the localizer, for beyond these limits adequate clearance of obstacles is not guaranteed.

The glide path necessarily must be $\pm 2\frac{1}{2}$ degrees wide in azimuth, the width here referring to the angular limits on the essentially flat planar wedge surface. For increased operational safety, the path is widened to the maximum possible by using an economically feasible array. It will be shown that with the addition
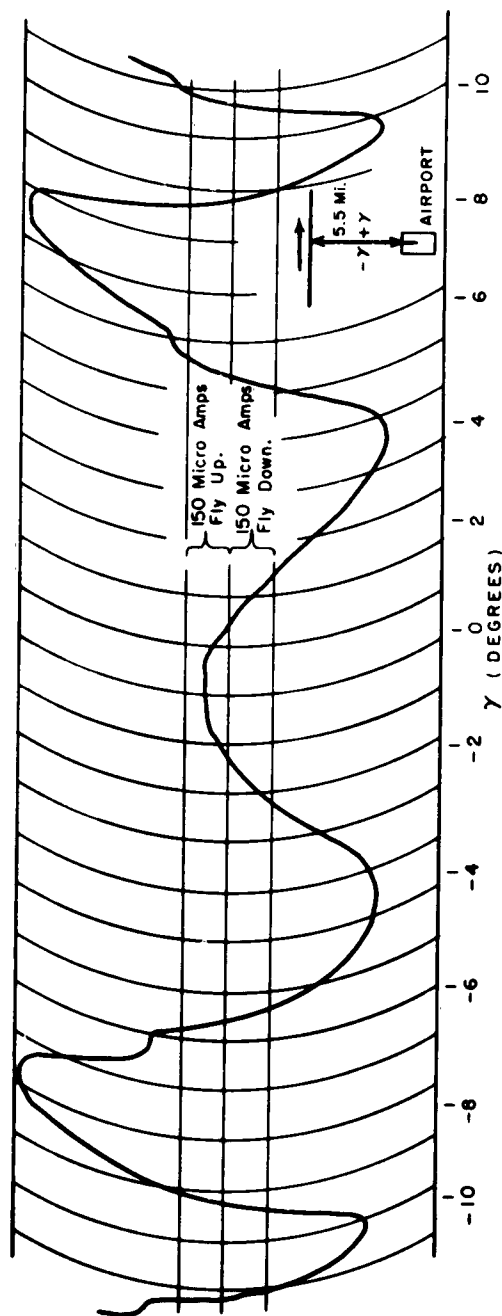
Fig. 51. In-flight recording of elemental array. Altitude 1500 feet above airport level. Gain of recording amplifier has been adjusted to allow peaks to remain on chart.

of three broadening antennas, the path can be made more than twice the width of the localizer path, or greater than ± 5 degrees. As previously mentioned, a flat wedge is not satisfactory for the region well removed from the runway centerline extension. For example, the approach path to an airport may be from east to west. This approach may be completely safe in spite of a 500-foot radio tower several miles northeast of the airport. Should the glide path be planar and of great extent in azimuth the path would intersect the tower.

From this illustration it is evident that the lateral guidance must be followed closely, and also for greatest safety, the regions on both sides of the lateral guidance limits should provide fly-up indications. This can be obtained by radiating a 150-cycle modulated signal in a pattern that would give a broad null on the centerline of the runway but would flood the regions beyond $\pm 6^\circ$ with the fly-up signal. This array with two or three antennas could be excited with energy from a separate transmitter displaced, say, 8 kc from the glide path carrier to utilize the capture effect of the receiver and avoid an audio beat.

Simply stated, the problem of path broadening by using additional antenna elements is one of determining the location, spacing, phasing, and amplitude distribution of an additional group of antennas both with respect to themselves and with respect to the elemental array.

When moving away from the centerline region, an increase in 90-cycle modulation is observed. To straighten the path it will be necessary to compensate for this region of excessive 90-cycle modulation. The amount of correction needed must be known so that an array may be synthesized that will be used to modify the fly-down condition.

To analyze this problem, consider the phase relations of the energies reaching a point P in the far field. For example, consider P with $\gamma = 3^{\circ}$ and $\theta = 3^{\circ}$. For a right tetrahedron

$$\cos \alpha = \cos \theta \cos \gamma \qquad (3\text{-}6)$$

then

$$\alpha = 4.24^{\circ}. \qquad (3\text{-}7)$$

From Equation (3-1) it can be calculated that

$$\delta = 39.64^{\circ} . \qquad (3\text{-}8)$$

This says that instead of the carriers being in phase at P as would be desired, producing an on-course indication, the signal from #2 antenna has advanced, thus giving a predominance of 90-cycle modulation (fly-down).[1] For the geometrical details refer to Figure 43 and assume #1 phasor = #2 in magnitude.

---

[1] An inspection of the phasor diagrams shows that maximum fly-down occurs when $\delta = 90^{\circ}$, maximum fly-up when $\delta = 270^{\circ}$, and an inverted path with carrier cancellation occurs when $\delta = 180^{\circ}$.

Equal quantities of modulation can be obtained by rotating the phasors of #1 39.64 degrees counterclockwise. To effect this, a signal with the character of #1 (i.e., with the same sideband resultant configuration) can be added to give a resultant parallei to # 2 , as shown in Figure 52 . It is evident, when recalling the sideband positions, that the result of the addition is an on-course signal. The problem now becomes one of supplying the correction signal with proper amplitude and phase.
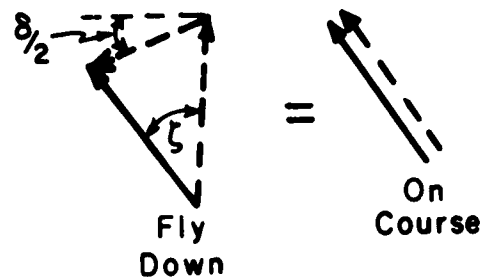
Fig. 52. Path correction by phasor addition.

From the geometry of closing the phasor triangle, it can be seen that the correction energy must have an angle of $90^{\circ} + \delta/2$ with respect to the vertical reference. This would suggest that the initial phasing of the broadening array would be advanced 90 degrees over the on-path reference condition. The angle $\delta/2$ indicates that the spacing which produces the phase difference between the broadening array and the #1 antenna be one-half of that which produces the phase differences between #1 and # 2 antennas, i.e., $\frac{1}{2} d_0$ or 120 feet.

In order to establish the spacing, phasing, and amplitude distribution of the broadening array, an analysis is necessary to determine what amplitude of correction signal will be needed to produce a straight path at $\theta = 3^\circ$ for γ values either side of zero. An amplitude $A(\gamma)$ will be derived by using only the expressions for the sideband energies. To simplify the mathematics, the reference for writing the sideband expression will be taken 45° counterclockwise from the vertical, with these sideband components having equal magnitudes normalized and proportional to the amplitude of their respective carriers.

Then writing the expressions for the sidebands from #1, #2, and some arbitrary correction array located midway between #1 and #2 antennas, gives:

$$E_{90-1} = e^{j0} \tag{3-8}$$

$$E_{90-2} = e^{j(\delta-90)} \tag{3-9}$$

$$E_{90-c} = A(\gamma)\, e^{j(90+\frac{\delta}{2})} \tag{3-10}$$

where the subscripts 90-1, 90-2, 90-c indicate the 90-cycle sidebands from #1 antenna, #2 antenna, and the correction antennas respectively. Similarly for the 150 cycle

$$E_{150-1} = e^{-j90} \tag{3-11}$$

$$E_{150-2} = e^{j(0+\delta)} \tag{3-12}$$

$$E_{150-c} = e^{j(0+\frac{\delta}{2})} \ . \tag{3-13}$$

Adding these gives

$$E_{90} = 1 + j\left(e^{j\frac{\delta}{2}} - e^{j\delta}\right) \tag{3-14}$$

$$E_{150} = e^{j\delta} + Ae^{j\frac{\delta}{2}} - j \ , \tag{3-15}$$

or, in trigonometric form,

$$E_{90} = \left(1 + \sin \delta - A \sin \frac{\delta}{2}\right) + j\left(-\cos \delta + A \cos \frac{\delta}{2}\right) \tag{3-16}$$

$$E_{150} = \left(\cos \delta + A \cos \frac{\delta}{2}\right) + j\left(\sin \delta - 1 + A \sin \frac{\delta}{2}\right). \tag{3-17}$$

Since the glide-path receiver will give path indications as a function of difference in modulation, the following is required for on-course:

$$|E_{90}| = |E_{150}| \tag{3-18}$$

or

$$|E_{90}|^2 = |E_{150}|^2 \ . \tag{3-19}$$

Substituting the sums of the squares of the real and imaginary components, expanding, and canceling terms gives

$$\sin \delta - A \sin \delta \sin \frac{\delta}{2} - A \cos \delta \cos \frac{\delta}{2} = 0 \ . \tag{3-20}$$

Using a trigonometric identity gives

$$\sin \delta - A \cos\left(\delta - \frac{\delta}{2}\right) = 0 \qquad (3\text{-}21)$$

which when solved for A gives

$$A = \frac{\sin \delta}{\cos \frac{\delta}{2}} = 2 \sin \frac{\delta}{2} \; . \qquad (3\text{-}22)$$

Since

$$\delta = d_o \left(\cos \alpha_c - \cos \alpha\right),$$

Then using equation (3-6) where $\cos \theta = \cos 3^o$ gives

$$A\,(\gamma) = 2 \sin\left[\frac{d_o}{2}\left(\cos \alpha_p - \cos \theta \cos \gamma\right)\right] \qquad (3\text{-}23)$$

$$\doteq 2 \sin\left[14468\left(1 - \cos \gamma\right)\right]. \qquad (3\text{-}24)$$

A plot of this function is shown in Figure 53. As would be expected there is no correction added when on the runway centerline ($\gamma = 0$). Incidentally, this same function can be obtained from an analysis of the carriers alone, provided there is a distinction made in their characters.

Experience has shown that no single element, nor a combination of two phased for a null, will furnish the proper shaped curve in the vicinity of $\gamma = 0$. A study of the difference pattern between a

$$E_C(\gamma) = 2C\left[1 - \cos\left(\tfrac{d_1}{2}\sin\gamma\right)\right] = 4C\,\sin^2\left(\tfrac{d_1}{4}\sin\gamma\right)$$

$$C = 0.6 \qquad d_1 = 21' = 2537°$$

$$A(\gamma) = 2\,\sin\left[\tfrac{d_0}{2}(\cos\alpha_p - \cos\theta\,\cos\gamma)\right]$$

$$\alpha_p = 3° \qquad d_0 = 28{,}936° \qquad \theta = 3°$$

γ In Degrees
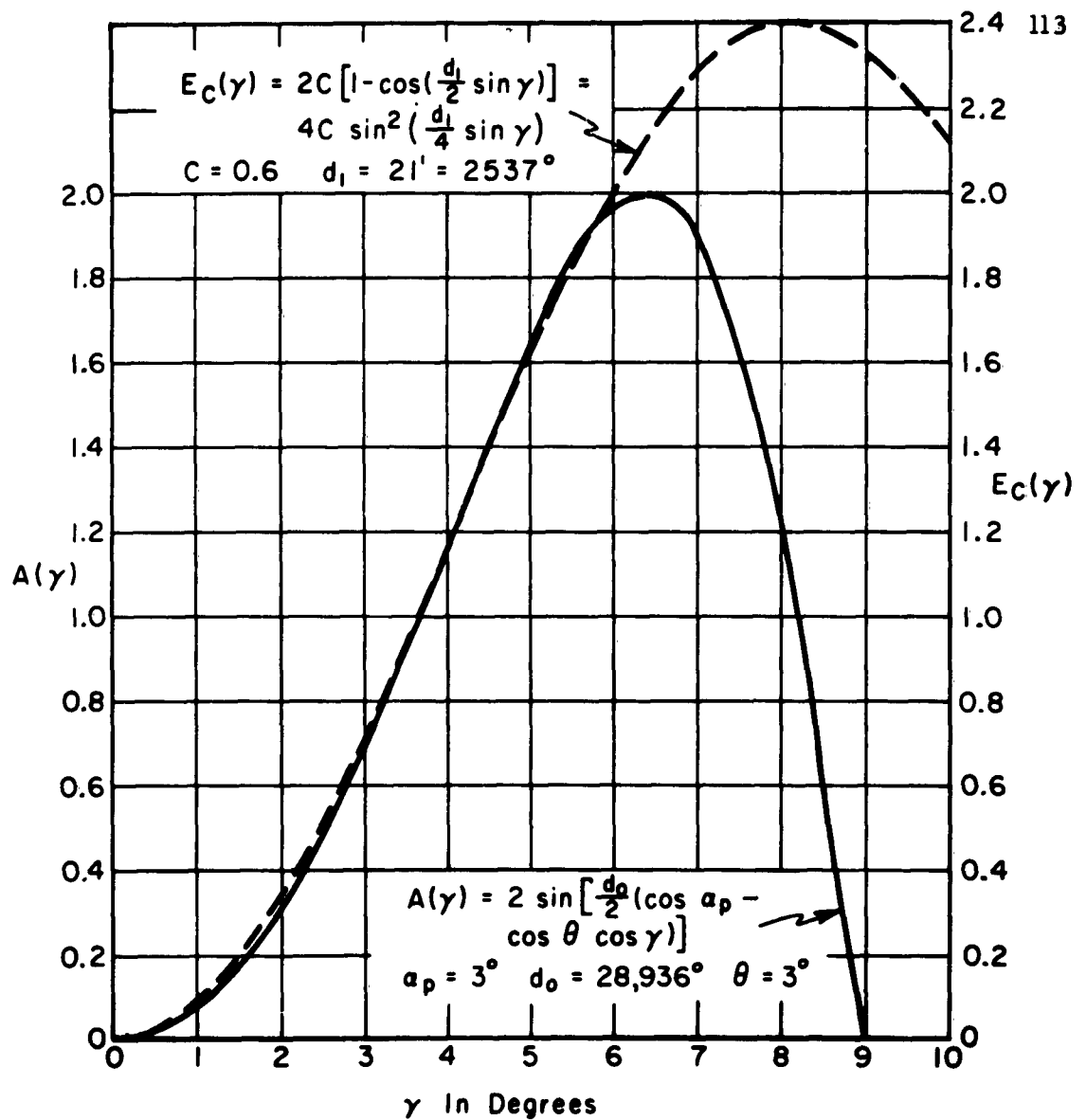
Fig. 53. Correction signal available from three modifier antennas compared with the required correction for a flat path in azimuth.

relatively constant source and two phased to give a null at $\gamma = 0$ does reveal a possible similarity.

Let a source producing constant radiation over the sector of interest be energized with an amplitude 2 C at a reference phase . On either side of this element, $d_1/2$ units, two similar sources are placed with amplitudes C and phased 180 degrees relative to the

center antenna. The expression for the resulting electric field magnitude becomes[2]

$$|E_c| = 2C - 2C \cos\left(\frac{d_1^o}{2} \sin \gamma \right)$$

$$= 2C \left[1 - \cos\left(\frac{d_1}{2} \sin \gamma \right) \right] \qquad (3\text{-}25)$$

Two undetermined parameters in this expression are the spacing and the amplitudes. These will be selected to best match the graph of this function with the graph of equation (3-15). These values will produce the smoothest and widest path when θ versus γ is plotted.

Equating (3-25) and (3-24) and using trigonometric identities give

$$\sin\left(28,936 \sin^2 \frac{\gamma}{2} \right) = 2C \sin^2\left(\frac{d_1}{4} \sin \gamma \right). \qquad (3\text{-}26)$$

From empirical evidence obtained by using dipoles, an optimum value for d_1 was found to be 21 feet. If d_1 is taken at 21 feet (2537 electrical degrees at 329.6 mc), the C becomes 0.596. By using this value of C, the correction provided is obtained. This function is plotted and compared with the required values in Figure 53.

---

[2]Kraus, J. D., Antennas, McGraw-Hill Book Co., Inc., New York, N. Y., p. 79; 1950.

As can be seen, the curves compare very well; hence, the glide

path would be expected to be nearly ideal over the range of coinci-

dence in Figure 53.

Solving for θ explicitly in (3-26) gives

$$\theta = \cos^{-1}\left\{\frac{\cos \alpha_p}{\cos \gamma} - \frac{2 \sin^{-1}\left[C\left\{1 - \cos\left(\frac{d_1}{2} \sin \gamma\right)\right\}\right]}{d_o \cos \gamma}\right\}. \quad (3-27)$$

A plot of equation (3-27) is shown in Figure 54 for $d_1 = 21$ feet

and $C = 0.6$. This curve represents the glide path as seen in a plane

perpendicular to the extended runway centerline. Tolerance limits

are shown on the graph as ± 1 dot. It is evident that for ± 5 degrees

in azimuth the tolerance is easily met.

3.5 Glide Path Measurements

To conduct the experimental phase of this glide-path work, a

sod runway at the Ohio State University Airport was made available.

This runway area produced a realistic environment for the operation

of a glide-path system. No obstructions except those deliberately

placed were present within one-fourth of a mile.

Fortunately too, the area north of the runway over which the

glide path extended was one of a low-density population. This

allowed extensive flight testing without hazard to persons or property.

Approximately 90 hours of actual flight tests were conducted to
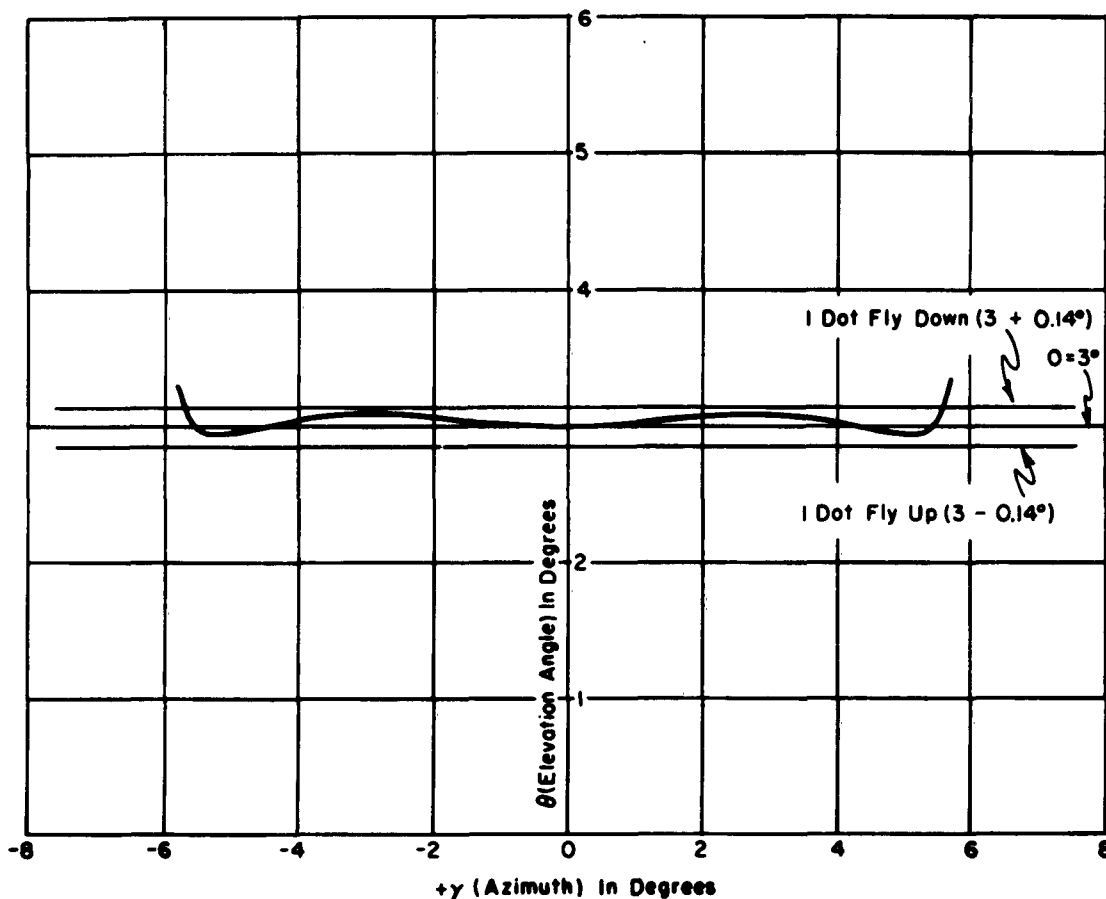
Fig. 54. Calculated cross section of the path.

investigate effects of changes in parameters, to view the actual path structure, and to confirm ground-based recordings and measurements.

3.51 Equipment

To give the reader a better understanding of the test site operation, a description of the type and location of the equipment will first be given, followed by a presentation of some significant

data and recordings. Details of the phase-stabilizing techniques will be included together with evidence of their effectiveness.

The radio frequency source for the glide path tests is a Federal Radio and Telephone Company TUS Glide Path Transmitter. This is the type of transmitter used in the Null-Reference glide-path system now installed at airports throughout the United States. Associated with this transmitter unit are the bridge circuits that determine the character of the output signals, which were discussed earlier in this chapter. Also housed in the same rack is the trombone in the line to #2 antenna used for setting the path angle. A photograph of this transmitter is shown in Figure 55. The signal source for early field strength tests was an AN/ARC-27 UHF transmitter, the airborne transmitter commonly used by the military for communication.

The transmission line coming from the final bridge with the signal character appropriate for #2 antenna first goes through a variable attenuator and trombone line stretcher unit before going to the #2 antenna. Note Figure 35.

The variable attenuator is a part of the original TUS unit and consists of a sliding "T" feeding a hybrid bridge. One output of this bridge is fed to a dummy load and the other to the trombone, also belonging to the TUS unit. By sliding the feed or stem position of the "T", power can be shifted in varying amounts from the dummy load
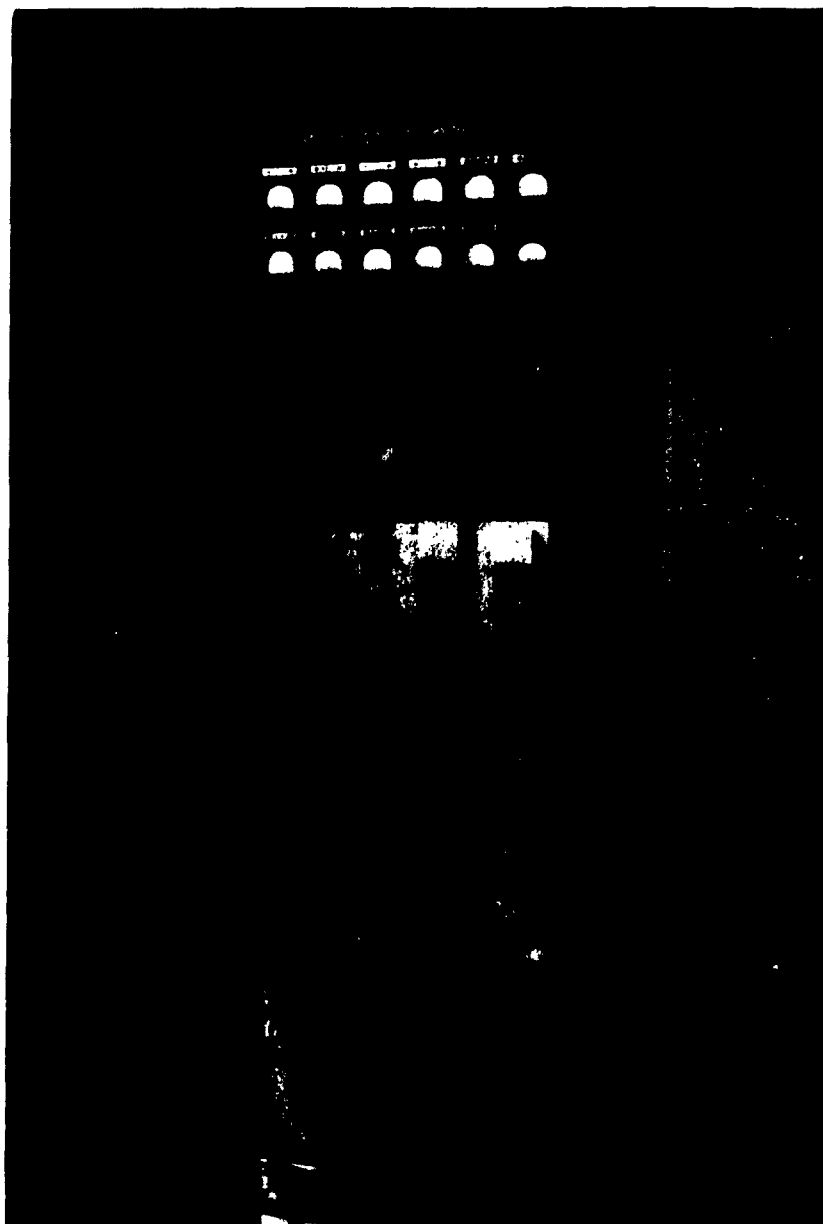
Fig. 55. Federal Radio and Telephone TUS glide-path transmitter. One of the trombones shown is used to set the glide path angle. The other is a spare. The vertical control to the left of the trombones is a sliding "T" which is used to adjust the power level of #2 antenna.

to the antenna. Operation of this is evident from the drawing in

Figure 56. It shoud be noted that this unit is basically a power

divider, a capability that will be used in the amplitude control for

the broadening array.
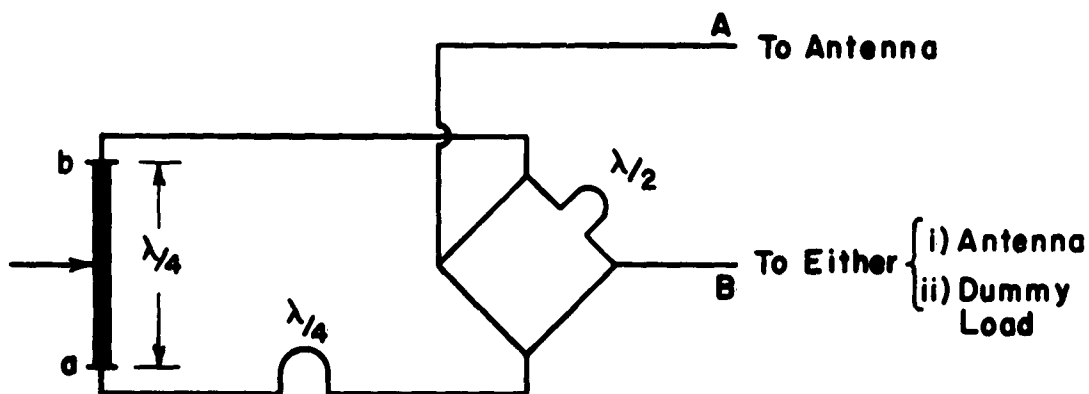
In Position **a** All Power Delivered To A

In Position **b** All Power Delivered To B

Fig. 56. Transmission-line power divider.

The second line coming from the final bridge goes directly to

a phase and amplitude control unit at the center of the array. It is

from this box that the power is distributed to elements 1, 3, 4, and

5. A schematic drawing and photograph are shown in Figure 57.

The transmission lines used to feed this array are one-half

inch sections of Styroflex, an air filled coaxial cable manufactured

by the Phelps Dodge Company. The cable should be pressurized for maximum phase stability and leak detection; however, because of connector problems, the data presented were obtained without pressurization.
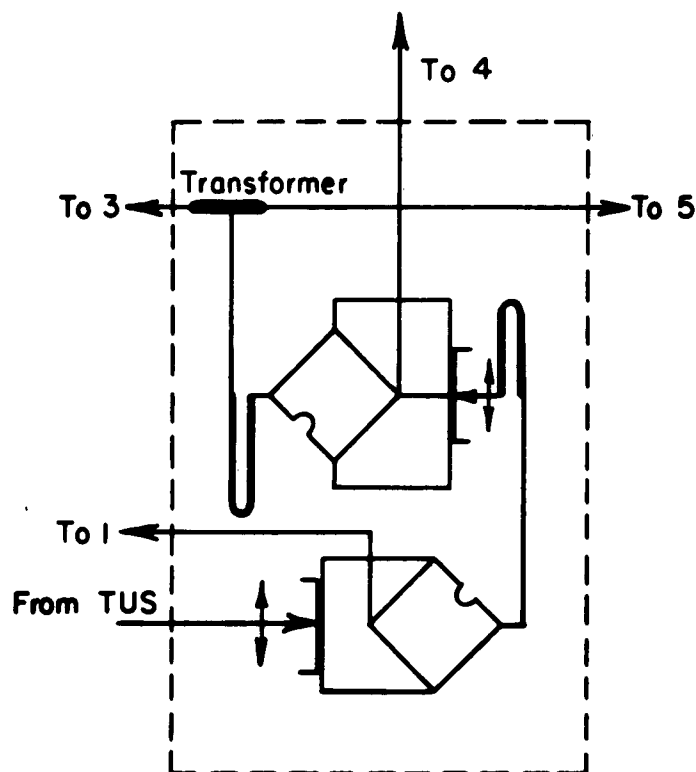
Fig. 57. Phase and amplitude control schematic drawing.

The array antennas were fabricated from one-eighth inch aluminum alloy 5086 H 32 which was welded to form a watertight trough. A fiberglass radome bolted to the top of the trough formed a completely sealed cavity for the polystyrene dielectric. Both the solid laminated polystyrene block and the stack of loose sheets performed equally well in the array. The electric probe used for

exciting the cavity is shown in Figure 58. Both the probe housing and the cavity can be pressurized for the detection of leaks. The short tuning stub can be seen in the photograph. The radome is also shown.

Spacing of the antenna elements is indicated in Figure 35. A view of the actual array is shown in Figure 59.

An eight-element yagi antenna one wavelength above ground, used as a pickup for the servo detector, is located approximately 900 feet north of #1 antenna. This simulates an area beneath the approach region to the runway. The detector is in a low shelter near the antenna.

The truck shown in Figure 28, with its telescoping tower, is used to raise a dipole as high as 50 feet above the ground for path recordings. The truck unit could be used either as a moble unit or as a fixed monitor. Extensive use was made of the truck equipment to obtain preliminary checks of the perpendicular structure of the glide path. This method was more convenient and less expensive than flight-checking for early work on the broadening array.

Recordings both on the ground and in the air were made by an Esterline Angus pen recorder driven by an amplified output from a Collins 51 V receiver. Both path indication and field strength were recorded by this method. The path indication was recorded as cross pointer deviation.
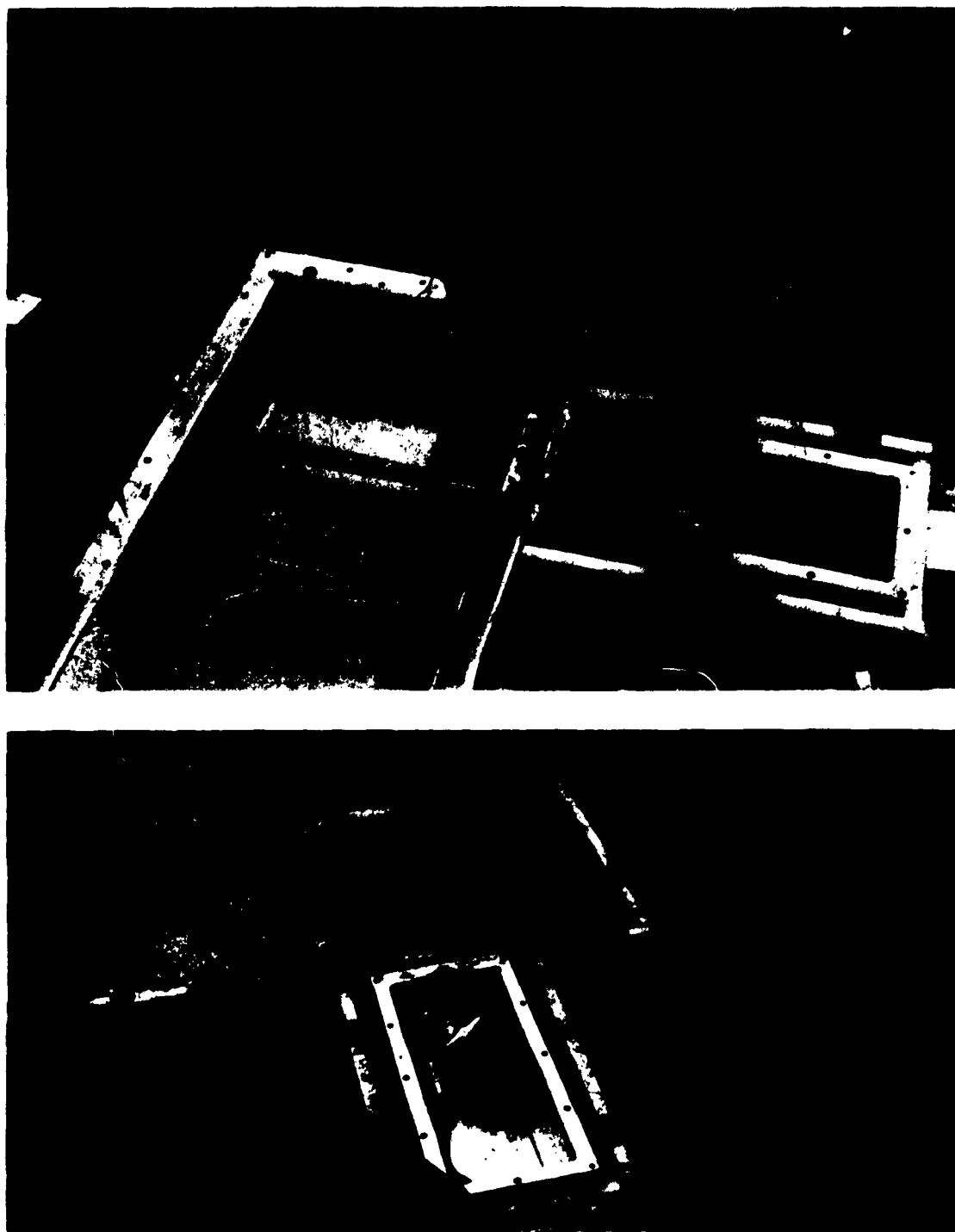
Fig. 58. (a) Close up view of probe assembly. (b) Probe box with probe and tuning stub adjusted to give 50/Ω ohms.

Fig. 59. View approaching touchdown region.

Amplification was in either of two forms. If long-time stability was not a factor, such as in flight recordings, a conventional DC amplifier stage was used ahead of the recorder for course-deviation indications. For long time periods it was found desirable to amplify the audio from the second detector of the Collins receiver and then proceed with the filtering and rectification at a higher level. This produced a very stable method of providing sufficient drive for the 1 milliampere recorder.

Airborne recordings were made of the system by using a Cessna 172 single-engine aircraft with a special rack containing a Collins 51 V receiver, DC amplifier, Esterline Angus 1 milliampere

recorder, course deviation indicator, altimeter, field strength

indicator and B+ voltage monitor. Provisions for calibrating the

recorder against a standard cell were available.

Several different antennas were used on the aircraft. A

conventional glide-path dipole mounted on the top of the fuselage

was used for the routine approaches. For field strength readings,

especially those involving high elevation angles, a 50-ohm standard

dipole was secured to a long wooden frame attached to the landing

gear, which positioned the dipole well to the side and ahead of

adjacent metal structures. In addition, a dipole was mounted on the

underside of the fuselage in order to receive the signal when flying

perpendicular to the runway centerline extended. Figure 60 illus-

trates the aircraft equipment. Baluns were used with the trans-

mission lines involving the balanced antennas.

Special flight recordings were made by using a Beechcraft

C-18 and a Douglas DC-3.

3.52 Measurements Based on the Basic Array

To determine systematically the characteristics of the glide

path, work began with the elemental path formed using but two

antennas. Airborne and ground-based measurements were made

with this array, and since the modifying array provides no signal

on the centerline, the final path available on the localizer path can

be investigated also. Of particular interest are the clearance below
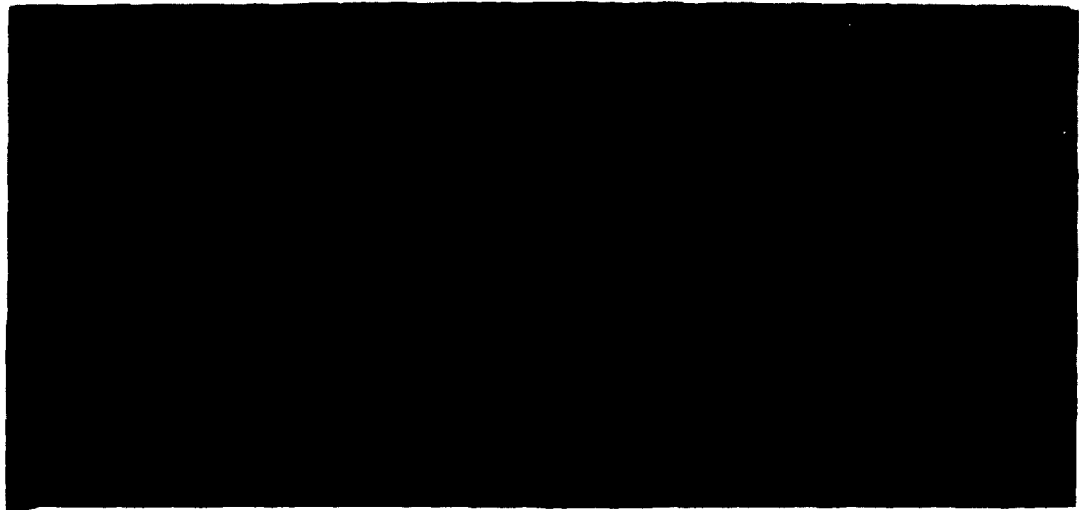
a) Standard glide-path dipole.   b) Special dipole for perpendicular
passes.

c) Airborne recorder panel.

Fig. 60. Airborne recording equipment.

path, straightness of the glide path, presence of transmitter anoma-
lies, presence of reflections, and the vertical path thickness.

In making a perpendicular pass the tight conical shape be-
comes evident (Figure 50). From this same recording, information,
which is a function of the spacing of the antennas, is obtained. The
parameters of the modifier array are directly related to the angles
at which the false paths and regions of maximum fly up or fly down
occur. A comparison of the calculated and measured values of the
basic structure is shown in Table 7.

TABLE 7

COMPARISON OF CALCULATED AND MEASURED VALUES OF

BASIC PATH STRUCTURE

	Calculated	Measured
On-Course	3°	3°
Max Fly-Down	4.53	4.25
Inverted Path	6.38	5.9
Max Fly-Up	7.83	8.0
On-Course	9.05	9.0
Max Fly-Down	10.13	10.0
Inverted Path	11.10	10.8
Max Fly-Up	12.0	12.0
On-Course	12.82	12.6

Control of the path sensitivity, i.e., the vertical thickness, is through the spacing d_o of #1 and #2 antennas. It is usually desired that a full-scale deflection of the pilot's indicator be obtained for a 0.7 degree elevation departure from the path. For the 240-foot spacing used, the following electrical phase shift is obtained in going from 0.7 degrees elevation below path to 0.7 above:

Calculated : 36 electrical degrees

Measured : 34 electrical degrees

The use of a standard glide-path receiver (calibrated for 2 db audio producing 77 micro amperes deflection) gives a path with vertical thickness of 1.00 degree (0.55° below , 0.45° above). This is a rather narrow path; however, there are two reasons for using it. First, to demonstrate that a tight path can be obtained, because longitudinal arrays have been known to be "soft" on the lower side. Second, to obtain measurements that are on the conservative side when considering path broadening. Figure 50 shows clearly that with a tighter path, the path broadening is more difficult and will not provide as large a region of smooth path in azimuth. Therefore, it is felt that path broadening accomplished by using this array can be duplicated more easily by using an array with a smaller d_o .

If desired, a certain amount of broadening in vertical width can be obtained by dephasing #3, #4, #5 antennas so they are not completely nulled on centerline.

3.53 Measurements of the Modifier Array

Proper adjustment of the amplitude and phase of the modifier antenna elements is essential in obtaining the optimum in horizontal path width. A rule of thumb for obtaining a first approximation for d_1 is to measure the azimuth angle where maximum fly-down is obtained from the elemental array at 3 degrees elevation and set d_1 so that the first null of antennas 3 and 5 falls at this angle. Further refinement can be obtained by matching curves , or by actual field measurements. Both were used in this work, giving nearly identical results.

In Figure 61 recordings are shown of the field strengths of the modifier elements taken in significant combinations. Because #3 and #5 are in phase with each other, but 180° out of phase with #4 , a subtraction takes place to yield the complete modifier array pattern. These were recorded at 600 feet at 3 degrees elevation.

3.54 Measurements on Full Array Using Airborne Equipment

Because actual utilization of this system is by aircraft, the logical method to evaluate the merits of the complete path is through airborne measurements. Several different flight patterns were used to investigate the entire structure of the path;

a. Level pass. This consists of a flight path starting approximately 10 miles from the array usually at 1500 feet above the surface (the interception altitude at the simulated
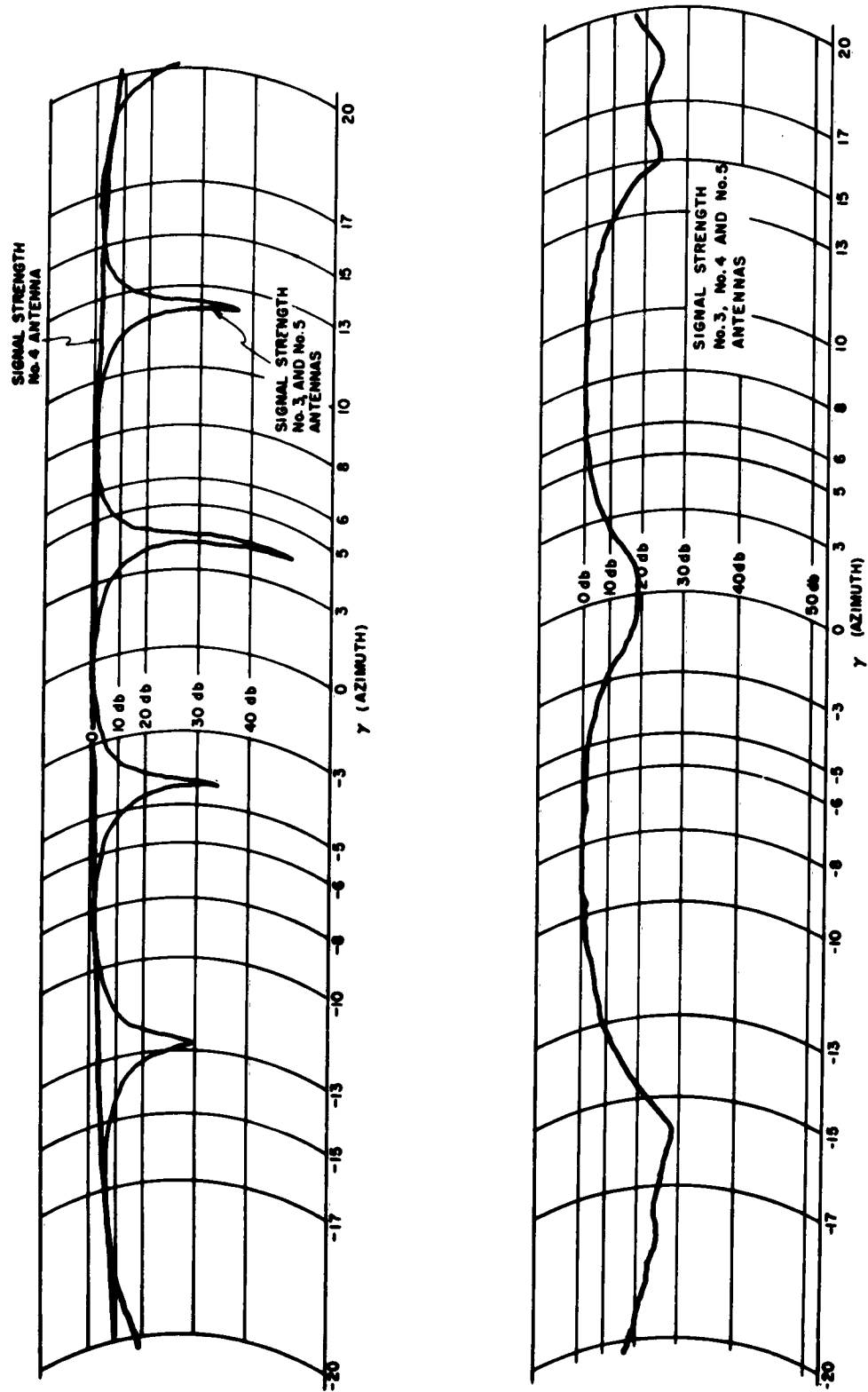
129

Fig. 61. Radiation patterns of modifier array.

outer marker) and proceeding at constant altitude on the run-
way centerline extended to the area above the runway. This
type of flight begins well below path, makes a transition
through the on-path region, and ends by going through the
false path structure. The characteristics of the path's vertical
cross section can be observed from this type of recording.

b. Low approach. This flight begins as the level pass, but
upon intercepting the on-course at the simulated outer marker,
a descent is below on the path, and proceeds to altitudes of
usually three to 10 feet. This measurement gives indication
of several quantities, namely, path straightness, path fly-
ability, turbulence, and pilot proficiency. By repeating the
flights, such variables as pilot proficiency and turbulence can
be eliminated.

c. Low clearence. This is a flight below the glide path, on
centerline, to show that with full fly-up signal on the indicator,
the aircraft will clear all terrain and obstructions. This also
proves the non-existence of false paths below course.

d. Perpendicular pass. This is a flight at an altitude 1500 feet
perpendicular to the runway centerline extended intersecting
it at the simulated outer marker. At the Ohio State University
site, this is five and one-half miles from the array. A three

degree path angle places the path at 1518 feet above the array at five and one-half miles.

Examples of data from some of the later flights are presented in Figure 62. These are recordings of the five-element flush-mounted glide-path system proposed as one independent of terrain in the approach region and one which can be used as a foundation for a system for landing aircraft completely blind.

3.6 Stability

No matter how perfect the glide path, it is of no value unless it is independent within acceptable tolerances of time and weather. Because the glide path must perform best when the weather is worst, it is necessary to build maximum stability into the system to ensure the safety of operations at all times. With modern control equipment available the first closed-loop glide path control system was incorporated into this glide-path system.

From early work with the dielectric-filled antenna, it was evident that the path was sensitive to material on the aperture surface. In fact, it will be recalled from Chapter II that at 3 degrees elevation, 1.5 electrical degrees phase shift occurs with each 0.001 inch of water covering the surface. The high dielectric constant of water makes even so thin a layer as .001 inch significant. A layer of oil ($\epsilon_r \approx 4$) on the surface causes no measurable phase shift.

Fortunately, the full effect of water layers is present only for
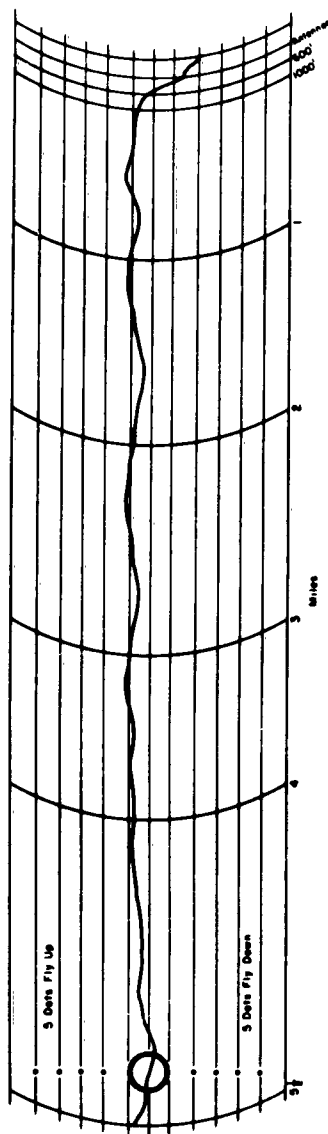
Fig. 62(a). Recording of low approach
Pilot: McFarland
Nov. 2, 1960
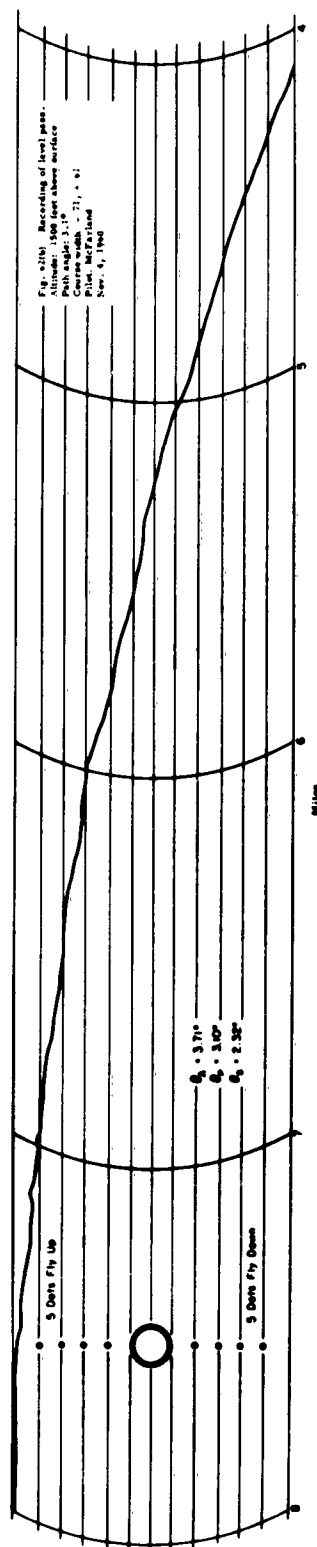
Fig. 62(b). Recording of level pass.
Altitude: 1500 feet above surface
Path angle: 3.1°
Course width: 71, + 6;
Pilot: McFarland
Nov. 4, 1960

$\theta_1 = 3.71°$
$\theta_2 = 3.10°$
$\theta_3 = 2.55°$
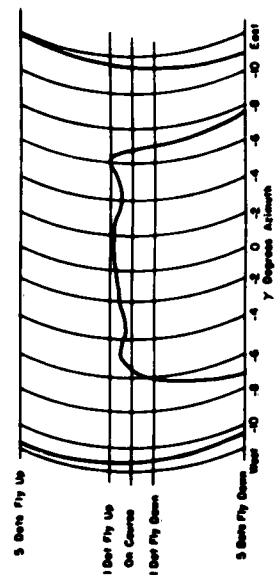
Fig. 62(c). Recording of perpendicular path at 5.5 miles.
Altitude: 1500 feet above surface
Width: 13.2°
Pilot: Copeland
Theodolite operator: Tye
Nov. 12, 1960

experimental purposes or for short periods, since in practice, rainfall is distributed nearly uniformly over an area the size of the array. With all antennas affected equally, there is no net phase difference produced between the signals arriving at the receiver because all retardations will be equal. To provide for increased stability, the crowns are used on the surface, thus decreasing the thickness of the water layer and making it more uniform. Basic stability is obtained, therefore, by balanced operating conditions.

Temperature can have a pronounced effect on the path and its structure since a transmission line will effectively lengthen with increase in temperature. In fact, with black RG-8/U feed cable lying exposed on the surface of the ground, the path can be observed to vary several dots as clouds obscure the sun. This extreme condition is not observed in practice, since RG-8/U cable is not used. Instead, 50-ohm Styroflex cable is used, and this is buried in the earth.

If a CDI deflection tolerance of one dot is required, the un- compensated or net undesirable electrical phase shift in the system must be held to less than four degrees, as seen in Figure 47 . A single cable feeding the antennas may be nearly 22,000 electrical degrees long. This means that a tolerance of one part in 5400 must be maintained. Without question this is a formidable requirement,

but one which may be achieved in two ways: by balanced self-compensating lines or by automatic control.

Spinner[3], in his work with yagi antenna arrays, reports that this tolerance was maintained in a test at Charleston, West Virginia. The system there depended wholly on self-compensating effects, since each transmission line running to the forward or number one group of elements had a counterpart in the feed to the rear elements.

With the five-element array used in this glide-path system, it is not possible to compensate entirely each antenna, since the feed to the modifier array coming from the line to #1 antenna introduces a kind of non-symmetry. Nevertheless, a great benefit is obtained, since the antennas are identical and an additional line is added going to the #2 antenna to make a length equal to that going to #1.

To obtain the path angle stability for the successful operation of this aircraft glide-path system, a closed loop-phase control system is employed. When the normal output of a monitor detector is used, this servomechanism allows a monitor to do more than merely shut down the system should a path-drift take place. With the feed-back loop, the path angle can be held constant throughout phase variations

[3] T.H. Bottoms, H.C. Hurley, L.N. Spinner, and J.W. Watt, "A Directional Glide Path", Technical Development Report No. 336, Civil Aeronautics Administration, February,1956.

of $\pm$ 70 degrees, resulting from disturbances in the transmission lines or in the antenna aperture.

Five months of night and week-end monitor records show that the servo phase controller is capable of holding the path angle to within $\pm$ one dot tolerance even with unpressurized cables, unequal line lengths, and shallow burial. Additional evidence of the effectiveness of the automatic phase controller can be seen in Figures 63 and 64.

In order to obtain the maximum benefit from the inherent stability potential and provide for the proper operation of the un-controlled modifier array, identical environments should be provided for each of the antenna elements.

136

ELEMENTAL PATH
WITHOUT SERVO

ELEMENTAL PATH
WITH SERVO
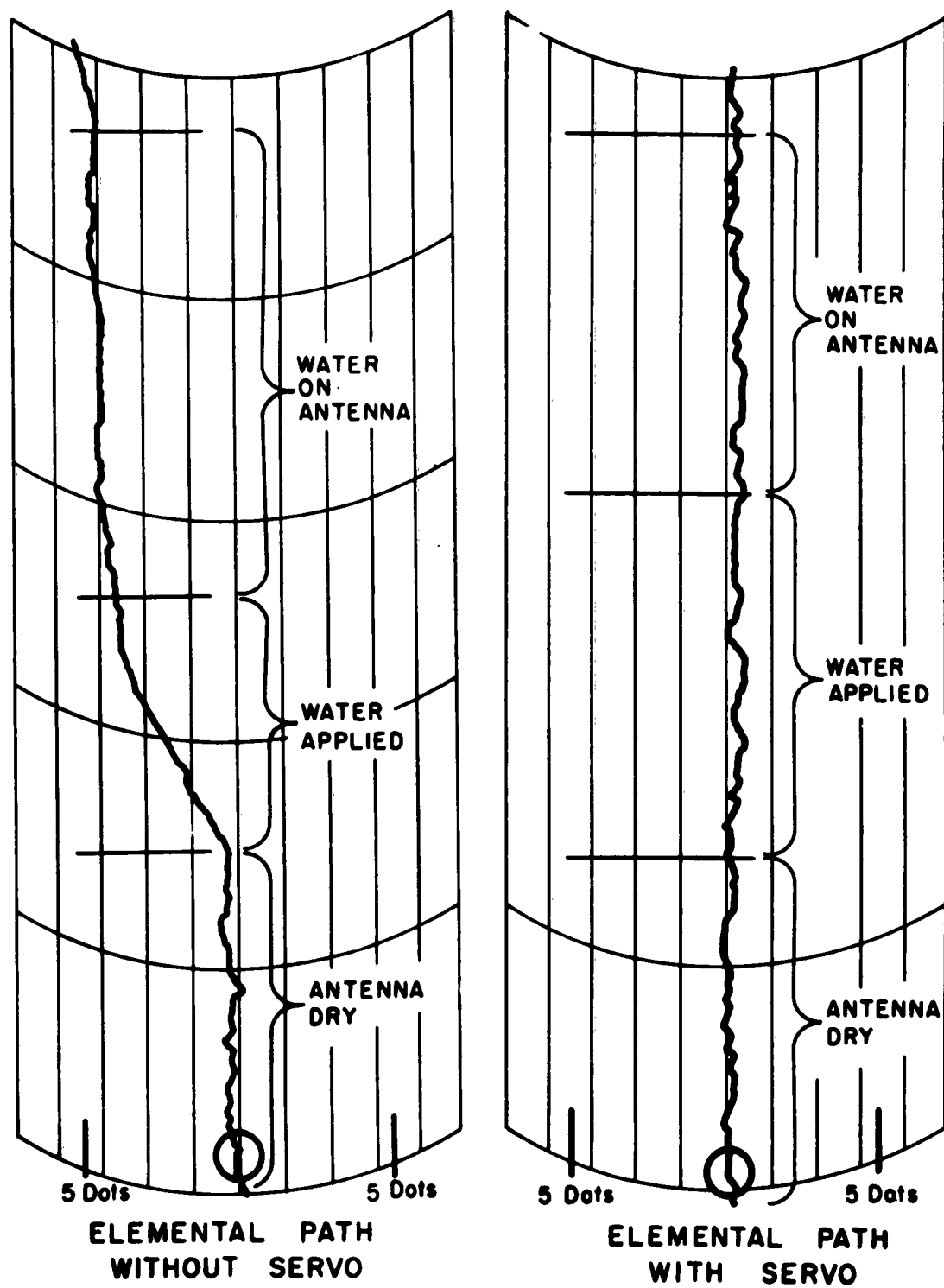
Fig. 63. Wetting antenna without servo.
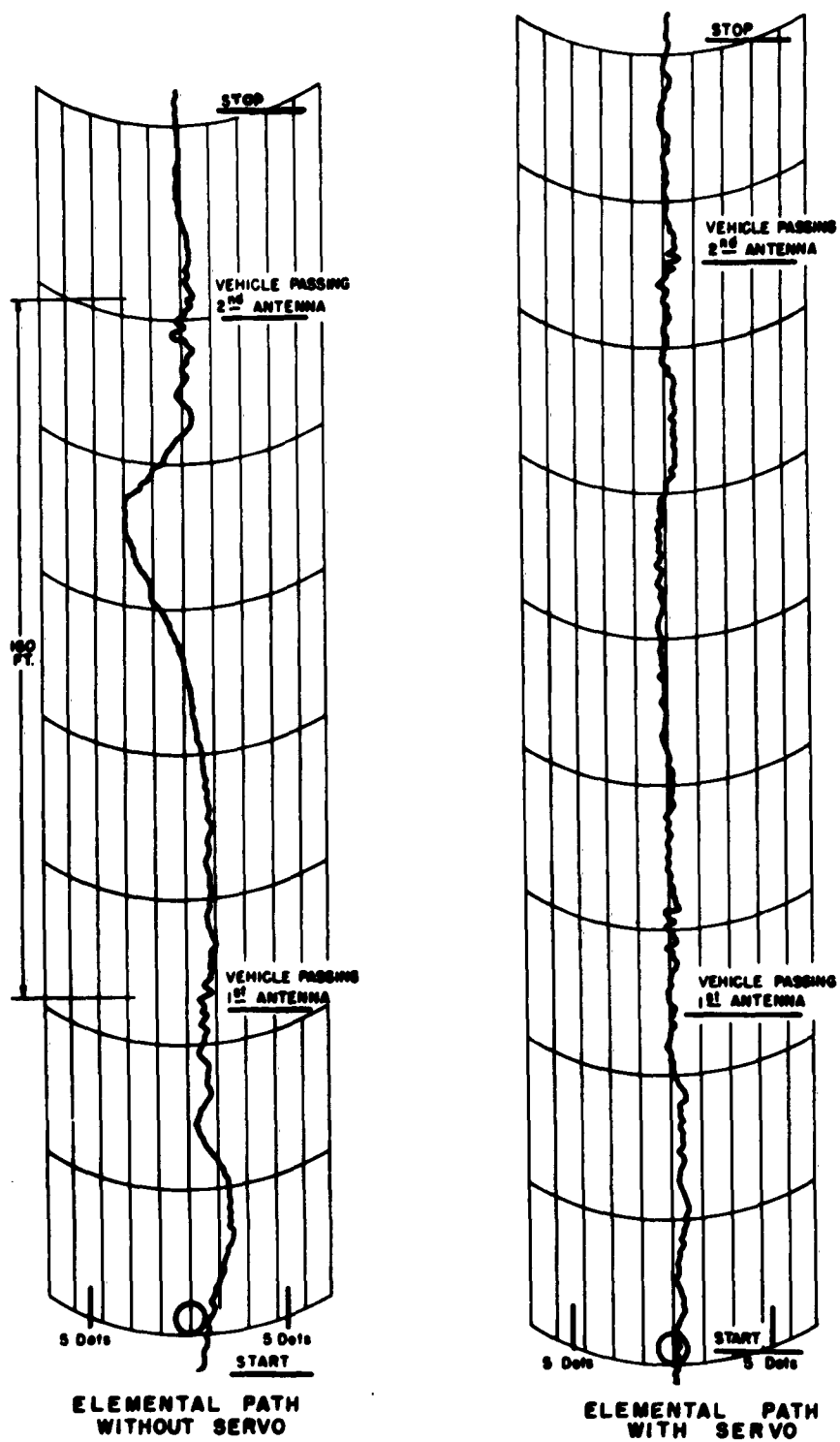
Fig. 64. Auto driving 10 feet aside array axis.

CHAPTER IV

CONCLUSIONS

Four significant conclusions follow   directly from the work done with the flush-mounted antennas and the five-element glide path using these antennas :

a. The 20-foot, dielectric-filled,traveling wave, flush-mounted runway antenna is one capable of satisfactorily serving as a radiator for a glide-path system.

b. The five-element glide path utilizing flush-mounted antennas installed in the runway proper provides a straight-line path extending over a sector more than twice the width of the localizer path.

c. The path may be flown to touchdown.

d. No modifications are necessary on present-day airborne equipment, i.e., the glide-path system is compatible with receivers now in use.

4.1 The Glide-Path Antenna

The dielectric-filled, transverse-electric, flush-mounted, runway antenna has performed well in the experimental glide-path system. Early array work with dipoles was directly applicable to the array using the flush-mounted antennas. With the spacings between elements,

that were used, no problem with coupling was observed. The antennas as can be seen from the evidence in chapters II and III perform as predict from theory and from model measurements. The calculated beam shapes, the number of lobes, and angles of maxima and minima are in good agreement with those observed.

An early consideration and concern when selecting the traveling-wave antenna for this application was its polarization pattern. This, however, proved to be no problem. Horizontally polarized energy exists over a region greater than 40 degrees (half power beam width), which is more than adequate for this glide path.

The flush-mounted antenna elements were found to have sufficient gain to allow full fly-up signal to be presented in regions as low as 1° elevation, while more than 15 miles from the runway. Full fly-up is present 150 feet above the surface at 7 miles and is present at tree-top level at 5 miles. This has been demonstrated with less than 1 watt total being fed to the #1 and #2 antennas.

The antenna is sufficiently broadbanded to be used on any frequency in the glide-path band. Obtaining a 50 /0 ohm input impe-dance is easily accomplished by means of the adjustable probe and the short capacitive stub. With observed temperature changes of 60^oF, impedances held within 10 per cent of the 50 ohm value.

Power handing capability is more than adequate for any future power increases.

The traveling-wave antenna is compatible with runway installation. Mechanical stress analyses show that the antenna is stable mechanically and capable of withstanding typical runway loading, which is important in maintaining electrical stability.

Insofar as stability is concerned, perhaps the greatest attention has been given to assessing and minimizing any undesirable effects of a water layer on the surface of the antenna. In a large measure this problem is solved by the gabled construction of the antenna radome and a good drainage system for the area immediately adjacent to the antenna. Any residual problem can be solved, with an adequate safety factor, by utilizing the output of a monitor detector to activate a closed-loop servocontrol to correct the system rather than merely shutting it down should a path change take place.

4.2 The Glide-Path Array

The strength of the five-element glide-path system lies in its ability to produce a glide path virtually independent of terrain, which can be flown with present-day equipment to the region of touchdown. It is conceived that in the future, with airborne computing equipment working on glide-path and distance information, a custom-built glide path can be formed by supplying information to the computer that would be peculiar to the airport, aircraft , and, perhaps, pilot. This type of path could be flown directly to touchdown in conditions of zero vertical and horizontal visibility.

In evaluating the glide-path system, reference will be made to the criteria outlined at the beginning of Chapter III.

The theory of the glide path calls for a straight-line path . Recordings showed this to be true except when spurious radiation from the transmitter was present. A signal 37 db down from the desired radiation can be seen as an irregularity in the path structure. It is therefore essential that stray radiation be eliminated. Attention should be given to thoroughly shielding transmitter. Oscillations in the perpendicular runs were evident, and calculations were made to determine the spacing. Calculations from ground-based and airborne data showed the second source to be 153 feet aside the array. The transmitter van was located 150 feet west of the array centerline. All evidence obtained in this glide-path work emphasizes the importance of ridding the glide-path region of stray signal. It is imperative that the TUS transmitter be extremely well shielded if a successful glide path is to be established.

The inverted, false path, a path more than twice the angle in elevation of the desired glide path, is of little concern, because the flag on the pilot's indicator will remain down, indicating an unsafe path. The first false path is at approximately three times the desired path angle, and if intercepted by gross error,could only be held by maintaining an abnormal rate of descent, which would alert the pilot to the error. In practice, these additional paths should present no

problem inasmuch as the present operational system with false paths has caused no difficulty.

By using an antenna with lower forward gain than most aircraft glide-path antennas, a fly-up signal was evident when over 20 miles from the runway at the interception altitude of 1500 feet. It is concluded that adequate signal is available from the flush-mounted antennas to establish a satisfactory glide path. The low angle radiation is limited by the sine θ factor to that which is essential to avoid unnecessary illumination of reflecting objects.

The region below path is abundantly filled with fly-up signal, providing a good safety factor. In fact, flight tests in the region from the outer marker to the airport indicate that ground obstructions, such as buildings, trees, and poles, are covered with sufficient signal to provide fly-up indication to the very low flying aircraft. In other words, any obstruction in this region would be indicated by a fly-up signal. No false paths are present below the established glide-path angle.

Vertical path width can be adjusted by the spacing which is set at the time of installation. Adjustment to a lesser degree can be made toward the broader side by dephasing the modifying array to allow some of its signal to appear on centerline. All properly adjusted paths recorded were less than 1.6 degrees total.

The horizontal path width, as measured with a theodolite, placed

50 feet to the rear of # 2 antenna, was measured at more than 13

degrees. The final runs averaged 13.3° .

Uniformity of the path sector appeared good from perpendicular

passes made at different elevations. Departures were noted at the

very edges of the flat sector where the path began falling off.

Stability of the glide-path system is excellent provided -

a. The transmission lines are of the air-filled type, are

pressurized and buried at least 24 inches in the ground.

b. Antennas are properly drained.

c. The servo system is maintained.

During the three-month monitor period, the path held to within $\pm$ 1 dot.

It should be pointed out that the modifier array depends on the

principle of self-compensation for stability, which can be expected

since the three elements are located in a relatively small region and

are symmetrically placed.

After a study of monitor sites it was concluded that a location in

the approach region below path was the most satisfactory area in which

to locate the servo monitor. For the complete fail-safe monitor it is

desirable to use the approach region also, but monitors should be

located at more than one position to detect changes in path width which

would be caused by a disturbance in the modifier array. All monitors

should possess long time constants, since they will receive transient

effects of aircraft passing over them as they use the system. The

question of fail-safe monitors is of paramount importance and should be given further study.

4.3   The Glide-Path System Concept

There is a certain finality about the decisions and actions of a pilot during an approach to an airport through fog, precipitation, and clouds. The pilot is called upon to exercise his utmost skill in maintaining the proper position of the aircraft; his attention must be devoted fully to this task of delivering his passengers safely upon the runway. The question of adequacy, proper operation, and erroneous indications of navigational aids must not be present, for in themselves these questions and doubts could mean the difference between a safe landing and tragedy. Indeed, the responsibility for the flight should and must be solely within the cockpit.

The glide-path system discussed in this paper is one that should command the respect of pilots. It offers to many airports the first opportunity to obtain the installation of a complete instrument landing system. It offers, also, the basis on which a fully blind landing system may be built.

It is hoped that further testing by the Federal Aviation Agency and the integration of the highest quality of monitors into the system will lead to installation of the flush-mounted glide-path system at selected airports throughout the United States.

The work for the completely blind landing system will continue at several research establishments, and it is believed that the work herein described will be fundamental to the permanent establishment and use of the zero-zero landing system.

APPENDIX

A detailed derivation of the expression for the far electric field from the flush-mounted runway antenna will be given here to supplement the discussion in Chapter II.

In working with discontinuous magnetic fields[1] the following expression is useful:

$$\bar{J}_{es} = \hat{n} \times \left(\bar{H}_{t1} - \bar{H}_{t2} \right) \qquad (A-1)$$

where

$$\bar{J}_{es} = \text{sheet current density (amperes/meter)}$$

$$\hat{n} = \text{unit normal}$$

$$\bar{H}_{t1}, \bar{H}_{t2} = \text{tangential magnetic fields in regions 1 and 2 .}$$

If a discontinuity could be present in the electric field, an analogous expression would be

$$\bar{J}_{ms} = -\hat{n} \times \left(E_{t1} - E_{t2} \right) \qquad (A-2)$$

The sign is changed to preserve symmetry in Maxwell's equations. A discontinuity does appear in the case of the equivalent currents

---

[1] J. D. Kraus, Electromagnetics, McGraw-Hill Book Co., Inc., New York, N.Y., p. 227 ; 1953 .

146

discussed in Chapter II when the value of the electric field goes from a finite value above the surface to zero below.

Maxwell's curl equations then appear as

$$\nabla \times \overline{E} = - J_m - \mu \frac{\partial H}{\partial t} \tag{A-3}$$

$$\nabla \times \overline{H} = J_e + \epsilon \frac{\partial E}{\partial t} \quad , \tag{A-4}$$

and the two associated retarded vector potentials are given by

$$\overline{A} = \frac{\mu}{4\pi} \int_{area} \frac{\overline{J}_{es} \, e^{-j\beta r}}{r} \, dS \quad \text{weber/meter} \tag{A-5}$$

$$\overline{F} = \frac{\epsilon}{4\pi} \int_{area} \frac{\overline{J}_{ms} \, e^{-j\beta r}}{r} \, dS \quad \text{coulomb/meter.} \tag{A-6}$$

Harmonic variation with time is assumed and suppressed.

It is well known that in the absence of magnetic currents the electric field is given by

$$\overline{E}_e = - j \omega A - \nabla V . \tag{A-7}$$

Analogous to the magnetic field case

$$\overline{H} = \frac{1}{\mu} \nabla \times \overline{A} \tag{A-8}$$

is the electric field due to magnetic currents

$$\overline{E}_m = - \frac{1}{\epsilon} \nabla \times \overline{F} . \tag{A-9}$$

Therefore,

$$\bar{E} = \bar{E}_e + \bar{E}_m = -j\omega A - \nabla V - \frac{1}{\epsilon} \nabla \times F, \qquad (A\text{-}10)$$

and from the continuity equation

$$V = \frac{j}{\omega \mu \epsilon} \nabla \cdot A \qquad (A\text{-}11)$$

the total electric field can be given wholly in terms of vector potential as

$$\bar{E} = -j\omega \bar{A} - \frac{j}{\omega \mu \epsilon} \nabla (\nabla \cdot A) - \frac{1}{\epsilon} \nabla \times F. \qquad (A\text{-}12)$$

By utilizing equations (A-5), (A-6), (A-1), and (A-2) the result from (A-12) is

$$
\begin{aligned}
E = \frac{-j\omega\mu}{4\pi} &\int_S \frac{(\hat{n} \times H_t) e^{-j\beta r}}{r} dS \\
&- \frac{j}{4\pi\omega\epsilon} \nabla \left[\nabla \cdot \int_S \frac{(\hat{n} \times \bar{H}_t) e^{-j\beta r}}{r} dS \right] \\
&+ \frac{1}{\epsilon} \nabla \times \left[\frac{\epsilon}{4\pi} \int_S \frac{(\hat{n} \times \bar{E}_t) e^{-j\beta r}}{r} dS \right] . \qquad (A\text{-}13)
\end{aligned}
$$

Because the fields below the surface are zero, an electric conductor can be brought infinitesimally close from below without disturbing the fields outside the surface, i.e., above the earth. When this is done, the image electric current element is of opposite phase to give the required E - field cancelation at the conductor. When the

limit is taken, the electric current elements cancel. However, the

magnetic current element will be in phase with its image to produce

cancelation of the E-field at the conductor, and in the limit these will

add to give double the original value (Figure 65).

(a)

(b)
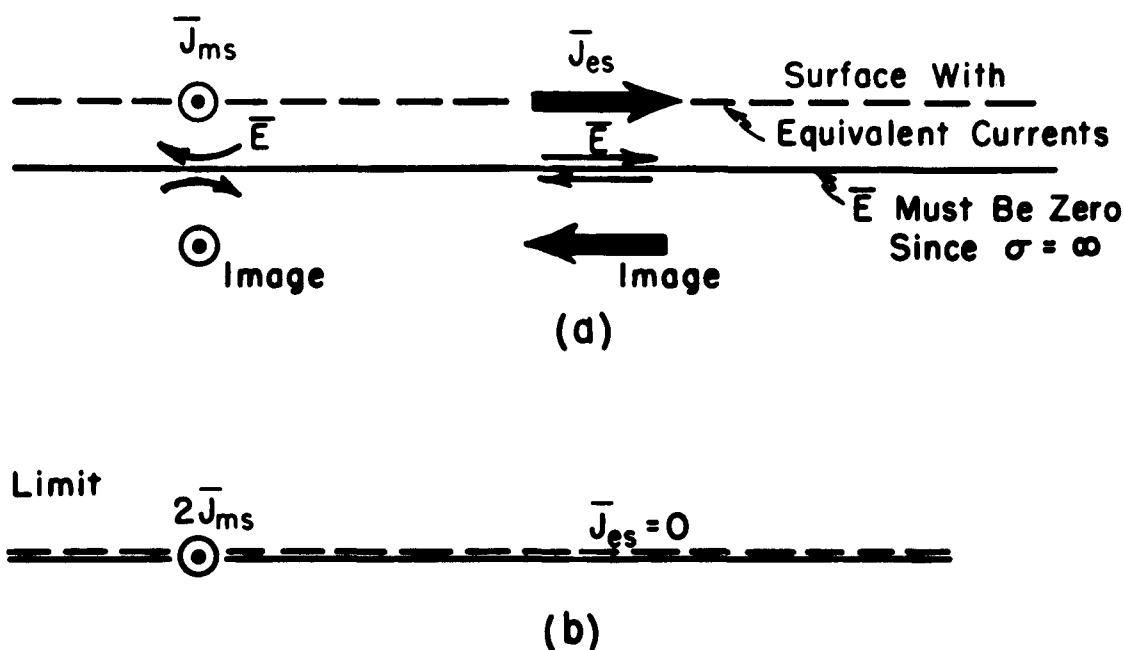
Fig. 65. Introduction of a perfect conductor of electricity
below the aperture surface for purposes of analysis.

Since J_{es} is now eliminated, the first two terms of (A-13) are

zero and the third term is doubled.

The earth's surface, excluding the aperture, has been assumed

to be a perfect conductor; tangential E is zero outside the aperture;

therefore, the integral in the remaining term for the expression for

E has values only when S is the aperture surface. $\bar{E}$, with the

coordinate of Figure 7, can now be written as

$$\overline{E}\,(x,y,z) = \frac{1}{2\pi}\,\nabla\times\int_{S}\frac{[\hat{n}\times\overline{E}\,(y',z')]e^{-j\beta r}}{r}\,dS\,. \qquad (A\text{-}14)$$

Because of the indepence of the variables associated with the curl and integration processes, $\overline{E}$ is

$$\overline{E}\,(x,y,z) = \frac{1}{2\pi}\,\int_{S}\nabla\times\frac{\{\hat{n}\times\overline{E}\,(y',z')\}e^{-j\beta r}}{r}\,dS\,. \qquad (A\text{-}15)$$

By recalling the vector identity

$$\nabla\times(f\overline{G}) = (\nabla f)\times\overline{G} + f\,(\nabla\times\overline{G}) \qquad (A\text{-}16)$$

and letting

$$f = \frac{e^{-j\beta r}}{r}\,, \qquad (A\text{-}17)$$

$$\overline{G} = \hat{n}\times\overline{E}\,(y',z') \qquad (A\text{-}18)$$

The expression for the electric field becomes

$$E\,(x,y,z) = \frac{1}{2\pi}\,\int_{S}\left\{\nabla\left(\frac{e^{-j\beta r}}{r}\right)\times\left[\hat{n}\times\overline{E}\,(y',z')\right]\right.$$

$$\left. +\left(\frac{e^{-j\beta r}}{r}\right)\nabla\times\left[\hat{n}\times\overline{E}\,(y',z')\right]\right\}\,dS\,. \qquad (A\text{-}19)$$

Since the curl involves operation with respect to the unprimed coordinates,

$$\bar{E}(x, y, z) = \frac{1}{2\pi} \int_S \nabla \left(\frac{e^{-j\beta r}}{r} \right) \times \left[\hat{n} \times \bar{E}(y', z') \right] dS. \quad (A-20)$$

The gradient can be written:

$$\nabla \left(\frac{e^{-j\beta r}}{r} \right) = \left(\frac{-j\beta}{r} - \frac{1}{r^2} \right) e^{-j\beta r} \left[\hat{x} \frac{\partial r}{\partial x} + \hat{y} \frac{\partial r}{\partial y} + \hat{z} \frac{\partial r}{\partial z} \right]. \quad (A-21)$$

But

$$r = \sqrt{(x - x')^2 + (y - y')^2 + (z - z')^2}, \quad (A-22)$$

and since the point of observation is in the far field

$$x \gg x', \quad y \gg y', \quad \text{and} \quad z \gg z',$$

$$\frac{\partial r}{\partial x} = \frac{x}{r}, \quad \frac{\partial r}{\partial y} = \frac{y}{r}, \quad \frac{\partial r}{\partial z} = \frac{z}{r}. \quad (A-23)$$

Neglecting higher order terms in the denominator gives

$$\nabla \left(\frac{e^{-j\beta r}}{r} \right) \approx \frac{-j\beta \, e^{-j\beta r}}{r} \left[\hat{x} \frac{x}{r} + \hat{y} \frac{y}{r} + \hat{z} \frac{z}{r} \right] \quad (A-24)$$

or transformed to spherical coordinates with $r \approx r_o$ in far field,

$$\nabla\left(\frac{e^{-j\beta r}}{r}\right) \approx \frac{-j\beta e^{-j\beta r}}{r}\left[\hat{x}\sin\theta\cos\phi + \hat{y}\sin\phi\sin\theta + \hat{z}\cos\theta\right] . \quad \text{(A-25)}$$

By referring to the geometry of Figure 7 and using the law of cosines,

$$r^2 = a^2 + r_o^2 - 2a\, r_o \cos\psi . \quad \text{(A-26)}$$

By approximating r with the first few terms of a binomial expansion,

$$r \approx r_o - a\cos\psi . \quad \text{(A-27)}$$

Let the end coordinates of the projection of a onto r be $(0,0,0)$ and (x_1, y_1, z_1) and this segment will be called $\bar{r}_1$. Then

$$\bar{r}_1 = \hat{x}x_1 + \hat{y}y_1 + \hat{z}z_1 \quad \text{(A-28)}$$

$$\bar{a} = \hat{y}y' + \hat{z}z' \quad \text{(A-29)}$$

where

$$|\bar{r}_1| = (x_1^2 + y_1^2 + z_1^2)^{\frac{1}{2}} = a\cos\psi . \quad \text{(A-30)}$$

Because the projection is made by dropping a perpendicular

$$\bar{r}_1 \cdot (\bar{r}_1 - \bar{a}) = 0. \quad \text{(A-31)}$$

Now

$$x_1(x_1 - 0) + y_1(y_1 - y') + z_1(z_1 - z') = 0 \quad \text{(A-32)}$$

or

$$|\bar{r}_1|^2 = y'y_1 + z'z_1 .$$ (A-33)

But

$$y_1 = |\bar{r}_1| \sin \phi \sin \theta$$ (A-34)

$$z_1 = |\bar{r}_1| \cos \theta .$$ (A-35)

Now

$$|\bar{r}_1| = y' \sin \phi \sin \theta + z' \cos \theta = a \cos \psi$$ (A-36)

thus

$$r \approx r_0 - y' \sin \phi \sin \theta - z' \cos \theta .$$ (A-37)

By working with the gradient operation,

$$\nabla \left(\frac{e^{-j\beta r}}{r} \right) =$$

$$\frac{\left\{ -j\beta e^{-j\beta r_0} e^{j\beta (y' \sin \phi \sin \theta + z' \cos \theta)} \right\} [\hat{x} \sin \theta \cos \phi + \hat{y} \sin \theta \sin \phi + \hat{z} \cos \theta]}{r_0 - (y' \sin \phi \sin \theta + z' \cos \theta)}$$

(A-38)

and recalling that for far field amplitude considerations $r_0 \gg |\bar{r}_1|$

gives

$$\nabla \left(\frac{e^{-j\beta r}}{r} \right) =$$

$$\frac{-j\beta}{r_o} e^{-j\beta r_o} e^{j\beta |\overline{r}_1|} \left[\hat{x} \sin\theta\cos\phi + \hat{y} \sin\theta\sin\phi + \hat{z} \cos\theta \right] \quad . \quad \text{(A-39)}$$

By using equation (A-20) and the fact that here $\hat{n} = \hat{x}$

$$E(r_o, \phi, \theta) =$$

$$\frac{1}{2\pi} \int_S \left[\frac{-j\beta}{r_o} e^{-j\beta r_o} e^{j\beta |\overline{r}_1|} \left\{ \hat{x} \sin\theta\cos\phi + \hat{y} \sin\theta\sin\phi + \hat{z}\cos\theta \right\} \right]$$

$$\times \left[- J_{ms} \right] dS \qquad \text{(A-40)}$$

The cross product in the integrand becomes

$$\overline{I} = \hat{x} \left[(J_{ms})_y \cos\theta - (J_{ms})_z \sin\theta\sin\phi \right] + \hat{y} \left[(J_{ms})_z \sin\theta\cos\phi \right]$$

$$+ \hat{z} \left[-(J_{ms})_y \sin\theta\cos\phi \right] \qquad \text{(A-41)}$$

Because the horizontal component is of interest in radiating glide-path signals, attention will be confined to the ϕ - component of the field; therefore, knowing

$$\overline{I}_\phi = -I_x \sin\phi + I_y \cos\phi \qquad \text{(A-42)}$$

gives

$$\overline{I} = \hat{\phi} \left[- (J_{ms})_y \ \cos\theta\sin\phi + (J_{ms})_z \ \sin\theta \right] \qquad (A-43)$$

Interest will be confined to the aircraft approach region to further simplify the integral.

$$E_{\phi} (r_o , \phi , \theta) = E_{\phi} (r_o , 0 , \theta) \qquad (A-44)$$

now

$$\overline{I} = \hat{\phi} \left[(J_{ms})_z \ \sin\theta \right] . \qquad (A-45)$$

Now it can be seen that the contributing electric field at the aperture consists only of the y-component, i.e.

$$E(y', z') = \hat{y} \ E_y . \qquad (A-46)$$

From this it can be seen that a horizontal electric probe in the cavity should be used. This also explains the basis for the name TE (transverse electric) that is applied to this type of antenna.

Since θ is not involved in the integration, the integral can be written

$$E_{\phi} (r_o , 0 , \theta) = \frac{-j\beta \ e^{-j\beta r_o}}{2\pi \ r_o} \ \sin\theta \int_S E_y(y', z') e^{j\beta |\overline{r}_1|} dS. \qquad (A-47)$$

By assuming

$$E_y = E_0 \, e^{-j \, k \, z'} \qquad \text{(A-48)}$$

as in a traveling wave where

$$k = \alpha_g + j \, \beta_g \quad , \qquad \text{(A-49)}$$

α_g = losses due to radiation, the dielectric and

the conductors with finite conductivity , and

$$\beta_g = \frac{\omega}{v} = \text{phase constant of cavity .}$$

Using equation (A-36) when (A-48) is substituted into (A-47), the exponential term becomes

$$e^{j\beta \sin\phi \sin\theta \, y'} \cdot e^{-j(k-\beta\cos\theta)z'} \qquad \text{(A-50)}$$

with the first factor being equal to 1 when the restriction of $\phi = 0$ is applied. Finally

$$E_\phi(r_0, 0, \theta) = \frac{j\beta e^{-j\beta r_0}}{2\pi r_0} E_0 \sin\theta \int_{-\frac{W}{2}}^{\frac{W}{2}} \int_{-\frac{L}{2}}^{\frac{L}{2}} e^{-j(k-\beta\cos\theta)z'} dz' dy' . \quad \text{(A-51)}$$

By integrating and letting

$$A = LW$$

give

$$E_{\phi} (r_0, 0, \theta) = \frac{-j\beta e^{-j\beta r_0}}{2\pi r_0} A E_0 \sin \theta \frac{\sin X_0}{X_0} \qquad (A\text{-}53)$$

where

$$X_0 = (k - \beta \cos \theta) \frac{L}{2} . \qquad (A\text{-}54)$$

These are equations (2-10) and (2-11) of Chapter II .

BIBLIOGRAPHY

Bottoms, T.H., Hurley, H.C., Spinner, L.N., and Watt, J.W.,
"A Directional Glide Path," Technical Development Report
No. 336, Civil Aeronautics Administration; February 1956.

Bronwell, A.B., and Beam, R.E., <u>Theory and Application of</u>
<u>Microwaves</u>, McGraw-Hill Book Co., Inc., New York, N.Y.,
p. 451; 1947.

Diamond, H., and Dunmore, F.W., "A radio beacon and receiving
system for blind landing of aircraft," Bureau of Standards
Journal of Research, vol. 5, paper 238, October, 1930, also
Proc. IRE, vol. 19, pp. 585-626; April 1931.

Iden, F.W., "Glide-slope antenna arrays for use under adverse
siting conditions," IRE Trans. on Aeronautical and Naviga-
tional Electronics, vol. ANE-6, pp. 100-111; June 1959.

Kandoian, A.G., "Glide Path Beacon," U.S. Patent 2,367,680,
U.S. Patent Office; 1942.

Kirschbaum, H.S., and Tsu, R., "A Study of a Serrated Ridge
Waveguide," IRE Trans. on Microwave Theory and Tech-
niques, vol. MTT-7, pp. 142-148; January, 1959.

Kraus, J.D., <u>Antennas</u>, McGraw-Hill Book Co., Inc., New York,
N.Y., pp. 79, 157, 344-348; 1950.

Kraus, J.D., Electromagnetics, McGraw-Hill Book Co., Inc.,

New York, N.Y., p. 227; 1953.

Oliner, A.A., and Rotman, W., "Periodic Structures in Trough

Waveguide," IRE Trans. on Microwave Theory and Techniques,

vol. MTT-7, pp. 134-142; January, 1959.

Rotman, W. and Oliner, A.A., "Asymmetrical Trough Waveguide

Antennas," IRE Trans. on Antennas and Propagation,

vol. AP-7, pp. 153-162; April, 1959.

Additional References

Anast, J.L., "All-weather landing," IRE Trans. on Aeronautical

and Navigational Electronics, vol. ANE-6, pp. 75-77;

June 1959.

Baechle, J.R., and McFarland, R.H., "A flush-mounted runway

antenna for use with the FAA directional glide path system,"

IRE Trans. on Aeronautical and Navigational Electronics,

vol. ANE-7, pp. 32-39; June 1960.

Buttner, H.H., and Kandoian, A.G., "Development of Aircraft

Instrument Landing Systems," Electrical Communications,

vol. 22, Number 3, pp. 179-192; 1945.

Cutrell, E.A., "Operational Flight Testing of Early Instrument

   Landing Systems," IRE Trans. on Aeronautical and Naviga-

   tional Electronics, vol. ANE-6, pp. 67-70; June, 1959.

Hampshire, R.A., and Thompson, B.V., "ILS-2 Instrument

   Landing Equipment," Electrical Communications, vol. 27,

   No. 2, pp. 112-122; June 1950.

Hines, J.N., Rumsey, V.H., and Walter, C.H., "Traveling-wave

   Slot Antennas," Proc. IRE, vol. 41, 1624-1631;

   November 1953.

Hines, J.N., and St. Clair, R.W., "The radiation characteristics

   of an end-fire, dielectric-filled TE traveling-wave antenna,"

   Quarterly Report 757-1, 19 June 1957, Antenna Laboratory,

   The Ohio State University Research Foundation.

Instrument Landing System Glide-Slope, Civil Aeronautics Adminis-

   tration Aeronautical Center Training Series Facilities Branch

   Manual 206, U.S. Department of Commerce, Oklahoma City,

   Oklahoma.

Jackson, W.E., "Improvements on the Instrument Landing System,"

   IRE Trans. on Aeronautical and Navigational Electronics,

   vol. ANE-6, pp. 85-94; June 1959.

Jackson, W.E., "The status of instrument landing systems,"

   Proc. IRE, vol. 26, pp. 681-699; June, 1938.

161

Jackson, W.E., Alford, A., Byrne, P.F., and Fisher, H.B.,
"Development of the Civil Aeronautics Authority Instrument
Landing System at Indianapolis," Electrical Communications,
vol. 18, pp. 285-302; April, 1940.

Kear, F.G., "Instrument Landing at the National Bureau of
Standards," IRE Trans. on Aeronautical and Navigational
Electronics, vol. ANE-6, pp. 61-66; June, 1959.

Lee, J.M., and Metz, H.I., "Development of a Straight-Line Glide
Path," Technical Development Report No. 55, Civil Aero-
nautics Administration; June, 1947.

McFarland, R.H., and Baechle, J.R., "A flush-mounted runway
antenna for the ILS glide path," Bulletin 171, Engineering
Experiment Station, The Ohio State University, Columbus,
Ohio; September, 1958.

Metz, H.I., "A survey of instrument approach systems in the
United States," IRE Trans. on Aeronautical and Navigational
Electronics, vol. ANE-6, pp. 78-84; June, 1959.

Pickles, S., "Army Air Forces portable instrument landing system,"
Electrical Communications, vol. 22, Number 4, pp. 262-294;
1945.

Stephenson, B.T., and Walter, C.H., "Endfire slot antennas,"
IRE Trans. on Antennas and Propagation, vol. AP-3, pp. 81-86;
April, 1955.

162

Wait, J.R. and Conda, A.M., "Radiation from Flush-Mounted Antennas on a Non-ideal Ground Plane," Part I National Bureau of Standards Report 5511, August 1957, Boulder Colorado.

Watts, C.B., "Theoretical consideration of an improved glide path antenna system," Technical Development Report No. 81, Civil Aeronautics Administration; March 1949.

Watt, J.W. and Saunders, A.L., "Some effects of terrain on the null-reference glide-path shape," Technical Development Report No. 169, Civil Aeronautics Administration; August 1952.